9

Groundwater–Surface Water Interactions

Vitaly A. Zlotnik
University of Nebraska-Lincoln

Adam S. Ward
Indiana University

Judson W. Harvey
U.S. Geological Survey

Laura K. Lautz
Syracuse University

Donald O. Rosenberry
U.S. Geological Survey

Philip Brunner
University of Neuchatel

9.1 Introduction

Surface water (SW) is linked to groundwater (GW) through myriad connections. Hydrological scientists from ancient times were aware of the water cycle concept, but not until the end of the twentieth century did the scale and dramatic effects of anthropogenic activity force scientists, engineers, and water users to start managing SW and GW within a water budget framework as a single resource (Winter et al., 1998; Healy et al., 2007).

We will use the abbreviation "GWSWI" to connote a groundwater–surface water interaction. GWSWIs exist at scales ranging from pores to formations. Globally, such interactions are characteristic of the terrestrial and oceanic components of the water cycle. In addition to stream–aquifer and lake–aquifer exchanges, GWSWIs include submarine GW discharge and saltwater intrusion that have attracted recent attention. Next, we will focus on more traditional terrestrial GWSWIs. This well-developed part of GW engineering is related to irrigation agriculture, which is the major GW consumer in the world (Konikow and Kendy, 2005; Wada et al., 2012). The topic is very broad, and we emphasize GW's role in this connection.

The renewal rates of GW are slow, and residence times are long compared to SW, and thus sustainability of a GW resource is an increasingly important consideration (Alley et al., 1999). Currently, estimates comparing aquifer recharge rates with GW extraction rates in various parts of the globe are not optimistic. To address theoretical and applied aspects of GW sustainability issues, a deeper and broader understanding of GWSWI is needed.

Examples of GWSWI issues include the usage of aquifer systems for temporary storage of SW during excessive flow, water rights adjudication when intensive use by one user (GW or SW) adversely affects another hydrologic component, bank storage effects and canal losses that may delay the time of discharge from headwater to stream outlet, effects of flood attenuation by modification of wetlands or stream–aquifer interface, effects of GW pumping on lake stages; denitrification in streams, and effects of temperature on fish habitats. Of course, this list falls far short of all connections. Management of one component of the hydrologic system is only partially effective when these components are treated separately (Winter et al., 1998).

This chapter begins with the hydraulics of GWSWIs (Section 9.2). This is one of the most developed fields of hydrogeology, evolving from engineering experience in designing well fields in alluvial valleys throughout the world. Typically, the interface between GW and SW was perceived as a layer with identifiable properties and simple geometry. Actual properties of mass and heat transfer are more complex. Section 9.3 elucidates properties of this interface (hyporheic zone [HZ]) using contributions from fluvial and lacustrine sedimentology, hydrodynamics of porous media, mass and heat transport, and laying out foundations for analysis of water, solute, and heat transfer across the interface. Section 9.4 focuses more specifically on solute transport across the interface. Section 9.5 addresses heat transport studies that gained strong momentum over the last decade. To support analyses of these processes, Section 9.6 addresses field methods needed for their quantification. Finally, Section 9.7 presents examples of usage of these principles, processes, and parameters in simulation of GWSWIs for theoretical and applied purposes.

9.2 Hydraulics of GW-SW Interactions

9.2.1 Basics

GWSWI studies emphasize water, solute, and heat exchanges across the interface in addition to GW flow and transport processes in the aquifer per se. Such studies are often a component of integrated watershed models (Rossman and Zlotnik, 2013) developed over past decades. They incorporate GW and SW including overland flow, vadose zone, land surface hydrology, and climate (e.g., reviews by AquaResource, Inc., 2011; Daniel et al., 2011). Sometimes, feedbacks between GW and SW, driven by climate variables and water resources management scenarios (Maxwell and Kollet, 2008; Green et al., 2011), are of primary interest.

Differences in GW role between streams and lakes: Water residence times and discharges differ significantly between streams and lakes. For a given water exchange rate between a body of GW and SW, the effects on stream discharge and stage might be dramatically different from those on a closed (endorheic) lake (Born et al., 1977). In the case of a stream, changes in the resulting stream regime may be negligible, while in the case of the lake, such changes can be quite dynamic.

Spatial-temporal nature of stream–aquifer interactions: Streams interact with GW in all types of landscapes in three basic ways (e.g., Winter et al., 1998): (1) streams gain water from inflow of GW through the streambed (gaining stream), (2) they lose water to the aquifer by outflow (losing stream), and (3) they do both, gaining at some reaches and losing in others. However, the transient nature of GWSWIs at annual or seasonal scales, affected by factors such as droughts or land use activities (e.g., GW withdrawals), may result in inversions of the flow direction. For example, some reaches undergo transitions from gaining to losing conditions as evident by the disappearance or reduction of flowing streams (e.g., Sophocleous, 2000).

Spatial-temporal nature of lake–aquifer interactions: Lakes, where substantial GW inflow exists compared to other components of the water budget, are often defined as GW-dominated lakes (Born et al., 1977). This dominance is especially important for shallow lakes (Rosen, 1994). In lakes, the flux direction across the interface may vary spatially. Lakes that receive GW over the entire lakebed are called discharge lakes (i.e., discharging GW); lakes that infiltrate SW over the entire lakebed are called recharge lakes; and lakes that have areas of both vertical upward and downward recharge are flow-through lakes (Born et al., 1977). Due to the transient nature of GWSWIs at various timescales, inversion of fluxes and change of the lake regime may occur.

Aquifer heterogeneity: Hydraulic conductivity (K) of an aquifer is inherently heterogeneous. The analysis of GWSWIs require data collection at appropriate scales (Bridge and Hyndman, 2004; Rubin and Hubbard, 2005) and quantitative data interpretation (Marsily et al., 2005) in terms of 3D K-distributions of the "bulk" mass of the aquifer. Substantial advances have been made in the past several decades (see Part II of the Handbook). In sedimentology, the distinction between short-term and long-term deposits in alluvial channels and floodplains is based on factors such as flow and sediment transport, flood frequency, tectonics, climate, and sea-level rise (Bridge, 2003; Sambrook Smith et al., 2013). This distinction defines the difference between the properties of the aquifer and HZ. In long-term deposits, adaptation of an SW regime to climate variations may result in sediment sequences that fine or coarsen with depth (Bridge and Demico, 2008).

GW-SW interface: The properties of the heterogeneous interface (e.g., Calver, 2001) are dynamic and are affected by physical, chemical, and biological processes. Over the past two decades, the term "hyporheic zone" has come to denote the region beneath and alongside a streambed, characterized by mixing of shallow GW and SW (Section 9.3). For practical purposes, several lithological traits and geometries are commonly recognized. The HZ may be incised to a full or partial depth into the same alluvial aquifer, or it can be incised into a lower permeability unit overlying the aquifer. Permeability properties at the interface are formed over "geological" time, but they might be affected by changes resulting from droughts, floods, or seasonal cycles (e.g., Doppler et al., 2007; Sambrook Smith et al., 2013). If the interface properties are well represented by the underlying alluvium, then a variety of different models can be used (e.g., Guin et al., 2010). Colmation (interface clogging) may reduce permeability under the effects of GW pumping in alluvial aquifers (Hiscock and Grischek, 2002).

GW models in GWSWIs: Flow and transport processes are inherently three dimensional. Considering the small aspect ratio of saturated aquifer thickness to horizontal aquifer extent, it is commonly assumed that vertical head gradients at a given location are negligible, which is Dupuit-Forchheimer assumption (Freeze and Cherry, 1979). In these cases, 2D GW flow models in Cartesian coordinates x and y are used. Exceptions are areas where streamline deformation occurs, for example, wells, seepage zones, and at or near aquifer boundaries. In these cases, 3D or combinations of 2D and 3D models are essential (Haitjema, 1995; Luther and Haitjema, 2000). Models focused on 2D analytical solutions are described in this section. With consideration of system complexity, such as 3D flow patterns, aquifer heterogeneity, irregular geometry, and various hydrologic processes across the SW-GW interface, numerical methods are used; these models are addressed in Section 9.7.

Boundary conditions: GW may occur in direct hydraulic connection with a stream or lake, or it may be "disconnected." In the latter case, the water table and capillary fringe are separated from the SW (e.g., Bouwer, 2002; Brunner et al., 2009a,b, 2011). In most models, hydraulic connection is commonly assumed. If additional resistance to fluxes between GW and SW exists due to fine sediments or anisotropy, a low-permeability horizontal layer is introduced. This was originally proposed by Grigoryev (1957) and later became commonplace after the release of the MODFLOW software (McDonald and Harbaugh, 1983), although heterogeneity and uncertainty of the layer shape are important (Brunner et al., 2011).

9.2.2 Stream–Aquifer Interactions and Capture

9.2.2.1 Capture and Stream Depletion

9.2.2.1.1 *Definitions*

Land use changes such as pumping and irrigation upset predevelopment equilibrium and cause stream depletion (and sometimes stream recharge) from the aquifer. In his classic study, Theis (1940, 1941) explained the dynamics of stream depletion resulting from GW withdrawals. During the early stage of pumping, a cone of depression (aquifer storage) is the main source of extracted water. With continued pumping, the pumping rate Q is supplied by capturing ambient GW flow (Figure 9.1a) that would discharge to the stream otherwise. However, at a sufficiently high pumping rate (equal to some critical value Q_C), the capture zone of a well located at a distance d may expand and reach the stream (Figure 9.1b). At even higher pumping rates, the aquifer is recharged by infiltration from the stream to the aquifer along some stream reach (AA' in Figure 9.1c).

The sum of two terms—decrease in discharge (ambient flow to the stream) plus increase in aquifer recharge (induced infiltration from the stream)—produces a new dynamic equilibrium under GW pumping referred to as *capture* (Lohman, 1972; Bredehoeft et al., 1982; Bredehoeft, 1997, 2002). Hantush (1965) used the term *stream depletion* as synonymous with capture to characterize changes in natural GW discharge to streams. Other sources of capture may include reduced evapotranspiration from the GW system and reduced rates of GW discharge to a coastal zone/ocean.

When stream and aquifer water qualities differ, intensive GW withdrawals from a well may result in a mixing of SW and ambient GW flow. If the quality of pumped water is a concern, a procedure for separating stream depletion into induced infiltration and captured discharge/ambient flow (*stream depletion separation* procedure, for brevity) is needed.

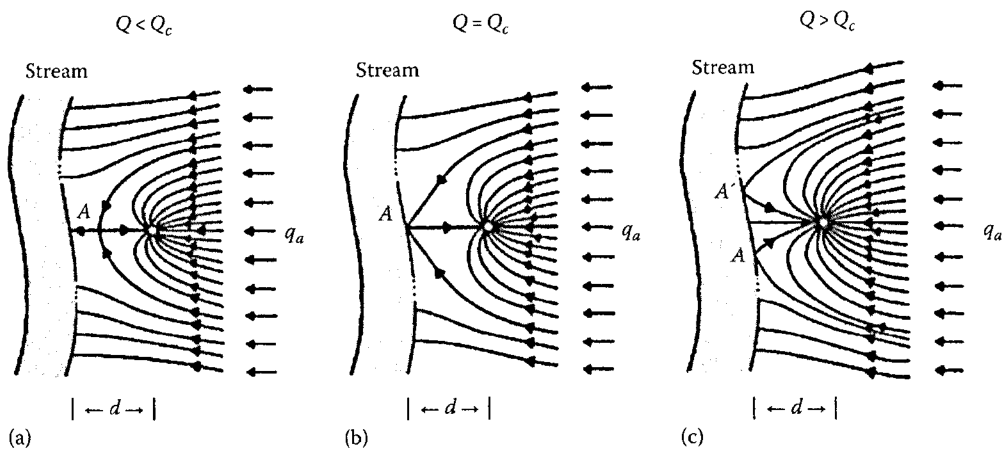

FIGURE 9.1 Schematic diagram of streamlines for steady-state GW flow near pumping well in plan view illustrating the stream depletion (capture) at different pumping rates: (a) well uses ambient flow only; (b) critical pumping rate Q_C, when stagnation point A reaches the stream; and (c) well uses ambient flow and infiltration from the stream between stagnation points A and A'. (Modified after Wilson, J.L., *Water Resour. Res.*, 29(10), 3503, 1993.)

With some land use changes, GW recharge can increase in various areas of the watershed. Such spatially distributed increases can result in *stream recharge by GW*, runoff increase, or associated SW quality changes (Knight et al., 2005; Stonestrom et al., 2009; Schilling et al., 2010).

Early studies of GWSWIs are largely focused on hydrogeological applications (irrigation supply, municipal well fields, pumped GW quality). An extensive body of literature, directed at understanding and managing the effects of GW pumping on streamflow, is summarized and illustrated by Barlow and Leake (2012) who describe the major factors controlling GWSWIs, including stream–aquifer geometry, streambed–aquifer properties, and GW withdrawal characteristics. We will highlight those aspects of hydraulics that serve as a basis of GW engineering decisions.

9.2.2.1.2 *Field Experiments*

Stream depletion rate observations and experiments must consider (1) time lag and attenuation of pumping effects that increase with distance from the location of GW withdrawal, (2) accuracy of stream discharge measurements to separate stream depletion rate changes from natural discharge variability, and (3) other factors that attenuate stream depletion rate such as phreatophytes (Bredehoeft et al., 1982; Bredehoeft, 2011) or aquifer leakage (Zlotnik, 2004). Two types of field studies are feasible: (1) short-time pumping tests, including well field operations in alluvium lasting from hours to months and (2) long-time analyses of pumping, utilizing hydrologic and climatic data collected over a period of many years.

Short-term tests are designed to determine local-scale effects of pumping, understand the geologic and hydrogeologic controls on streamflow depletion, and test the predictive capability of models to determine streamflow depletion under actual field conditions. Such studies typically make use of multiple data types to provide a comprehensive picture of how stream–aquifer systems respond to pumping and are not numerous. They include those described by Sophocleous et al. (1988), Christensen (2000), Hunt et al. (2001), Nyholm et al. (2002, 2003), Kollet and Zlotnik (2003), Fox (2004), and Lough and Hunt (2006). There are also cases of applied nature, when the quantity and quality of captured SW are of interest (see Barlow and Leake, 2012).

Long-term studies utilize hydrologic and climatic data collected over several years and aim to determine whether changing streamflow conditions can be correlated to long-term, basin-wide development of GW resources (e.g., Wahl and Tortorelli (1997) for the period 1938–1996, Sophocleous (2000) for 1950–1995, Fleckenstein et al. (2004) for 1941–1981, and Prudic et al. (2006) for 1950–2000). In these cases, water balance over a long period permits estimations of stream depletion rate in the SW budget and long-term trends in streamflow conditions.

9.2.2.1.3 *Streamflow Response to GW Pumping*

The properties of the aquifers controlling stream depletion include saturated thickness (b), hydraulic conductivity (K), transmissivity ($T = K \cdot b$), specific yield for an unconfined aquifer or storage coefficient for a confined aquifer (both denoted as S), and diffusivity defined as $D = T/S$. Typically, GWSWI studies have utilized 2D frameworks with Cartesian coordinates x and y but may also require vertical dimension z, as outlined earlier. If the stream boundary is aligned with the y-axis and a well is located on the x-axis at a distance d, stream depletion rate $q(t)$ is found by integrating Darcy's fluxes along the stream–aquifer interface along the y-axis (Figure 9.2a) as follows:

$$q(t) = -T \int_{-\infty}^{\infty} \frac{\partial s(0, y, t)}{\partial x} \mathrm{d}y \tag{9.1}$$

Here, $s(x, y, t)$ is a head change at the watershed, resulting from transition from predevelopment to development conditions over time t. Geometry and properties of the streambed may result in various modifications of this equation. The resulting stream depletion volume $V(t)$ for this stream is found by summation of *SDR* over time as follows:

$$V(t) = \int_0^t q(\tau)\mathrm{d}\tau \tag{9.2}$$

Due to the near-linear nature of the GW flow equation, the effects of multiple wells located at various distances from the stream are treated by superposition of the effects of individual wells with individual pumping rates.

The classic solution was obtained by Theis (1940, 1941), and the results were refined by Glover and Balmer (1954). Jenkins (1968, 1970) analyzed this Theis–Glover–Balmer solution, $q(t)$, as a function of dimensionless time t_d and introduced a *stream depletion factor* (*sdf*)

$$t_d = \frac{t}{t_A}, \quad t_A = \frac{Sd^2}{T} = sdf \tag{9.3}$$

that reflects the aquifer properties (T and S) and GW withdrawal geometry (d). Stream depletion rate at time t is defined as follows:

$$\frac{q(t)}{Q} = erfc\left(\frac{1}{2t_d^{1/2}}\right), \quad erfc(x) = \frac{2}{\sqrt{\pi}} \int_0^{\infty} e^{-u^2} du \tag{9.4}$$

This equation indicates that 100% of GW withdrawal will eventually come from stream depletion, that is, $\lim_{t \to \infty} V(t)/(Qt) = 1$. There are several simplifications in the Theis assumptions regarding the properties of the streambed, stream penetration of the aquifer, transient pumping rate, heterogeneity of the aquifer (alluvial valley), and a nonstraight stream shape. They have been addressed by different authors and tools as discussed next.

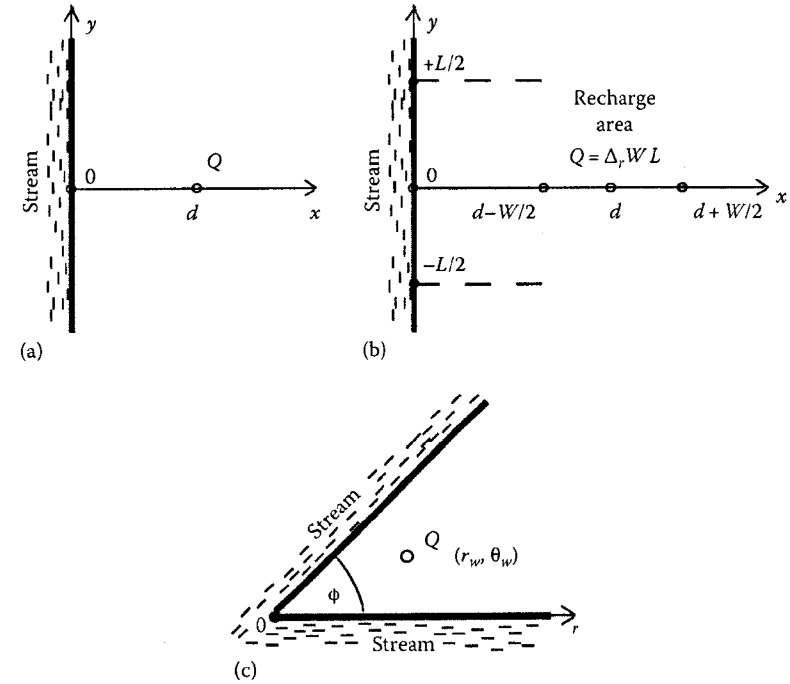

FIGURE 9.2 Geometry of GWSWI with different sinks/sources of strength Q: (a) a single well (pumping rate Q); (b) rectangular sink/source with strength $Q = \Delta_r \cdot W \cdot L$; and (c) a single well near a stream confluence at angle ϕ, located at polar coordinates (r_w, θ_w).

9.2.2.1.4 *Stream Recharge from Land Use Changes*

Typically, land use changes are spatially distributed (various crops, irrigation technologies, etc.). If increase in recharge is a result, the change of water levels may result in changes of baseflow and runoff in general (Schilling et al., 2010). Hantush (1967b) developed several 2D solutions for GW mounding resulting from circular and rectangular sources but without considering effects on stream runoff. Knight et al. (2005) obtained and applied analytical solution for stream recharge rates $q(t)$ originating from GW recharge increase (Δ_r) over a rectangular patch, aligned along the stream with dimensions W and L as shown in Figure 9.2c.

$$\frac{q(t)}{Q} = \frac{2t_d^{1/2}}{w}\left[ierfc\left(\frac{1-w/2}{2t_d^{1/2}}\right) - ierfc\left(\frac{1+w/2}{2t_d^{1/2}}\right)\right],$$

$$ierfc(x) = \frac{e^{-x^2}}{\sqrt{\pi}} - x \cdot erfc(x) \qquad (9.5)$$

where $Q = \Delta_r \cdot W \cdot L$ is the strength of sink, centered at the patch, and $w = W/d$. Zlotnik (2015) presented a summary for this and other stream–aquifer geometries and stream recharge volume estimates. The role of the patch shape becomes less significant over time or with distance from the stream.

9.2.2.1.5 *Other Factors in Stream–Aquifer Hydraulics*

9.2.2.1.5.1 ***Partial Penetration of Stream*** Concepts of streambed properties and geometry have substantially evolved since Theis (1940) considered only streams fully incised into the aquifer (Figure 9.3a). Hantush (1965) investigated the effects of reduced stream/aquifer connections by introducing an imaginary thin incompressible "vertical" layer of reduced hydraulic conductivity K_S ($K_S < K$) with thickness m_S (Figure 9.3b). His stream depletion rate

$$\frac{q(t)}{Q} = erfc\left(\frac{1}{2\sqrt{t_d}}\right) - e^{t_d v^2 + v} erfc\left(\frac{1}{2\sqrt{t_d}} + v\sqrt{t_d}\right), \quad v = \frac{d}{B_S} \qquad (9.6)$$

utilizes the retardation coefficient B_S, which accounts for streambed properties

$$B_S = \frac{K m_S}{K_S} \qquad (9.7)$$

Compared to the Theis-Glover-Balmer solution dynamics, the pace of the stream depletion rate increases more slowly over time; the term "retardation" characterizes the later onset of time needed to develop full capture.

Grigoryev (1957) proposed a scheme that accounts for streambed incision, resistance, geometry (width), and partial penetration for designing water supply in alluvial aquifers (Figure 9.3c). Zlotnik et al. (1999), Hunt (1999, 2014), Butler et al. (2001), Fox et al. (2002), and Singh (2003) used different versions of this scheme. The resulting stream depletion rate is again Equation 9.6, although the retardation factor B_S is modified to account for stream width W, thickness of

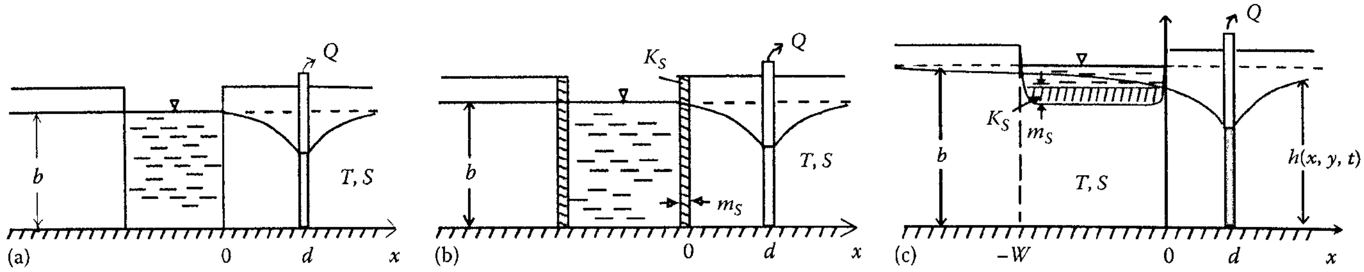

FIGURE 9.3 Stream–aquifer interface in hydraulic models: (a) stream, fully penetrating the aquifer, (b) stream separated from the aquifer by a vertical layer of elevated resistance, and (c) stream of shallow penetration with a horizontal layer of reduced hydraulic conductivity. (a: After Theis, C.V., *Civil Eng.*, 10(5), 277, 1940; b: From Hantush, M.S., *J. Geophys. Res.*, 70(12), 2829, 1965.)

streambed sediments m_S, and hydraulic conductivity K_S as follows (Zlotnik et al., 1999):

$$B_S = B\coth\left(\frac{W}{2B}\right), \quad B = \sqrt{\frac{m_S T}{K_S}} \tag{9.8}$$

For a small stream width ($W \ll 2B$), Hunt (1999) used B_S as follows:

$$B_S \approx \frac{2m_S T}{WK_S} \tag{9.9}$$

Simulation of the partial stream penetration the aquifer allows for the propagation of GW drawdown under the stream and the resulting GW storage changes on the side of the stream opposite to the well (Hunt, 1999; Butler et al., 2001).

An important assumption common to all of these approaches is that the aquifer head at the stream remains above the streambed, that is, it remains hydraulically connected with the stream (Banks et al., 2011b; Brunner et al., 2011). Finding the streambed thickness (parameter m_S) is not a well-defined procedure and may be inconsistent with the aquifer stratigraphy, which complicates B_S calculations. Therefore, it is actually more of a fitting parameter, incorporating effects of various factors (Hunt et al., 2001; Kollet and Zlotnik, 2003). Reeves (2008) and Reeves et al. (2009) provided empirical approach for finding parameter B_S, which still needs validation (e.g., by comparing with Theis–Glover–Balmer or numerical models). For example, Traylor and Zlotnik (2016) found that a model based on Equation 9.6 in alluvial aquifers does not improve estimates of stream depletion compared to the Theis–Glover–Balmer model (Equation 9.4).

9.2.2.1.5.2 Aquifer Heterogeneity at Large Scale (Layers and Bands) Additional solutions have been developed to address flow conditions along the lower and upper boundaries of the aquifer. Streams located within an overlying aquitard that provides a source of leakage to the underlying pumped aquifer are shown in publications by Hunt (2014). Zlotnik (2004), Butler et al. (2007), and Zlotnik and Tartakovsky (2008) developed solutions for leaky aquifer systems in which the upper pumped aquifer is separated by an aquitard from a high-permeability aquifer below. Theoretically, stream depletion may be less than 100% of the pumping rate if the lower aquifer has its own recharge zones (Christensen et al., 2010). Miller et al. (2007) considered alluvial aquifer width, and Butler et al. (2001, 2007) accounted for both aquifer width and structure by considering different properties of alluvium between banks and streambed (bands) but for linear stream shape.

9.2.2.1.5.3 Multiple Streams Stream depletion rate in Equation 9.4 is commonly assessed over the entire straight stream length. The stream depletion rate distribution was explored by Kollet et al. (2002) and Ward and Callander (2010). This rate varies among stream segments. If a confluence of two streams exists (Figure 9.2c), rates for each stream are of interest. Partitioning of this rate for a right-angle confluence was given by Hantush (1967a), and Yeh et al. (2008a) provided estimates for various confluence angles (wedge-shaped aquifer). This partitioning is essential for each stream above the confluence.

9.2.2.1.5.4 Transient Pumping Regime Pumping is inherently transient and often cyclical. In the majority of practical problems, one cycle amounts to a year, with distinct pumping and no pumping periods. Due to linearity of the 2D GW models, the stream depletion rate can be addressed by using various convolution methods (Wallace et al., 1990; Darama, 2001). The resulting magnitude depends on the distance d and the fraction of a year with pumping. Cyclic pumping close to a stream results in highly variable stream depletion rates through time, with peaks that may approach the maximum pumping rate. In contrast, the effect of cyclic pumping at greater distances is less variable through time, with depletion peaks that may only be slightly greater than the long-term average pumping rate. When the pumping period becomes longer, variability in capture diminishes at all distances.

9.2.2.2 Stream Depletion Separation

Steady-state and transient stream depletion estimates address total rates and volumes but do not differentiate between induced infiltration and captured ambient flow. Separation of these components is important for the management of quantity and quality of GW-SW resources. Such separation requires analysis of the flow net. Wilson (1993) provided such analysis for most common cases of GWSWI in 2D format (Figure 9.1). They include a semi-infinite aquifer of width $L \gg d$ near a stream, a finite width aquifer between a stream and an impermeable boundary, located at distance L from the stream, and a finite width aquifer between two streams, separated by distance L; in each case, a well is located at distance d near a stream. The size of the capture and location of stagnation point A associated with an individual well depends on pumping rate Q (e.g., Bear, 1979). At some critical pumping rate Q_C, stagnation point A reaches the stream, and further increase of pumping rate Q results in emergence of a stream segment AA' with induced infiltration into the aquifer (Figure 9.1c). In each case, three parameters are of interest: (1) value of critical Q_C, (2) location of the segment boundaries (AA' on Figure 9.1), and (3) induced infiltration Q_S. They are defined as functions of two dimensionless parameters, $\beta = Q/(\pi d q_a)$ and $\delta = \pi d/(2L)$. Here, q_a [L^2T^{-1}] is the uniform ambient flow velocity (discharge per unit aquifer width) resulting from lateral inflow to the aquifer from a remote boundary and diffuse GW recharge into the aquifer. Critical pumping rate for all three cases can be calculated as follows (Wilson, 1993):

$$Q_C = \pi d q_a f(\delta) \tag{9.10}$$

where function $f(\delta)$ is specific to each case. Coordinates of A and A' of the segment for any pumping rate $Q > Q_C$ are then calculated as functions of parameters δ and β. Infiltration rate Q_S is then simple closed-form function of these coordinates (Wilson, 1993).

There are several factors that may be encountered in practice as follows:

- Transient GW flow effects on location of the infiltration segment (e.g., Glover and Balmer, 1954; Chen, 2001; Kollet et al., 2002; Ward and Callander, 2010) are present.
- Multiwell interference, as illustrated by Nelson (1978), requires delineation of multiple capture zones (e.g., Fienen et al., 2005).
- Deviation of ambient flow direction from the normal to the stream may require modification of procedures for delineation of the AA' segment (Newsom and Wilson, 1988).
- Consideration of stream penetration is important for capture-zone delineation because it may extend from one stream bank (with well) to another (Bakker and Anderson, 2003).
- Heterogeneity of the aquifer may require a stochastic framework for delineation of the well capture zone, but such studies do not account for stream–aquifer exchanges explicitly (Stauffer et al., 2005; Enzenhoefer et al., 2012).

9.2.2.3 Applications

Estimation of capture is important for adjudication of water rights (Bouwer and Maddock, 1997) and engineering design. Uncertainty in available parameters often results in equal validity of analytical and numerical evaluations, and both approaches are currently used widely. Analytical methods and their modifications (including transfer functions, see Barlow and Leake (2012)) are applied to each individual well. Afterward, the integral effect is estimated using the superposition principle and often facilitated by geographic information systems. Numerical methods assess capture by considering well networks in their entirety, rather than well-by-well, but assigning capture to individual wells requires special procedures (Leake et al., 2010).

Underlying assumptions of analytical methods disregard some factors that complicate stream depletion assessment (Barlow and Leake, 2012). These include aquifer heterogeneity, finite sizes, irregular boundary shapes, stream meandering, and multiple tributaries and their orientations. However, in practice, such solutions (most commonly the Theis–Glover–Balmer solution) are used with success (e.g., COHYST Technical Committee, 2004; Reeves et al., 2009; Foglia et al., 2013; Kuwayama and Brozović, 2013). The approximate nature of such estimates is compensated for by the ease of direct assessment of annual capture rates for each well. On the other hand, numerical methods have the advantage of utilizing all hydrogeological and hydrological information for collective assessment of all wells rather than superimposing individual well effects. In practice, their accuracy in estimating stream depletion rates converges for the following practical reasons:

1. Analytical estimates are conservative; almost all solutions indicate that the stream will supply 100% of the well water, which is the highest and sometimes the fastest capture if one neglects salvage effects described by Bredehoeft et al. (1982) or aquifer leakage (Christensen et al., 2010).
2. Watersheds have multiple wells, and while estimates for an individual well may be biased, errors of different signs tend to balance each other. This is often apparent when runoff observations are available (Traylor and Zlotnik, 2016; Foglia et al., 2013).
3. The approach has broad merit in the initial phases of designing GW management strategy to identify broad areas of potentially feasible projects and to convey information on the scope of potential projects and expected outcomes. Addressing heterogeneity and (or) uncertainty of parameters in GWSWIs should be addressed by numerical modeling at subsequent stages.

Of practical interest is a capture from each SW body for a given year. Leake et al. (2010) proposed a convenient method for generating maps of capture for each year of interest since the development. For any given year, a ratio of capture-to-pumping rate is calculated for each well or location associated with a SW body of interest. Such a ratio ranges between 0 (absence of capture) and 1 (pumping rate is fully based on stream depletion). This ratio can be mapped for each year and each SW body involved in GWSWIs, as it was successfully developed and applied for both analytical and numerical methods (COHYST Technical Committee, 2004; Leake et al., 2010, respectively).

In adjudication of water rights or meeting certain constraints (e.g., on capture or on streamflow requirements), there are two approaches. For simple systems with few wells, a trial-and-error technique can be used for conjunctive water resources management. For multiple wells and stream reaches, however, a simulation–optimization technique might be more appropriate due to complexities in finding optimal solutions according to some criteria. An analytical or numerical simulation model is combined with a mathematical optimization technique, which allows identification of well locations and pumping schedules that best meet management objectives and constraints. The simulation model accounts for hydraulics of the stream–aquifer system under a given management scenario, whereas the optimization model allows for defining the best management strategy among possible scenarios. Some of these aspects are described by Barlow and Leake (2012), but the subject of water resources management is beyond the scope of this chapter.

9.2.3 Stream-Stage Fluctuations and Baseflow Generation

An important problem of GWSWIs is determining the streambed and aquifer parameters. Because many pumping experiments last from hours to months and require substantial effort in data collection, a possible alternative is offered by the variability of the stream stage and resulting propagation of head changes into the aquifer. Changes in recharge or transient boundary conditions may result in baseflow changes. Analyses of these perturbations in various locations may yield information both on bulk aquifer properties and their heterogeneity. There are four different types of such studies that do not involve pumping: (1) assessment of bank storage effects, (2) baseflow analyses, (3) river tomography, and (4) recharge from ephemeral streams.

9.2.3.1 Assessment of Bank Storage Effects

In conditions that are undisturbed by pumping, stream-stage fluctuations are sources of perturbations in the GW regime. Unlike analyses of pumping wells near streams, these fluctuations can be treated as 1D, at distances on the order of the aquifer thickness away from the streambed. The pioneering study by Ferris (1951) estimated well response to the cyclic stream-stage hydrograph. Then, Stallman (1962) developed a solution for wellhead response $h(d, t)$ to a sudden change of stream stage s_0 from an initial head h_i as follows:

$$h(d,t) = h_i + s_0 erfc\left(\frac{1}{2t_d^{1/2}}\right) \tag{9.11}$$

similar to Equation 9.4, where t_A is equivalent to sdf (see Equation 9.3). Typically, such perturbations operate at timescales from hours to months and propagate into the aquifer perpendicular to the stream channel. To be detectable or comparable to s_0, changes at a characteristic length scale d from the stream to observation points/wells are detected by piezometric variations, which can then be assessed at times $t_d < 1$, or $t < t_A = Sd^2/T$ after perturbation. This technique is often used because of minimal needs for data collection, namely, only drawdown responses $h(d, t)$ in a piezometer s.

To estimate stream-stage function as a function of time $h_0(t)$, well response can be obtained by a convolution integral (see Barlow and Moench, 1999) as follows:

$$h(d,t) = \int_0^t \frac{dh_0(\tau)}{d\tau} erfc\left(\frac{d}{2\sqrt{D(t-\tau)}}\right) d\tau \tag{9.12}$$

Barlow and Moench (1999), Moench and Barlow (2000), and Barlow et al. (2000) also provided a detailed summary of studies addressing the following aspects: temporal form of the stream stage; numerical convolution techniques; specifics of confined, unconfined, and leaky aquifer types; effect of nonlinearity in GW flow; comparison of 1D and 2D approximations of GW equations; and examples of field applications. The least developed aspect of these models was partial stream penetration: accuracy of solutions is low at distances on the order of aquifer thicknesses b (e.g., Luther and Haitjema, 2000) due to violations of Dupuit– Forchheimer assumptions. This issue was partially addressed analytically by Zlotnik and Huang (1999) using the Grigoryev (1957) streambed model that presents the well response function to a sudden change of stream stage s_0 as follows:

$$h(d,t) = h_i + s_0\left[erfc\left(\frac{1}{2\sqrt{t_d}}\right) - e^{t_d v^2 + v} erfc\left(\frac{1}{2\sqrt{t_d}} + v\sqrt{t_d}\right)\right], \quad v = \frac{d}{B_S} \tag{9.13}$$

where B_S is defined by Equation 9.8 in general and by Equation 9.9 for small stream widths. Later, Chen and Chen (2003) investigated effects of various assumptions numerically using examples of similar geometry.

9.2.3.2 Baseflow Generation

Baseflow evaluation remains an important part of GWSWI studies and one of the fundamental issues in modern hydrology (Brutsaert, 2005). Unlike stage-initiated perturbations, baseflow variations may be triggered by water table perturbations (e.g., associated with infiltration from storm runoff), which result in GW outflow changes. Baseflow variation and baseflow rate Q_{bf} can be described by various simplified stream–aquifer models that in general obey the relationship

$$\frac{dQ_{bf}}{dt} = -aQ_{bf}^b, \quad Q_{bf}(0) = Q_{bf}^0 \tag{9.14}$$

where

Q_{bf}^0 is the initial flow rate

a is the aquifer characteristic (reflecting hydraulic conductivity, thickness, storage properties)

b is a constant ranging from 1 to 3 (Brutsaert and Nieber, 1977) for a variety of reasons

For $b = 1$, the equation represents exponential flow rate decay. Much effort has been spent on identifying b in field studies for interpretation of baseflow stages (e.g., Szilagyi, 2003; Chen et al., 2006); however, uncertainty remains in the appropriate selection among a variety of simple models (Brutsaert, 2005). The hope is that this approach can be used for parameter identification from readily available stream runoff observations.

9.2.3.3 Stream Tomography

Tomographic surveys (Yeh et al., 2008b) are a relatively new approach designed for delineation of aquifer heterogeneity. Such surveys of the subsurface use well-defined natural (e.g., stream stage, earthquakes, tides) or artificial (e.g., injections of water or air) hydraulic head perturbations at different locations. After each perturbation, responses of a certain parameter in the subsurface are collected at a large number of locations. An inverse model then synthesizes all the responses to generate a 3D model of the distribution of hydraulic parameters in the subsurface. These surveys produce more detailed information about the subsurface than the more traditional model. Yeh et al. (2009) suggested combining the multiple data sets of accurately defined spatial and temporal stream-stage fluctuations and related sets of aquifer head responses. In contrast to the previously discussed 1D analytical methods, this approach explicitly requires a 2D or 3D framework. For example, Sophocleous (1991) and Yeh et al. (2009) used 2D models and considered flood routing, while Rötting et al. (2006) considered 3D but without routing modeling. In both of the latter cases, the stream–aquifer interface was treated by the Grigoryev (1957) model. Rötting et al. (2006) and Yeh et al. (2008a) utilized geostatistical inversion, while Sophocleous (1991) relied on sensitivity analyses. Both Sophocleous (1991) and Rötting et al. (2006) relied heavily on available stratigraphic data, while Yeh et al. (2008a) worked with a synthetic aquifer. Apparently, the development of dense monitoring networks, advancements in inversion techniques, and fusing data from geophysical techniques has substantial promise for applications. For example, Rötting et al. (2006) supplemented data from stream-stage analyses with pump test data that supplied additional information for effective inversion.

9.2.3.4 Ephemeral Streams

If direct hydraulic connection between stream and aquifer is absent along a stream reach, this reach can provide recharge to the aquifer and is a major source of GW in arid regions of the world (Shanafield and Cook, 2014). They identified seven methods for quantifying ephemeral and intermittent stream infiltration to the aquifer: (1) controlled infiltration experiments, (2) monitoring changes in water content, (3) heat as a tracer of infiltration, (4) reach length water balances, (5) flood wave front tracking, (6) GW mounding, and (7) GW dating. Detailed analyses of temporal and spatial scales and the advantages and limitations of each method were illustrated with examples from the literature. As is common, appropriate uses of each field method can be enhanced using multimethod approaches, avoiding the potential drawbacks inherent in any single method. Important challenges, however, still remain. These include parameter uncertainty, long-term data collection and processes, role of riparian vegetation, and matching transmission losses and infiltration estimates with actual aquifer recharge. Numerical modeling of such streams is briefly addressed in Section 9.7.

9.2.4 Lake–Aquifer Interactions and Flow Regime Identification

9.2.4.1 Definitions

Most of the concepts and terminology particular to the study of SW-GW systems have evolved through attempts to describe and classify steady-state GW flow systems near lakes. Lake–aquifer interactions are inherently 3D and transient. The best-known lake classification (Born et al., 1977) identifies lakes as recharge, discharge, or flow-through, depending on the distribution and direction of flow across the lakebed with respect to the aquifer. Field methods of seepage across the lakebed are described in Section 9.6. However, lake classifications generally compare net inflow with net outflow from the lake. Recharge lakes lose water across their entire lakebed and recharge the aquifer; discharge lakes gain GW across their entire lakebed and discharge the aquifer. Flow-through lakes lose water over part of their lakebed and gain water over the other parts; at any instant, a flow-through lake can be a source or sink for GW, depending on the net balance between GW inflow to the lake and lake water outflow to the aquifer. This approach also applies to playas (Rosen, 1994). Transient conditions may alter lake regimes. To address complexity, theoretical analyses of such systems have tended to assume steady-state frameworks for lake–aquifer systems (Townley and Trefry, 2000; Smith and Townley, 2002).

9.2.4.2 Water Table Configuration Effects

For classification of steady-state flow regimes of lakes, the geometry of their GW flow nets can be used. These nets identify dividing streamlines, delineating zones of GWSWI in 2D as local-, intermediate-, and regional-scale GW flow systems. This approach originated from a hypothetical closed 2D GW basin in a vertical cross section (Tóth, 1963). Local systems are shallow, small-scale flows that occur between adjacent water table highs and lows (e.g., between a lake and adjacent water table mound or depression). Intermediate-scale systems are typically deeper, consisting of flow lines that extend over several high and low water tables. Regional systems extend over the full length of the basin near bedrock and along boundaries, and a flow model shows the distribution of stagnation points on the flow net. Winter (1978, 1999) explicitly applied this steady-state approach to lake systems in 2D and 3D. A 3D example of a discharge lake with a complex flow net is shown in Figure 9.4. The fundamental assumption was made that the water table is a replica of the land surface and the lake is merely an element of the GW system. Several studies, however, have shown that there are limitations to this concept (Winter, 1986; Haitjema and Mitchel-Bruker, 2005; Gleeson and Manning, 2008), indicating more nuanced relationships between GW recharge and terrain parameters.

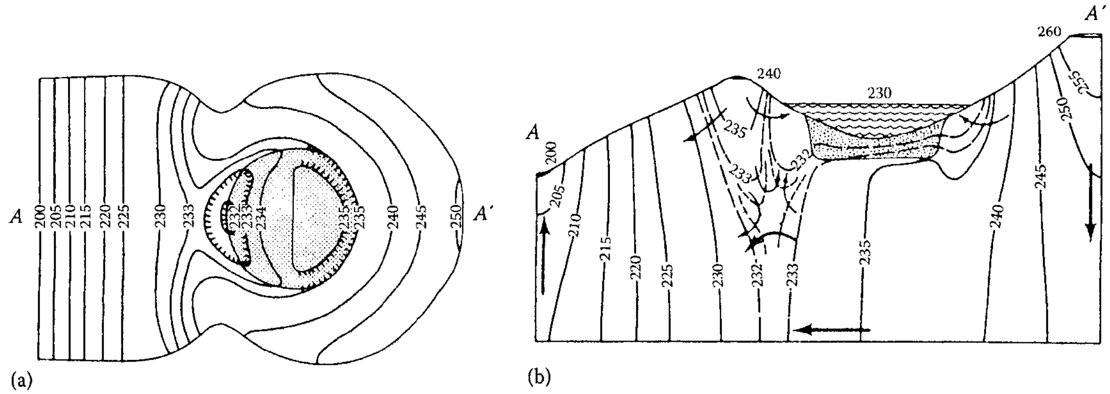

FIGURE 9.4 Steady-state 3D flow near lake with permeable lakebed: (a) plan view of a circular lake with areas of upward fluxes and (b) vertical cross section. (Modified after Winter, T.C., *Water Resour. Res.*, 14(2), 245, 1978.)

9.2.4.3 Water Budget Approach

In variance with classic approaches, Townley and Trefry (2000, see also references therein) did not explicitly use water table configuration. They singled out a shallow lake of radius a in a regional system (Figure 9.5a) in a uniform, box-shaped aquifer of known width (W), length (L), and thickness (b) with hydraulic conductivity (K_h and K_z in horizontal and vertical directions, respectively).

Instead of using water table data, they assumed that the GW flow rates upgradient and downgradient from the lake (U_- and U_+, respectively) are known, together with fluxes at all other facets of the box, including GW recharge (R) on the upper boundary and differences between evaporation (E) and precipitation (P) on the lake surface. At high resolution, a finite-difference method for computing head distribution and particle tracking allowed for delineation of capture and discharge zones in 3D (Figure 9.5b). Using a steady-state model, Smith and Townley (2002) and Townley and Trefry (2000) developed an approach for the identification of discharge, recharge, and flow-through regimes for various combinations of lake–aquifer parameters and illustrated the corresponding flow patterns in the vertical plane of symmetry in a 3D flow field, defined by dimensionless parameters $(RL)/(U_+ b)$, (U_+/U_-), and lake diameter/aquifer thickness ratio a/b.

Important characteristics of GWSWIs for lakes included seepage magnitude along the lake circumference, role of regional aquifer setting, lakebed resistance, aquifer anisotropy, lake elongation, and transient GW flow. Their results are briefly outlined below.

Seepage along the lake edge: McBride and Pfannkuch (1975) and Pfannkuch and Winter (1984) showed high fluxes near the lake shore using 2D models, but some 3D details were missing. High-resolution computations by Townley and Trefry (2000) clearly illustrated the 3D nature of seepage along the lake shore in a typical case of a flow-through system (Figure 9.6). The magnitude of vertical fluxes along the circumference of the lake varies, being largest (V_z^{max}) near the upstream and downstream margins, but opposite in sign, and varying between positive and negative extremes with zero fluxes at intermediate points on the shore. Only adequate grid resolution can address flux distribution numerically (see Genereux and Bandopadhyay, 2001; Bakker and Anderson, 2002).

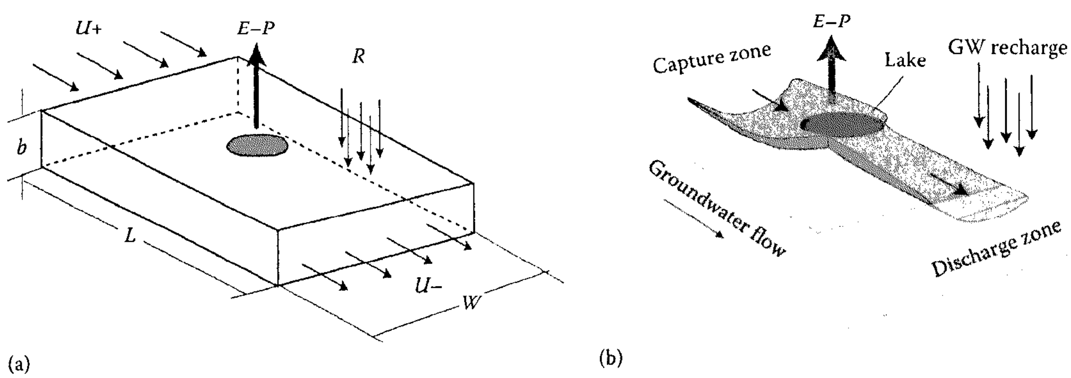

FIGURE 9.5 Shallow lake of radius a, embedded in a box-shaped aquifer: (a) upgradient and downgradient GW flow rates (U_+ and U_-, respectively), GW recharge R, and lake water budget (E–P); (b) upstream capture zone and downstream discharge zone. (Modified after Townley, L.R. and Trefry, M.G., *Water Resour. Res.*, 36(4), 935, 2000.)

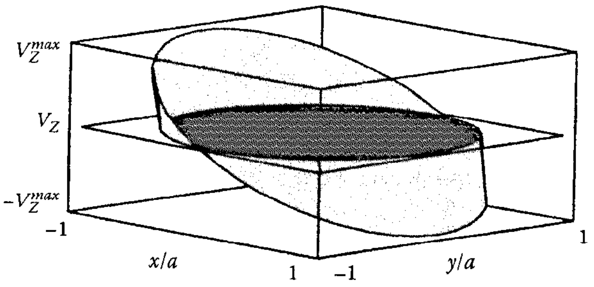

FIGURE 9.6 Schematic depiction of the flux magnitude along the circular lake circumference. Horizontal lake surface is shown in black and the flux magnitude and direction in different points are shown by the height of the gray cylindrical surface. (Modified after Townley, L.R. and Trefry, M.G., *Water Resour. Res.*, 36(4), 935, 2000.)

Regional aquifer setting is important for analyses of interactions between a single shallow lake and the regional aquifer system (Smith and Townley, 2002). In general, lakes positioned downgradient in a closed GW basin have stronger components of GW inflow (Cheng and Anderson, 1994).

Lakebed resistance, aquifer anisotropy, and lake elongation are important for constraining the flux distribution across the lakebed (Nield et al., 1994) because increased sediment resistance, anisotropy (K_r/K_z), and a/b ratios shift stagnation points downward. Decreased lakebed resistance and K_r/K_z, as well as increased length compared to the aquifer thickness, favors flow-through regimes.

Transient regimes result from (1) GW flow response to transient recharge and boundary conditions at the watershed and (2) lake response to climatic forcing. In such cases, the developing flow regimes must be described by streaklines instead of streamlines (Bear, 1972). Numerical modeling by Anderson and Munter (1981) and Townley (2015) indicates that shifts between flow-through and other regimes may be rapid.

9.2.4.4 Consideration of Water Table and Water Budget Properties

It should be noted that the water table, required by classic models (e.g., Winter, 1978), is a more easily measured aquifer property than the upstream and downstream GW flow rates needed for models based exclusively on water budget (e.g., Townley and Trefry, 2000). The reason is due to noise in water table data (or any other piezometric data), which is strongly amplified in spatial derivatives needed for estimating upstream and downstream GW discharge and especially for comparison of U_- and U_+. A combined approach can utilize the water table as a GW flow and lake–aquifer exchange driver and take into account the water budget for an individual lake. Zlotnik et al. (2009) considered a conceptual steady-state model of a shallow lake embedded in an unconfined aquifer (Figure 9.7a) and suggested that flow-through regimes develop when regional GW flow exceeds capture of water by the lake, resulting from lower water level compared to the regional water table. A robust criterion for distinguishing flow-through and discharge regimes is based on a dimensionless gradient ratio $G = i/(H/a)$, where i is the regional head gradient or slope of the regional piezometric surface, a is the lake radius, and H is an offset between the lake center and regional water table. This offset is a product of regional water table topography and hydrological conditions. (In arid conditions, this offset is positive, but in humid conditions, H will have an opposite sign.)

If G exceeds some critical value G_c, which is a function of dimensionless aquifer thickness $\bar{b} = b(K_r/K_z)^{1/2}/a$, the flow-through regime is present. In this case, captured ambient flow overwhelms the evaporative losses that operate as a pumping from a shallow, large-diameter well. Otherwise, all captured ambient GW is balanced by evaporation. This criterion indicates that the decrease in anisotropy and (or) aquifer thickness and (or) increase in lake radius facilitates the existence of flow-through regimes (Zlotnik et al., 2009), which is consistent with the findings of Nield et al. (1994), but emphasizes the role of the water table configuration.

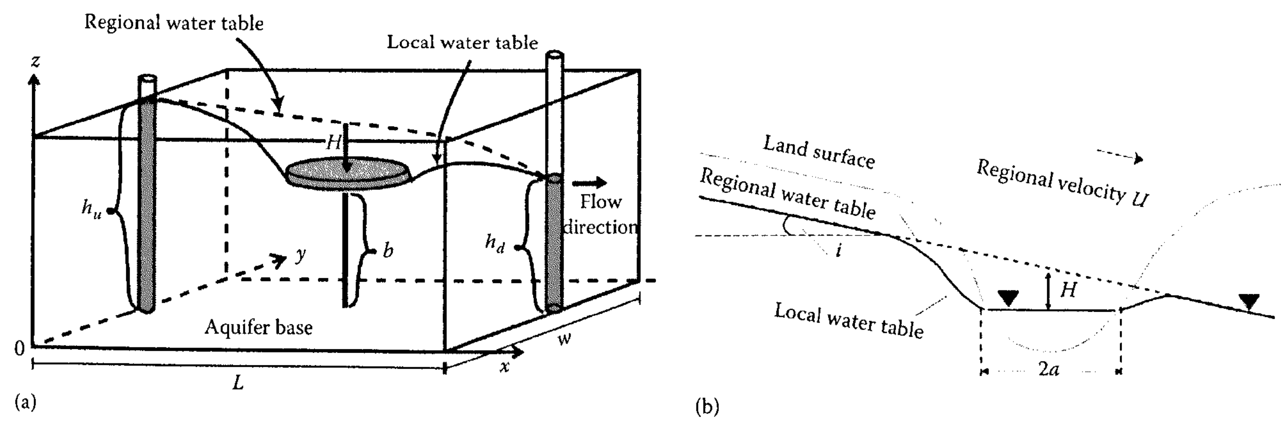

FIGURE 9.7 GWSWI between lake and unconfined aquifer: (a) aquifer, water table, and lake geometry; here $h_u > h_d$ and (b) parameters for calculating the gradient ratio G. (Modified after Zlotnik, V.A. et al., *J. Hydrol.*, 371, 22, 2009.)

9.2.4.5 Applications of Lake Classifications

Transient recharge and boundary conditions, heterogeneity, water table topography, lake bathymetry, and other factors have strong influences on the magnitude and direction of water fluxes. Field methods of determining local water fluxes are elucidated in Section 9.6. Hydraulics of lakes at watershed scales is commonly addressed using modeling of piezometric heads only (Anderson and Munter, 1981; Cheng and Anderson, 1994). For example, Smerdon et al. (2007) presented a study including detailed system characterization, long-term observations, with consideration of geology and local climate, and modeling including calibration. This study, conducted at the scale of several km^2, utilized an integrated watershed model involving the vadose zone, land surface hydrology, GW, and lake. The high-resolution model (243,000 subsurface prism elements) showed GW flux distribution over the lakebed consistent with Winter (1978) patterns, similar to Figure 9.4a.

Starting from Krabbenhoft et al. (1990a,b), lake studies supplement modeling with geochemical methods (e.g., Hunt et al., 2005). Turner and Townley (2006) applied water budget approach to classification of lakes in Perth, Australia, explicitly, following the approach by Townley and Trefry (2000). With developments in geophysics, lake classification studies combining the water table and water budget analyses can use electrical resistivity and electromagnetic methods. For example, Ong et al. (2010) and Befus et al. (2012) applied geophysical methods explicitly for lakes in western Nebraska, United States.

9.3 Hyporheic Zone

9.3.1 Definitions

The term "hyporheos" was coined by Orghidan (1959) to describe the organisms living in pore spaces formed within the mixture of coarse sand, gravel, and rocks in the shallow subsurface near streams and rivers. Hyporheos originates from the root words "hypo" (meaning below) and "rheos" (meaning flow), literally describing the areas below and adjacent to flowing water bodies (Orghidan, 1959). Since this first appearance in the literature, the HZ has been more broadly defined based on a host of physical, chemical, and biological metrics.

Biological and ecological definitions have focused on the presence or activity of biological organisms (Stanford and Ward, 1988, 1999, 1993) or the presence of a dynamic subsurface ecotone (Gilbert et al., 1990; Vervier et al., 1992; Boulton et al., 1998). Physically based definitions include the saturated sediments beneath or adjacent to a stream (Valett et al., 1990; White, 1993; Winter et al., 1998; Findlay and Sobczak, 2000) or the area in the subsurface affected by flowpaths of SW returning to the stream (Valett et al., 1993; Findlay, 1995; Harvey et al., 1996; Wroblicky et al., 1998; Wondzell and Swanson, 1999; Harvey and Wagner, 2000; Woessner, 2000; Storey et al., 2003). Chemically based definitions focus on the mixing percentage of SW versus GW in subsurface flowpaths, with 10% or more SW typically being considered the lower threshold for hyporheic flow (Triska et al., 1989; Wondzell and Swanson, 1996).

Hydrologists typically define HZ flow as SW entering subsurface flowpaths that return to the stream, thereby crossing the streambed interface more than once. In contrast, GW fluxes are generally envisioned as crossing the interface only once (either discharging from subsurface to stream or recharging from stream to subsurface). Also, GW fluxes may originate in areas other than the stream (e.g., recharge of precipitation on uplands). These distinctions between HZ and GW fluxes may depend on spatial and temporal variability of the HZ and may be affected by the length of the stream reach under consideration, which may introduce difficulties in establishing a rigid definition of the HZ. Harvey and Bencala (1993) used a mass balance approach to distinguish HZ fluxes within a reach from GW exchanging with areas outside the study reach. Still, even with a precise definition, very long hyporheic flowpaths that leave the stream in one reach and return to the stream in another reach could be difficult to distinguish from GW fluxes. Larkin and Sharp (1992) used both flowpath length and timescale to distinguish the HZ from larger-scale and longer-term interactions of GWSWIs. Proposed definitions including a temporal scale have included the GW volume hydraulically interactive with the channel over timescales on the order of hours (Stanford and Ward, 1993) and days (Wroblicky et al., 1998).

Following Brunke and Gonser (1997), we suggest the following definition: the HZ (1) is in the subsurface, (2) near a stream, (3) influenced by SW, (4) including water flowpaths that return to SW, and (5) within a temporal and spatial scale relevant to the process of interest and fluvial structure. This definition notably encompasses spatial and temporal variability by suggesting the HZ may be differently defined for varied scales or processes of interest.

9.3.2 HZ as Part of a Nested Hierarchy of Hydrological Systems

HZs are one part of the interconnected elements of a hydrological landscape (Winter et al., 1998). In contrast to the view of hydrological elements as individual, isolated elements (e.g., GW, streams, lakes), the perspective of hydrological landscapes considers a continuum of interacting hydrological elements. The HZ, then, exists at the interface between the flowing SW and GW as part of this hydrological landscape. HZs are nested within the landscape with controls and processes spanning several spatial and temporal scales.

Hyporheic exchange is scale dependent. Therefore, a hierarchical approach allows the study of a process of interest at a scale of interest, while recognizing that other processes are operating concurrently at other scales. Given the physical controls of hyporheic exchange, natural break points may exist between scales of interest (Dent et al., 2001), which may align with geological or geomorphological hierarchies (Valett et al., 1997). Theoretical (Tóth, 1963) and empirical (Dahm et al., 1998; Fisher et al., 1998) results identify generally local, intermediate, and regional scales of GWSWIs. Indeed, any hierarchal classification of hyporheic exchange must fit within existing, well-established systems of geomorphic (increasing stream size) and hydrologic (flowpath length) concepts (Stanley and Jones, 2000).

Specific to hyporheic exchange, a small number of hierarchal relationships have been put forth for consideration. Hyporheic corridor concept by Stanford and Ward (1993) links spatial relationships between chemical, physical, and biological characteristics attributed to the HZ, loosely linking these to yet another hierarchy, Strahler stream order. Subsequently, Dent et al. (2001) proposed a hierarchy well linked to existing concepts, which includes five levels (from largest to smallest spatial scale): segment, reach, channel unit, channel subunit, and particle. Indeed, recent reviews consider the drivers of hyporheic exchange across these spatial scales (Kaser et al., 2009; Wondzell and Gooseff, 2013; Boano et al., 2014). Gomez-Velez and Harvey (2014) proposed a scaling of hyporheic flow through river networks based on how physical features of channel evolve in the downstream direction. The scaling of downstream hydraulic geometry and the downstream fining of sediments and their effects on the hydraulic properties of the surrounding aquifers determine how hyporheic exchange varies from low- to higher-order streams.

9.3.3 Functions of HZs in the Aquatic Systems

9.3.3.1 Interactions of the Physical, Chemical, and Biological Systems

The HZ provides a host of functions to the stream ecosystem. A key review of hyporheic functions has been written by Brunke and Gonser (1997), Boulton et al. (1998), Sophocleous (2002), Krause et al. (2011), and Merill and Tonjes (2014). These functions are the characteristic of the physical, chemical, and biological systems that interact and cooperate in the environment (Figure 9.8).

They vary widely in their study, scales, drivers, and ability to parse one from the others. It is the specific combination of physical, chemical, and biological systems that give rise to the HZ as a unique landscape element. The ecological importance of hyporheic exchange primarily arises from the combination of rapid reaction rates with exchange flux or the intersection of processes and transport (Vidon et al., 2010). This perspective is parallel to that widely used in the study of wetlands, where wetlands are defined by their unique combination of physical, chemical, and biological conditions. Indeed, the interaction of the physical, biological, and chemical systems is necessary to sustain any hyporheic function (Boulton et al., 1998; Battin et al., 2008; Pinay et al., 2009).

9.3.3.2 Physical Functions

The physical system sets the initial template upon which hyporheic exchange may occur (Battin, 1999, 2000; Ward et al., 2011); that is, physical transport is a convenient starting point for the analysis of the hyporheic system, with feedbacks and feedforwards with chemical and biological systems inferred from these initial conditions. We acknowledge that the physical system is intimately linked to other systems at other scales; for example, a newly fallen tree (biological system, in a broader context) may cause stream water to pool, creating a newly enhanced head gradient and new flowpaths. Still, the physical transport along hyporheic flowpaths is the basis of mixing of SW and GW in this interface.

Harvey and Wagner (2000) note that one key function of hyporheic exchange, as a physical process, is in keeping SW in close contact with the biogeochemically reactive subsurface.

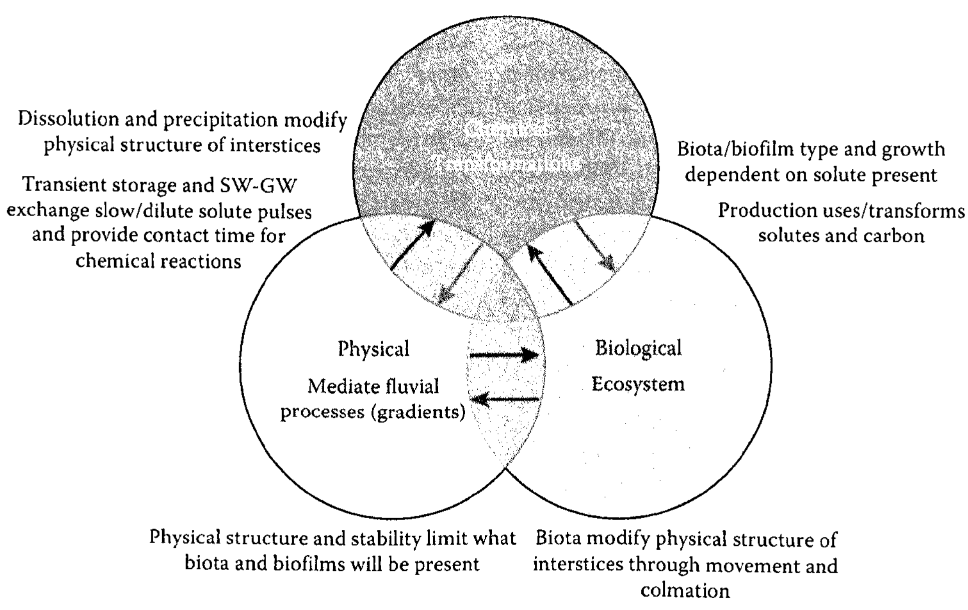

FIGURE 9.8 The interaction of physical, chemical, and biological systems in the HZ gives rise to a host of ecological functions and ecosystem processes.

The key physical function of the HZ is the regulation of energy and material fluxes and residence times at scales ranging from individual flowpaths to stream reaches. Commonly, studies of the HZ have focused on transit time distributions at the reach scale, where exchange of water happens between the advection-dominated main channel and slower-moving domains, including in-stream dead zones and HZs. In these slower-moving domains, water from the stream channel has extended contact time with biogeochemically active HZs.

Hyporheic exchange flux, in turn, regulates the transport of water, energy, and materials (e.g., organic carbon) between the stream and subsurface. As water flows along hyporheic flowpaths, hydrogeologic properties (i.e., hydraulic conductivity, porosity, tortuosity) and hydraulic drivers (i.e., hydraulic gradient) control the residence time of water along hyporhehic flowpaths. Contact time with hyporheic sediment, and the delivery of limiting reagents from the stream to the subsurface, gives rise to a host of chemical and biological functions described in the subsequent sections. Finally, hyporheic hydraulics control the flushing of products from the HZ to the stream.

While the discussion earlier is focused primarily on water and the transport of dissolved species, HZs also regulate the exchange of thermal energy between the stream and subsurface. Arrigoni et al. (2008) describe hyporheic interactions as buffering, lagging, or cooling stream waters (i.e., adjusting the mean value, phase, or amplitude of temperature differences between the cool subsurface and SW). Indeed, thermal processes in the stream have key linkages to biological functions, where cool hyporheic water provides a permanent and temporary habitat used by a host of species, as discussed further in Section 9.3.3.4. Finally, HZs provide physical filtration of stream water (Brunke, 1999).

9.3.3.3 Chemical Functions

The chemical system mediates both chemical and biogeochemical functions of the HZ and is a source of some of the most critical ecosystem functions provided by hyporheic exchange (e.g., sequestration of heavy metals, denitrification). The chemical system transforms fluxes of materials from both SW and GW as it is transported across gradients of physical and chemical conditions (e.g., temperature, redox, pH; Triska et al. (1989)). While the physical system controls the fluxes of water into and along HZs, the chemical system transforms these material fluxes. HZs may be important locations of mineral dissolution or precipitation based on chemical conditions and mineral composition.

Many HZ functions are primarily attributed to the substantial contact time between SW and the biogeochemically active subsurface, where microbial activity is key to mediating chemical processes in the subsurface. Solutes are generally retained initially by physical and chemical transient storage, while biotic uptake dominates the process of retention at longer timescales (Bencala et al., 1984; McDowell, 1985; Triska et al., 1989; Kim et al., 1992). Microbial processes contribute to the chemical function of the HZ, but note that it is, indeed, the unique interaction of chemical and biological spheres that enables these microbial communities to exist and give rise to these functions. For example, HZs are a key source of reach-scale stream respiration, processing both natural and anthropogenically sourced organic matter. Redox gradients generated from microbial respiration drive a host of other reactions, including denitrification. The aerobic–anaerobic transition between the stream and subsurface has also been documented to retain heavy metals (Gandy et al., 2007).

In addition to biogeochemical processes, the chemical system has a direct impact on both physical and biological systems. Physically, the chemical system controls weathering of hyporheic minerals or active porosity. Biologically, the chemical system mediates chemical conditions necessary to support life (e.g., upwelling of cool, well-oxygenated water for spawning habitat, cycling of nutrients that control primary production).

9.3.3.4 Biological Functions

The HZ contributes to both primary and secondary production in the stream ecosystem. Primary production includes a microbial community in the stream and on the streambed. As noted in Section 9.3.3.3, microbial communities catalyze an array of biogeochemical processes integral to carbon fluxes and nutrient cycling in sediments of aquatic ecosystems (Chapelle, 1992). Biofilms may temporarily buffer embedded bacteria from fluctuating resource supply. Notably, physical characteristics govern the surface area for biofilm formation and greatly influence both resource availability and predation pressure to biofilms (Findlay and Sobczak, 2000). At larger scales, HZs support primary production in the stream channel. Upwelling water can be enriched in nutrients by storage and mineralization. This hyporheic delivery can increase algal standing crop and shorten recovery times after disturbance and thus enhance the resilience of primary producers (Valett et al., 1994). Exchange with subsurface zones can affect primary production in the stream, mainly due to enhanced nutrient concentrations at upwelling and outwelling zones (Dent et al., 2000, Chapter 16). Secondary production in the stream is also supported by hyporheic exchange. Hyporheic invertebrates are prey for fish and generate nutrients for in-stream and riparian production (Boulton, 2007). Additionally, the grazing consumers in the stream may benefit from this supplementation, and hence upwelling exerts a control on secondary production (Ward, 1989).

Additionally, the HZ was initially studied as a unique ecosystem existing between the SW and GW, supporting a complex food web. Hyporheic organisms are abundant in the HZ, with at least some species uniquely adapted to commonly low oxygen levels (Hakenkamp and Palmer, 2000). These organisms provide a link between the microbial community (where they act as predators) and the macroinvertebrate and higher trophic levels (where they are prey). The presence of these meiofauna may interact with rates of microbial processes by enhancing the availability of limited resources in the subsurface. At the next highest trophic level, a class of macroinvertebrates exist, which are uniquely adapted to spend a majority of or their life in the HZ.

Finally, HZs provide a temporary habitat for organisms that primarily exist in the stream. Some insects may use HZ as a refuge against strong currents (shear stress) and extreme temperatures (during winter ice formation on the stream bottom and physiologically dangerous surface temperatures in summer) and offer stable substrates during bedload movement. The HZ also provides predictable conditions for the development of fish embryos, for the immobile life stages of insects (Pugsley and Hynes, 1986). Furthermore, the HZ may provide protection from large predators (Brunke and Gonser, 1997) or even anthropogenically induced toxic pulses (Jeffrey et al., 1986).

9.3.4 Controlling the HZ Functions

The physical, chemical, and biological functions of HZs are critical to healthy stream ecosystems. The U.S. Army Corps of Engineers and the U.S. Environmental Protection Agency have issued new guidance for the regulation of the waters of the United States (Department of Defense and Environmental Protection Agency, 2014). In particular, the near-stream environment, including HZs, riparian zones, and wetlands, may now be regulated under the Clean Water Act due to their clear relationship with the physical, chemical, and biological integrity of traditionally regulated waters.

Interest in the restoration of ecosystem functions, particularly via stream restoration, is growing rapidly (e.g., Bernhardt et al., 2005). A number of recent studies suggest hyporheic restoration as a path forward for promoting healthy stream ecosystems (e.g., Bernhardt and Palmer, 2007; Boulton, 2007; Boulton et al., 2010; Hester and Gooseff, 2010, 2011; Krause et al., 2011; Ward et al., 2011; Merill and Tonjes, 2014). With a widespread interest in hyporheic restoration, there are few studies comparing the performance of natural and artificial structures in terms of ecosystem benefits, including Lautz and Fanelli (2008), Daniluk et al. (2013), and Gordon et al. (2013). In conclusion, restoration of hyporheic exchange may be possible, if the objectives and relevant timescales are clearly defined and structures are engineered for this purpose (Ward et al., 2011).

9.4 Chemical Interactions between GW and SW

Water fluxes across interfaces and chemical interactions between GW and SW interactions have been characterized using models of various levels of sophistication, ranging from simple water mass balance models (e.g., Krabbenhoft et al., 1990b) to fully dynamic implementations of the advection–dispersion equation with time-varying hydrologic and chemical inputs and complex reaction expressions (e.g, Runkel et al., 1996a,b; 1999). Simple approaches are illustrated here that are widely applicable to any SW body in contact with saturated permeable sediments where water budgets can be constructed. Mass balance approaches are a practical means for quantifying water and solute mass fluxes across the GW-SW interface that are difficult to measure over large areas.

The mass balance approach relies on the rapid mixing in SW compared to GW. As a result, SW tends to integrate the physical and chemical signatures that can be used to quantify GWSWIs. The wide availability of existing SW data and generally easier data collection compared with GW are also the benefits of constructing mass balances around a SW control volume. In addition to the principal use of the mass balance to quantify GW and SW exchange fluxes, this method can be used for quantifying chemical reactions in the waters being exchanged across the sediment interface. Streams provide the most ubiquitous examples; however, the equations are general and can easily be applied wherever a hydraulic connection to GW exists (rivers, wetlands, lakes, or estuaries). This section provides fundamentals of chemical GWSW interactions, and field applications are relegated to Section 9.6.

9.4.1 Water and Chemical Mass Balance near Interface

Streams interact with surrounding aquifers in three principal ways: they may receive GW discharge, or they may recharge the GW system, or they may interact by both receiving GW discharge and recharging the aquifer simultaneously in different areas of the stream (Winter et al., 1998). The water balance for a stream can be expressed in terms of the rate of change in SW storage in a stream, which is defined as the sum of the inflow rates minus the outflow rates in a given stream reach

$$\frac{dV}{dt} = Q(0,t) + Q_{gw}^{in} + Q_{hz}^{in} - Q(L,t) - Q_{gw}^{out} - Q_{hz}^{out} \tag{9.15}$$

where

t is the time [T]
x is the distance [L] along the reach's centerline with $x = 0$ upstream and $x = L$ downstream
L is the length of stream reach over which exchange fluxes are averaged
V is the volume of stream water [L^3]
$Q(x, t)$ is stream volumetric discharge at a distance x [L^3T^{-1}]
Q_{gw} and Q_{hz} are GW volumetric flux and hyporheic volumetric flux [L^3T^{-1}], respectively, which are assumed not to vary spatially

Superscripts on GW and hyporheic fluxes designate the discharge components, *into*, and the recharge components, *out of*, respectively, the stream reach. GW discharge and recharge fluxes per unit area of streambed [LT^{-1}] are easily calculated by dividing total fluxes by the product of reach length and the average stream width. Only surface–subsurface exchange fluxes are considered here. However, other exchange fluxes could be added to equations to distinguish tributaries, springs, seeps, etc. Precipitation and evapotranspiration fluxes are generally neglected in stream mass balances because of small surface area and short water residence times; however, these fluxes are easily included for wetland and lake mass balances.

For practical applications, Equation 9.15 is often simplified by assuming that flow in the stream is steady or nearly so, which eliminates the storage term, that is, $dV/dt \cong 0$, and constrains the accuracy of a mass balance by field measurements of streamflow. Surface flows are typically measured by a combination of velocity gaging and solute tracer-dilution techniques, leaving the more difficult to measure GW exchange fluxes to be solved for by difference. Note that Equation 9.15 has too many subsurface fluxes to solve for individual subsurface components by difference. The equation can be simplified by assuming that the stream reach is long enough to encompass many small hyporheic flowpaths that enter and leave (Figure 9.9), with the net effect being zero during steady flow, that is, $Q_{hz}^{in} - Q_{hz}^{out} = 0$, such that, at steady state

$$0 = Q(0) + Q_{gw}^{in} - Q(L) - Q_{gw}^{out} \tag{9.16}$$

Rearrangement of Equation 9.16 defines a *net* GW exchange in the stream reach

$$Q_{gw}^{net} = Q(L) - Q(0) = Q_{gw}^{in} - Q_{gw}^{out} \tag{9.17}$$

Equation 9.17 is the basis of a commonly used technique referred to as "differential stream gaging" or sometimes known simply as "seepage run" (Riggs, 1972). In essence, the technique uses differences in streamflow to quantify SWGI. It can be confusing that differential gaging does not actually estimate magnitudes of GW discharge and recharge because there is only enough information to solve the mass balance equation for the difference between discharge and recharge in streams. Differential stream gaging has sometimes been incorrectly used to estimate GW discharge (e.g., Cox et al., 2002), which is accurate only if GW discharge and recharge do not co-occur in the reach (Harvey and Wagner, 2000). It is widely recognized that GW discharge and recharge often co-occur in different zones of the same SW body, for example, in streams that flow at an angle across a regional gradient in GW hydraulic head. In such cases, GW discharge typically occurs on the upgradient side and GW recharge occurs on the downgradient side. Therefore, in the absence of additional evidence demonstrating that either recharge or discharge is zero, differential gaging is best interpreted as an estimator of the *net difference* between GW discharge and GW recharge, $Q_{gw}^{in} - Q_{gw}^{out}$.

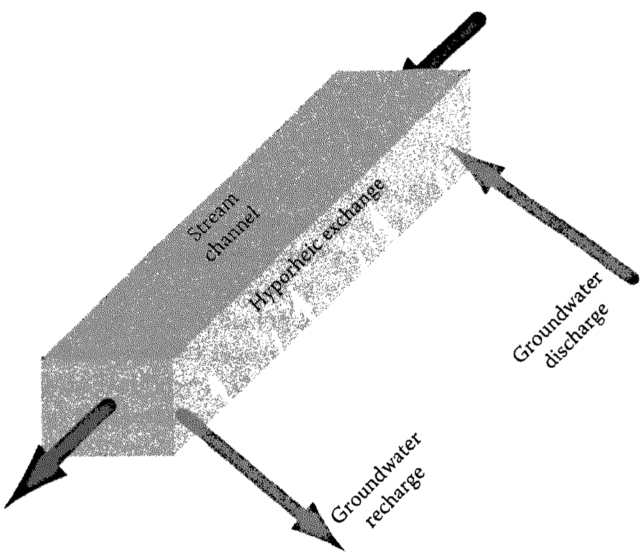

FIGURE 9.9 Mass balance analysis of stream–subsurface water interactions. GW exchange flows enter (GW discharge) or leave (GW recharge) the stream reach along unidirectional flowpaths as compared with hyporheic exchange, which leaves and then reenters the stream along many short flowpaths. Any imbalance in GW discharge and recharge may cause a change in streamflow and may alter solute concentrations and mass fluxes. At steady state, many bidirectional exchanges with hyporheic flowpaths are commonly assumed not to affect water balance or mass fluxes of conservative solutes, although reactive solutes may be strongly affected by hyporheic exchange.

To quantify both discharge and recharge to a stream using mass balance, an additional constraint is needed such as an independent information provided by a solute tracer. Combining an equation for water mass balance with an equation for chemical mass flux will allow a solution for both GW discharge and GW recharge by solving for two unknowns in two equations. The chemical mass balance equation expresses the rate of change in storage of solute mass M in the reach with the sum of the solute inflows minus the sum of the chemical outflows

$$\frac{dM}{dt} = Q(0,t)C(0,t) + Q_{gw}^{in}C_{gw}^{in} + Q_{hz}^{in}C_{hz} - Q(L,t)C(L,t) - Q_{gw}^{out}\bar{C} - Q_{hz}^{out}\bar{C} \tag{9.18}$$

where

- $C(x, t)$ is the solute tracer concentration [ML^{-3}] at distance x at time t
- C_{gw}^{in} is the average concentration in discharging GW
- C_{hz} is the concentration in the HZ
- $\bar{C}$ is the average concentration in SW

The concentrations $\bar{C}$ and C_{hz} are often difficult to estimate for transient conditions, which may necessitate more advanced modeling (see Section 9.4.3).

For steady mass transport conditions (i.e., $dM/dt = 0$), hyporheic terms are canceled because the solute mass fluxes into and out of hyporheic flowpaths are equivalent, that is, $Q_{hz}^{in}C_{hz} = Q_{hz}^{out}\bar{C}$

$$0 = Q(0)C(0) - Q(L)C(L) + Q_{gw}^{in}C_{gw}^{in} - Q_{gw}^{out}\bar{C} \tag{9.19}$$

where $\bar{C}$ is the average of measurements at upstream and downstream end points because stream concentration changes linearly through the reach.

Both GW discharge and GW recharge fluxes are quantified by combining the steady-state water mass balance, Equation 9.16, with the steady-state solute mass flux, Equation 9.19, and solving for two unknowns using backward substitution. The first step is to rearrange the solute mass balance equation to express Q_{gw}^{out}

$$Q_{gw}^{out} = \frac{Q(L)C(L) - Q(0)C(0) + Q_{gw}^{in}C_{gw}^{in}}{\bar{C}} \quad (9.20)$$

The right-hand side of Equation 9.20 is substituted for Q_{gw}^{out} in the water mass balance equation (Equation 9.16), which produces an expression with only one unknown, Q_{gw}^{in}. In a final step, the water mass balance equation (Equation 9.16) yields Q_{gw}^{out} after inserting the value of Q_{gw}^{in} in Equation 9.16 or Equation 9.20 to solve for Q_{gw}^{out}.

Uncertainties of the resulting estimates of GW discharge and recharge can be estimated using first-order assumptions. Errors associated with each individual measurement are assumed to be independent and propagate in calculations based on two or more measured variables according to simple rules based on assumptions of independence of errors. Examples of calculating error terms associated with coupled GW-SW mass balances for lakes, streams, and wetlands are given in Winter (1981b), Krabbenhoft et al. (1990b), and Choi and Harvey (2000).

Time-varying GW exchanges can be calculated from water and solute mass balances if field data (e.g., water level and concentration data) allow estimation of the change in storage terms. For example, Choi and Harvey (2000) solved the transient water and solute balance equations using Equations 9.15 and 9.18 to quantify time-varying GW discharge and recharge fluxes and their associated uncertainties. The work was performed in a large constructed wetland that is designed to remove phosphorus before water enters the Everglades in south Florida (Figure 9.10).

Applications of mass balance models to quantify in-stream and subsurface reactions may be found in Mulholland (1992), who examined nutrient uptake in a forest stream, and Kim et al. (1995), who examined biodegradation of toluene in a contaminated stream.

9.4.2 Chemical Mass Transport across Interface

The mass balance approach has been used to estimate fluxes and reaction rates near the interface between GW and SW. The approach discussed here emphasizes the quantification of hyporheic fluxes and residence times, mixing with GW, and subsurface reaction rates. The approach builds on early work by Triska et al. (1989), Bourg and Bertin (1993), and Valett et al. (1996) and specifically follows Harvey and Fuller (1998) and Harvey et al. (2013).

For a steady flow condition, the SW that crosses the interface has a solute concentration reflecting the mixing between SW and GW

$$C_{hz} = f_{sw}C_{sw} + f_{gw}C_{gw} \quad (9.21)$$

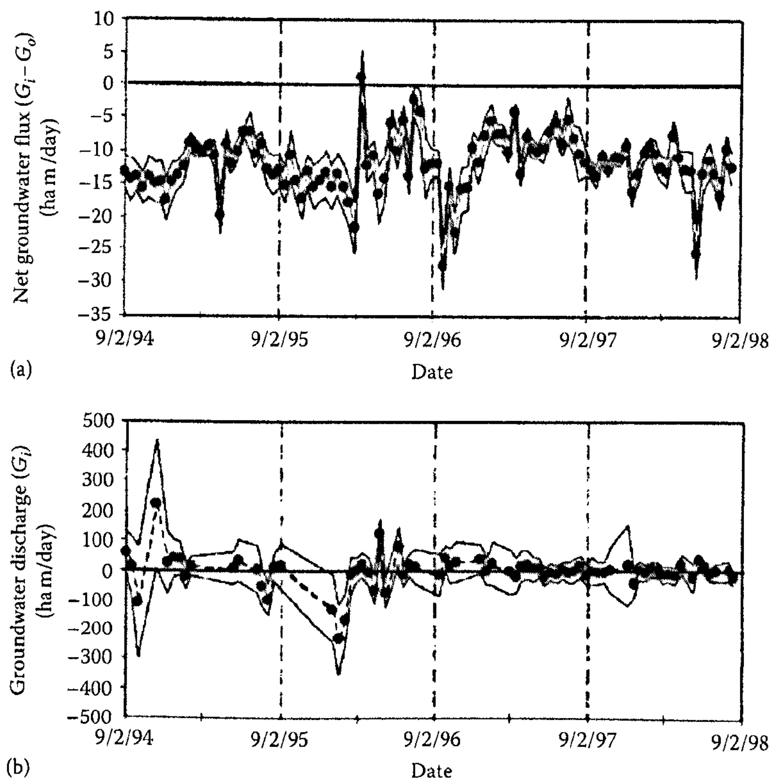

FIGURE 9.10 A dynamic water and solute mass balance approach quantified both GW discharge (G_i) and recharge (G_o) with uncertainty estimates in a large (1544 ha) wetland constructed for water treatment on agricultural land formerly a part of the Everglades, south Florida: (a) GW recharge nearly always exceeded discharge and varied with time, being generally greater in fall and lower in summer, (b) GW discharge was generally small except for a few brief time periods.

(Continued)

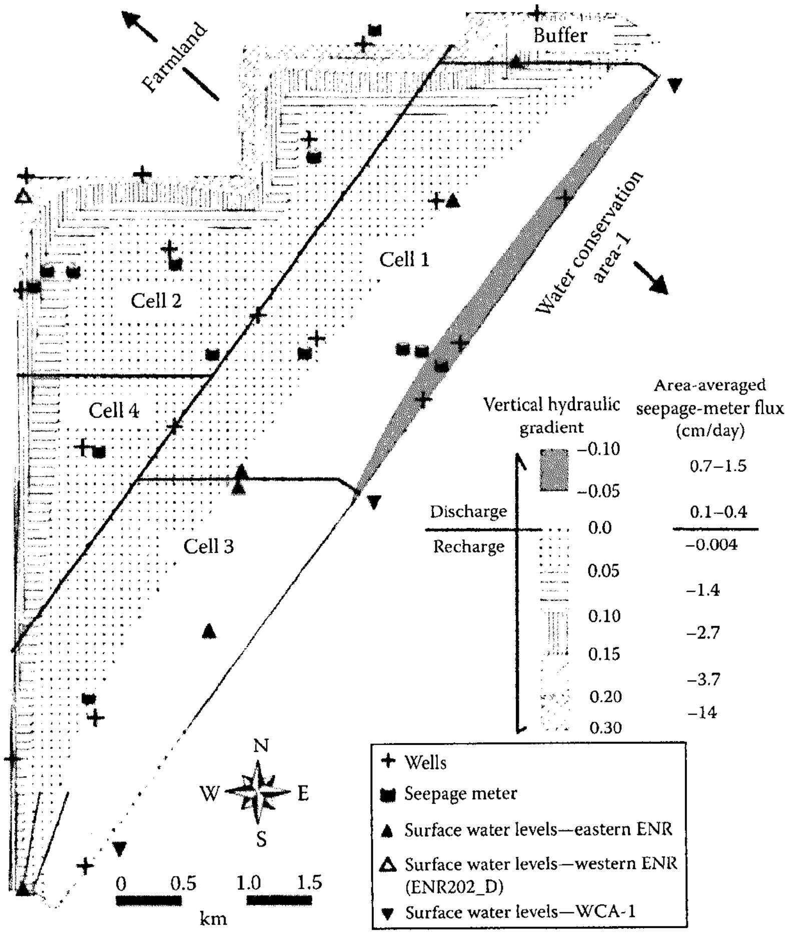

(c)

FIGURE 9.10 (*Continued*) A dynamic water and solute mass balance approach quantified both GW discharge (G_i) and recharge (G_o) with uncertainty estimates in a large (1544 ha) wetland constructed for water treatment on agricultural land formerly a part of the Everglades, south Florida: (c) discharge occurred on the east side of the wetland adjacent to a water conservation area where water level was maintained at a relatively high elevation, whereas recharge occurred on the west side adjacent to drained farmland. (Used from Choi, J. and Harvey, J.W., *Wetlands*, 20(3), 500, 2000. With permission.)

where

C denotes the concentration of any conservative solute

f_{sw} and f_{gw} are mixing fractions of water contributed from SW and GW, respectively

Subscripts denote the measured concentration in the hyporheic zone (*hz*), the end member concentrations of SW (*sw*) entering the HZ from above, or deeper GW (*gw*) entering with a GW flux from below. The mixing fractions are estimated from measurements of the steady-state concentrations of a conservatively transported solute tracer (e.g., specific conductivity or bromide)

$$f_{sw} = \frac{C_{hz} - C_{gw}}{C_{sw} - C_{gw}}, \quad f_{gw} = 1 - f_{sw} \tag{9.22}$$

For a reactive solute, the concentration in the HZ may be affected by both mixing and reaction according to

$$C'_{hz} = f_{sw}C'_{sw} + f_{gw}C'_{gw} - C^{*}_{hz} \tag{9.23}$$

where

C'_{hz} is the average HZ concentration of a potentially reactive solute

C'_{sw} and C'_{gw} are the SW and GW end member concentrations of the potentially reactive solute, respectively

C^{*}_{hz} is the mass concentration of the solute lost or gained by reaction in the HZ, with dimensions [ML^{-3}]

To quantify reaction rates using Equation 9.23, an estimate of the subsurface residence time is needed. For example, for a constant-rate injection of a solute tracer into the stream, the median subsurface residence time, τ_{hz}, is estimated as the elapsed time from the first arrival of the tracer in the stream to the time at which the subsurface tracer concentration achieves the 50th percentile concentration relative to its eventual plateau concentration. The hyporheic water flux across the streambed is estimated as

$$q_{hz} = \frac{d_{hz}\theta}{\tau_{hz}} \tag{9.24}$$

where

q_{hz} is the flux of water per unit area crossing the streambed interface, with dimensions [LT^{-1}]
θ is the sediment porosity
d_{hz} is the depth of the measurement below the streambed

The mass concentration of the solute lost or gained by the reaction in hyporheic flow is calculated by dividing C^*_{hz} by the hyporheic water residence time τ_{hz}, which expresses the reaction rate per unit volume of water [$ML^{-3}T^{-1}$]

$$r_{hz} = \frac{C^*_{hz}}{\tau_{hz}} \tag{9.25}$$

Typically, there is interest in expressing the reaction rate as a vertical mass flux of the reactant crossing a unit area of streambed, which is referred to as the reaction flux, U_{hz}

$$U_{hz} = C^*_{hz}q_{hz} = \frac{C^*_{hz}d_{hz}\theta}{\tau_{hz}} = r_{hz}d_{hz}\theta \tag{9.26}$$

A useful expression of the strength of a reaction that can be compared between different streams with different concentrations of reacting solutes is the first-order (concentration dependent) reaction rate coefficient where the coefficient, λ_{hz} [T^{-1}], is related to C^*_{hz} as follows:

$$C^*_{hz} = \hat{C}_{hz}(1 - e^{-\lambda_{hz}\tau_{hz}}) \tag{9.27}$$

where $\hat{C}_{hz}$ is defined as the expected concentration for nonreactive transport in the HZ. $\hat{C}_{hz}$ is calculated using Equation 9.23, which accounts for the dilution effect of mixing between SW and GW in the HZ (i.e., C^*_{hz} is set to zero). The reaction rate coefficient is solved for by rearranging Equation 9.27

$$\lambda_{hz} = \frac{-\ln\left[\left(\hat{C}_{hz} - C^*_{hz}\right)/\hat{C}_{hz}\right]}{\tau_{hz}} \tag{9.28}$$

The analysis of subsurface fluxes and reactions based on a single subsurface sampling point generally will only provide an accurate estimate if unidirectional subsurface flow occurs and if reaction rates are constant with depth. These assumptions could be appropriate for GW recharge, but generally the fluxes near the interface are more complicated and involve mixing between GW and hyporheic flow. Hyporheic flowpaths, for example, are generally distributed as a set of shallow flowpaths nested with deeper subsurface flowpaths, with flowpaths at greater depths contributing a diminishing fraction of the overall flux. Physically based models of hyporheic flow by Elliott and Brooks (1997) and Boano et al. (2007) support the hypothesis that hyporheic flux decreases rapidly as a function of depth in the HZ (e.g., model fluxes decrease exponentially), which is consistent with field observations indicating an exponential or lognormal decrease in flux as a function of depth (e.g., Jonsson et al., 2003; Harvey et al., 2013). Therefore, a single sampling depth potentially only represents a small part of the HZ, and calculations using data from a single sample depth may underestimate water fluxes and chemical reactions, especially if the sample point is located deep in the HZ where transport is slower.

Improved accuracy in field estimation of hyporheic flow is possible by sampling with multiple subsurface points deployed vertically at different depths and then using flux weighting to combine the results. The needed flux weighting functions are easily estimated from data or, alternatively, could be fit with theoretical weighting functions such as exponential or lognormal functions. Estimating a depth weighting function from field data is simplified by assuming that fluxes to each layer are independent. For these conditions, the total hyporheic flux across the sediment interface is the sum of the individual mass fluxes reaching each layer

$$q^{tot}_{hz} = \sum_{i=1}^{n} q_{hz,i} = \sum_{i=1}^{n} \frac{d_{hz,i}\theta_i}{\tau_{hz,i}} \tag{9.29}$$

where

q^{tot}_{hz} is the sum of contributions from total n layers
$q_{hz,i}$, where $d_{hz,i}$ is the thickness of the ith layer
θ_i is the sediment porosity of the ith layer
$\tau_{hz,i}$ is the subsurface water residence time in the ith layer measured as previously defined (i.e., elapsed time from the tracer arrival time at the sampling point in that layer minus the tracer arrival time in SW at the location of subsurface sampling)

Layer boundaries are usually determined by the spacing of subsurface sampling points (i.e., midpoint depth between measurement points), but also could be defined by transitions between actual sediment layers.

The depth weighted analysis of the vertical mass flux of a solute per unit area of streambed gives

$$U^{tot}_{hz} = \sum_{i=1}^{n} W_i \cdot U_{hz,i} \tag{9.30}$$

where

U^{tot}_{hz} is the total mass flux of solute to the streambed
$W_i \cdot U_{hz,i}$ is the flux-weighted contribution to reaction in the ith layer

The flux weight, W_i, is calculated as the fraction of the HZ flux reaching layer i

$$W_i = \frac{q_{hz,i}}{\sum_{i=1}^{n} q_{hz,i}} \quad (9.31)$$

where $q_{hz,i}$ is the flux contribution from the ith layer as previously defined in Equation 9.29.

Mass balance methods, such as the one described earlier, were used by Bourg and Bertin (1993) and Von Gunten and Lienert (1993) to investigate microbial processes affecting metal transport through the HZ and their influence on drinking water supply in alluvial aquifers. Triska et al. (1989) and Valett et al. (1996) used the approach to characterize nutrient uptake in alluvial sediments surrounding streams in different geologic settings. Harvey and Fuller (1998) used the approach to quantify metal uptake rates by precipitation of metal oxides and sorption of trace metals onto oxides in the HZ of a stream contaminated by acid mine drainage. Conant et al. (2004) assessed controls on GW discharge of a organic contaminant plume at preferential locations in the streambed. Lautz et al. (2006) determined the effect of debris dams on biogeochemical reactions in the streambed of a semiarid stream. Krause et al. (2009) and Kennedy et al. (2009) determined controls on nitrogen delivery in discharging GW to streams. Harvey et al. (2013) determined that denitrification in HZs could account for the cumulative removal of nitrate occurring in the stream as a whole. Although the reaction occurred throughout the full depth of the HZ, only denitrification in the shallow hyporheic flowpaths (<4 cm deep) was significant to the nitrate mass balance in the whole stream. The physical and chemical controls were hyporheic residence time, dissolved organic carbon concentration, and nitrate concentration, which can be summarized by a reaction significance factor for the whole stream equal to the ratio of hyporheic transport and reaction timescales multiplied by the proportion of streamflow being exchanged with the HZ for a given length of the stream (Harvey et al., 2013).

9.4.3 Coupled Modeling of Stream–Hyporheic–Aquifer Systems

Water and solute transport processes near streams can be integrated in a coupled model of transport in stream corridors. An example is the transient storage model, which simulates in-channel advection and longitudinal dispersion in a stream that also has hydrologic connections with GW and with "transient storage zones," that is, slowly moving SW at channel sides and in shallow subsurface (hyporheic) waters (e.g., Thackston and Schnelle, 1970; Valentine and Wood, 1979; Bencala and Walters, 1983; Jackman et al., 1984; Runkel, 1998; Harvey and Wagner, 2000; Fernald et al., 2001), as shown in Figure 9.11. Other models in the transient storage model family have more detailed characterization of the storage-exchange processes (e.g., Choi et al., 2000; Haggerty et al., 2002; Wörman, 2000; Wörman et al., 2002; Briggs et al., 2009; Neilson et al., 2010; Bottacin-Busolin et al., 2011).

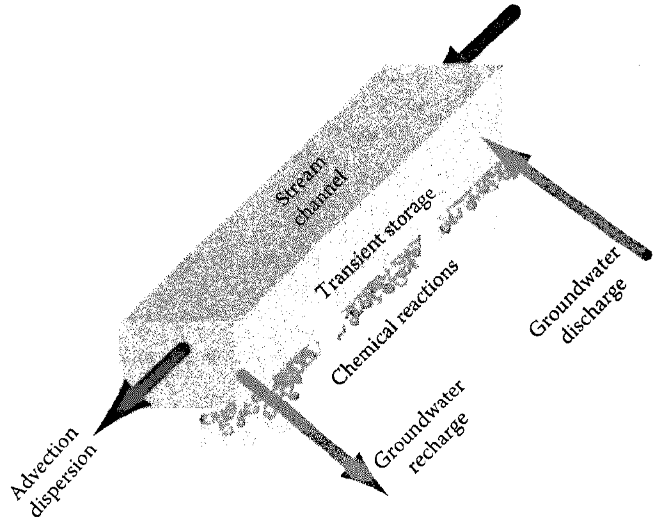

FIGURE 9.11 Dynamic analysis of solute transport: the transient storage model. Mass transport by advection and longitudinal dispersion is modeled in a stream that exchanges mass with transient storage zones, that is, well-mixed storage reservoirs of a specified size and residence time alongside the main channel that may represent much more slowly moving surface or subsurface (or both) waters. The effect of transient storage is to delay downstream mass transport and to increase opportunities for chemical reactions in contact with geochemically and biologically active surface coatings on vegetation leaves and sediment grains. (Used from Harvey, J. and Gooseff, M., *Water Resour. Res.*, 51, 6893, 2015. With permission.)

The governing equations for transient storage consider width- and depth-averaged transport through a stream channel with GW exchange. The advection–dispersion is as follows:

$$\frac{\partial C}{\partial t} = -\frac{Q}{A}\frac{\partial C}{\partial x} + \frac{1}{A}\frac{\partial}{\partial x}\left(AD\frac{\partial C}{\partial x}\right) + \frac{q_L^{in}}{A}(C_L - C) + \alpha(C_S - C) - \lambda C \quad (9.32)$$

where

terms in the right-hand side represent advection, dispersion, lateral inflow, exchange with storage, and reactive chemical losses
A is the stream cross-sectional area [L^2]
D is the stream longitudinal dispersion coefficient [L^2T^{-1}]
q_L^{in} is the lateral inflow rate in the stream [L^2T^{-1}]
C_L is the solute concentration of lateral inflow [ML^{-3}]
α is the storage zone exchange coefficient [T^{-1}]
$C_S(t)$ is the solute concentration in the storage zone [ML^{-3}]
λ is the stream sorption rate coefficient [T^{-1}]

A first-order mass exchange equation in the transient storage zones is given as follows:

$$\frac{dC_S}{dt} = \alpha\frac{A}{A_S}(C - C_S) - \lambda_S C_S \quad (9.33)$$

where

terms on the right-hand side represent exchange with the stream and reactive chemical loss in the storage

A_S is the cross-sectional area of storage zone [L^2]

λ_S is the sorption rate coefficient of the storage zone [T^{-1}]

Like all models based on the advection–dispersion equation, the transient storage models characterize complex physical and chemical processes in a simple way, which is useful for modeling field data. Both steady-state and dynamic hydrologic and chemical conditions can be modeled with the available numerical codes. Some codes also offer an objective means for identifying parameters and for estimating uncertainty (Wagner and Gorelick, 1986; Wagner and Harvey, 1997; Runkel, 1998).

Often the needed field data are acquired by injecting a conservatively transported solute tracer at a constant rate into a stream for a period of hours to days and monitoring the arrival and flushing of the tracer at downstream locations. A first step in data analysis is to quantify GW discharge and recharge in the reach. Using the background solute tracer concentration measured before the injection and the steady plateau concentration achieved after a period of time, the streamflow at the downstream end of the experimental reach can be estimated using the end-member mixing via tracer dilution gaging equation

$$Q_{tracer}^{dwn} = \frac{C_I Q_I}{C_{sw}^{dwn} - C_B} \quad (9.34)$$

where

Q_{tracer}^{dwn} is the streamflow estimated by tracer dilution to concentration C_{sw}^{dwn} at the downstream end of the reach

C_I and Q_I are the tracer injectate concentration and injection rate, respectively

C_B is the background concentration of the solute tracer

From Equation 9.34, it is apparent that the tracer-based measure of streamflow, Q_{tracer}^{dwn}, is sensitive to mass inputs from discharging GW but is not sensitive to GW recharge because any loss of tracer mass into GW flowpaths has no effect on the in-stream solute tracer concentration (see Equation 9.34). As a result, GW discharge, Q_{gw}^{in}, is estimated as

$$Q_{gw}^{in} = Q_{tracer}^{dwn} - Q(0) \quad (9.35)$$

However, Q_{gw}^{out} also can be estimated as long as streamflow at the downstream end of the reach is measured two ways, that is, using both tracer dilution, that is, Q_{tracer}^{dwn}, and velocity gaging, that is, $Q(L)$. Outflow of GW is calculated by substituting Equation 9.35 into the stream mass balance, Equation 9.16, and rearranging to give

$$Q_{gw}^{out} = Q_{tracer}^{dwn} - Q(L) \quad (9.36)$$

Thus, both GW discharge and recharge are quantified by tracer-dilution gaging supplemented with velocity gaging at the downstream end of the stream reach.

These estimates of GW discharge and recharge fluxes are used as inputs to the transient storage model. For example, using the freely available U.S. Geological Survey (USGS) one-dimensional transport with inflow and storage model with parameter estimation (OTIS-P model, Runkel, 1998) to solve Equations 9.32 and 9.33 typically involves specifying GW exchange as outlined earlier and then identifying four additional parameters: stream advection, longitudinal dispersion coefficient in the stream, transient storage zone cross-sectional area, and stream–storage zone exchange coefficient. OTIS-P uses statistical inverse fitting routines to search for the combination of parameters that provide the best fit simulation to the tracer breakthrough data. If, in addition, a reactive solute tracer was co-injected with the conservative tracer, or if measurements were made of a naturally occurring reactive solute, then a solute reaction rate also may be estimated. Thus, compared with the very simple mass balance models that were previously discussed, there is considerably more to be revealed about solute transport and reaction processes with solute tracer experiments and transient storage modeling.

Transient storage fluxes are distinguished from GW fluxes in the bidirectional nature of the fluxes exchanging with relatively small zones of nearly stagnant or recirculating water at channel sides or in the shallow subsurface. In contrast, GW discharge and recharge water only flow across the sediment interface once (i.e., either discharging to the stream or recharging the aquifer). The model conceptualization of transient storage is extremely basic. It assumes that the stream water and solute exchange repeatedly with well-mixed storage zone. Parcels of water that enter transient storage are held in storage for variable lengths of time. The reach-averaged parameters determined by fitting include an exchange coefficient, an average size of the storage zone, and the average residence time in storage, which by rearrangement produces the reach-averaged water exchange flux per unit length of stream [$L^3T^{-1}L^{-1}$] that is defined as the storage zone cross-sectional area divided by the average residence time in storage (Harvey et al., 1996). The mathematical form of the residence time distribution for a well-mixed storage reservoir is exponential, which often fits tracer data in real streams quite well. That the fit to field data is reasonable does not mean that transient storage zones are actually well-mixed reservoirs but rather that transient storage zones comprise an exponentially distributed assemblage of many short exchange pathways and a few much longer exchange pathways. Closer examination of field tracer data often suggests that solute residence times in storage zones of real streams are often more broadly distributed than exponential, exhibiting lognormal or power law distributions (Haggerty et al., 2002; Wörman et al., 2002).

Additional storage zones may be added to the transient storage model, with different exchange fluxes, storage-zone sizes, water residence times, and rates of chemical reaction. In practice, the modeling of multiple storage zones with different sizes, and different hydrologic turnover rates and reaction rates, has been difficult to constrain simply by modeling in-stream solute tracer breakthrough curves. Usually, independent measurements are needed within representative storage zones of various types (e.g., subsurface HZs versus SW storage zones in channel side cavities) to parameterize multiple storage zones. Models are improved by simultaneously measuring solute tracer dynamics at the reach scale and also at representative locations where storage actually occurs. For example, working in a boulder bed coastal stream in California, Bencala et al. (1984) was the first to demonstrate that in-stream transport was strongly affected by hyporheic exchange. Harvey et al. (1996) showed that only one class of hyporheic flowpaths through gravel bars was observable with injected tracers. Larger and longer timescale hyporheic flow through alluvium up to several meters away from the stream was observed through the measurement of head gradients and verified through the release of a subsurface tracer, but was not detected by a 4-day injection of tracer into the stream. Gooseff et al. (2005) directly compared stream reaches differing primarily in one being underlain by alluvium and the other by bedrock. Ensign and Doyle (2005) investigated reach-scale effects on storage dynamics of creating SW storage zones by adding wood baffles as surrogates for wood debris. Harvey et al. (2005) simultaneously measured SW transient storage and hyporheic transient storage and contrasted the resulting storage areas and residence times with reach-scale quantities that had been inversely estimated by modeling the dynamics of the injected tracer. Similarly, Briggs et al. (2009) directly measured the surface transient storage component in SW storage zones and accounted for hyporheic transient storage as the remaining unexplained component of storage in the reach-scale model. O'Connor et al. (2010) and Jackson et al. (2013) added solute tracers directly to SW storage zones and measured their flushing rate to estimate surface transient storage residence times. Those authors demonstrated that relatively simple physical measurements could be used to estimate the surface transient storage zone size and water residence time as a means to parameterize the surface transient storage component of reach-scale transport models.

9.4.4 Reactive Transport Modeling in Stream–Hyporheic–Aquifer Systems

Chemical reactions in stream corridors often are characterized by first-order uptake or production terms in the main channel and in the storage zone of transient storage models. However, a wide variety of chemical reactions can be simulated in addition to first-order decay. For example, Equations 9.32 and 9.33 can be modified to consider sorption by adding additional terms for solute sorption in the main channel onto streambed sediments, $\rho\hat{\lambda}(C_{sed} - K_d C)$, and sorption of solutes entering the storage zone onto sediment surfaces, $\hat{\lambda}_S(\hat{C}_S - C_S)$, respectively (Bencala, 1983). Using the term for sorption of main channel solutes onto the streambed in Equation 9.32 would require an additional equation for sorbed solute on the streambed

$$\frac{dC_{sed}}{dt} = \hat{\lambda}\left(K_d C - C_{sed}\right) \tag{9.37}$$

where the new terms in the two sorption equations are defined as follows: $\hat{C}_S(t)$ is the background storage zone solute concentration [ML^{-3}]; ρ is the mass of accessible sediment per volume of water [ML^{-3}]; $\hat{\lambda}$ is the main channel sorption rate coefficient [T^{-1}]; $\hat{\lambda}_S$ is the storage zone sorption rate coefficient [T^{-1}]; C_{sed} is the sorbate concentration on the streambed sediment [MM^{-1}]; and K_d is the sorbed solute distribution coefficient [L^{3}M^{-1}].

An easily used and widely available model of in-stream transport with dispersive mixing and first-order uptake terms and sorption terms is available from the USGS in its well documented OTIS-P code (Runkel, 1998) that provides a built-in statistical code for inversely estimating parameters. The OTIS model has roots in similar models described by Newbold et al. (1983), Stream Solute Workshop (1990), Mulholland et al. (1997), DeAngelis et al. (1995), and Jones and Mulholland (2000). All of these modeling studies describe the use of tracer injections and modeling, and a wide variety of chemical reactions can be simulated in addition to first-order decay, including gas exchange (Choi et al., 1998), sorption from main channel waters onto the streambed, sorption within the storage zone, and various other equilibrium speciation or kinetically controlled speciation reactions (Bencala, 1983). Mulholland et al. (1997) used transient storage modeling to show that HZs increase important biogeochemical reactions such as heterotrophic metabolism and phosphorus uptake in streams. Several other detailed examples of transient storage modeling are given by Kim et al. (1990, 1992) who simulated transient storage and nitrate uptake kinetics of a periphyton community in a flume and then in a stream. Kimball et al. (1994) conducted tracer injections to measure metal loading from acid mine drainage and to determine reaction rates that attenuate metals in the stream and in HZs. Broshears et al. (1996) manipulated stream pH and simulated the controls on aluminum and iron chemistry. The role of HZs in denitrification was investigated using transient storage modeling by Gooseff et al. (2004) and Harvey et al. (2013). Ensign and Doyle (2006) examined results from many tracer experiments that quantified nutrient retention in streams and assessed the possible role of hyporheic flow. The reactive solute transport capabilities of OTIS were expanded in the One-Dimensional Transport with Equilibrium Chemistry (OTEQ) model that solves the equilibrium submodel MINTEQ in the context of transport with GWSWIs (Runkel, 2010). This model has been extensively tested in applications involving the fate of metals released by acid mine drainage.

One of the valuable outcomes of transient storage modeling is the reach-scale estimates of transport that are relevant to many issues of water quality and stream ecology. However, there are several limitations in the physical interpretation of storage processes. First is the difficulty of specifying where transient storage occurs, that is, in surface side zones of streams or in the subsurface, which potentially affects the amount of reaction that occurs. The difficulty of specifying where the dominant storage occurs is problematic for predicting water quality effects. For example, whether transient storage occurs in SW dead zones of streams or in hyporheic flowpaths is particularly important for understanding controls on chemical reactions such as denitrification. Second, because transient storage is the result of an assemblage of processes that are difficult to predict based on easily measured physical attributes, it means that results from one experiment cannot be transferred to other streams or even within the same stream at a different discharge (Wörman et al., 2002; Harvey et al., 2003), which implies that expensive tracer experimentation may always be needed. A third problem is that tracer-derived parameters tend to contain biases that reflect the timescale of the stream tracer experiment and how it affects the observable range of transient storage. For example, arbitrary choices of tracer injection time and the length of the experimental reach can interact with the actual exchange characteristics in a stream reach in a way that limits the spatial and temporal scale of exchange flows that can be detected (Ward et al., 2013b). The consequences can be overcome to an extent using principles of experimental design and lengthening the time of injections (Harvey and Wagner, 2000). However, there are practical limits of labor expenses. As a response to these challenges, there has been an increasing effort to develop physically based modeling approaches for stream and river corridors that explicitly simulate specific storage types and their cumulative contributions to transient storage (Wörman et al., 2002; O'Connor et al., 2010; Stonedahl et al., 2013; Boano et al., 2014). Progress also is being made in developing physically based models of river corridor transport processes at the scale of large drainage basins based on widely available physical data (e.g., Battin et al., 2008; Gomez-Velez and Harvey, 2014; Kiel and Cardenas, 2014).

9.5 Heat Transport across the Interface

9.5.1 Introduction

Water temperature is an important environmental variable because temperature influences habitat suitability for aquatic life, rates of geochemical processes, and hydraulic conductivity of near-stream sediments (Hayashi and Rosenberry, 2002; Stonestrom and Constantz, 2004; Anderson, 2005). Temperature dynamics at the GW-SW interface are particularly important because they integrate the distinct temperature regimes of SW and GW; GW temperatures are typically stable relative to SW temperatures, at approximately the mean ground surface temperature, while SW temperatures fluctuate through time diurnally and seasonally (Hayashi and Rosenberry, 2002). The distinct contrast in temperatures daily and seasonally between SW and GW makes heat an ideal tracer of water exchange across the SW-GW interface. A renewed interest in heat transport and tracing in hydrologic systems has led to several detailed reviews, particularly of heat tracing in near-stream zones (Stonestrom and Constantz, 2004; Anderson, 2005; Rau et al., 2014).

Heat tracing has a number of advantages over traditional methods of measuring SW-GW interaction. Heat is a naturally occurring tracer (Constantz et al., 2003), and thermal properties of sediments, such as thermal conductivity, are much more tightly constrained than hydrologic properties, such as hydraulic conductivity, which can vary over orders of magnitude (Lapham, 1989; Stonestrom and Constantz, 2004). 1D heat transport in near-stream vertical profiles has been well understood and described for decades (Suzuki, 1960; Bredehoeft and Papadopulos, 1965; Stallman, 1965), and advances to improve heat tracing parameterization continue to develop (e.g., Rau et al., 2012). Inexpensive and accurate temperature data loggers (e.g., Hubbart et al., 2005; Johnson et al., 2005) are now commonly available, and new methods for obtaining high-resolution profiles of stream and subsurface temperatures have been developed using fiber-optic distributed temperature sensing (e.g., Vogt et al., 2010; Briggs et al., 2012). Just as data acquisition is becoming more detailed and cost-effective, straightforward analytical techniques are being developed to interpret data (Hatch et al., 2006; Keery et al., 2007; McCallum et al., 2012; Luce et al., 2013). These new techniques are coded in publicly available, free computer programs and graphical user interfaces that integrate the latest research on temperature signal processing, analytical and numerical modeling, and model error analysis (Swanson and Cardenas, 2011; Gordon et al., 2012; Voytek et al., 2014). The limitations of heat tracing under a variety of field conditions have been explored in several recent studies, including limitations imposed by streambed heterogeneity (Schornberg et al., 2010; Ferguson and Bense, 2011), multidimensional flow (Lautz, 2010; Cuthbert and Mackay, 2013), strong upwelling of GW (Briggs et al., 2014), and uncertainty of thermal properties (Munz et al., 2011; Shanafield et al., 2011), etc. As a result of these recent advances, field examples of heat tracing are now abundant in the literature.

In this section, we summarize the developments in theory of heat transport in near-stream sediments, common solutions to the heat transport equation that are used to model rates of SW-GW exchange, parameterization of heat transport models, and heat tracing limitations.

9.5.2 Heat Transport Theory

9.5.2.1 Governing Equations of Heat Transport

The heat transport equation describes heat flow through porous media and is analogous to the advection–dispersion equation for solutes in GW (see Chapter 4). For fully saturated conditions, without sources or sinks of heat internal to the system, the governing equation in 1D form for vertical heat flow in z-direction is as follows:

$$c\rho\frac{\partial T}{\partial t} = \kappa_e\frac{\partial^2 T}{\partial z^2} - c_w\rho_w q\frac{\partial T}{\partial z} \tag{9.38}$$

where
- T is the temperature (°C)
- t is the time (s)
- κ_e is the effective thermal diffusivity of the sediment–water matrix ($m^2 s^{-1}$)
- q is the specific discharge ($m\ s^{-1}$)
- c and ρ are the specific heat ($J\ kg^{-1}\ °C^{-1}$) and density ($kg\ m^{-3}$), respectively, of the sediment–water matrix
- c_w and ρ_w are the specific heat ($J\ kg^{-1}\ °C^{-1}$) and density ($kg\ m^{-3}$) of water (Suzuki, 1960; Bredehoeft and Papadopulos, 1965; Stallman, 1965; Domenico and Schwartz, 1998; Anderson, 2005)

Often, an analogue of pore velocity in advective solute transport, v_t, is used

$$v_t = \frac{c_w\rho_w}{c\rho}q \tag{9.39}$$

The first term on the right hand side of Equation 9.38 represents heat transport by conduction and the second term represents heat transport by water flow, termed advection or convection (Anderson, 2005).

9.5.2.2 Concepts of Heat Transport in GWSWI

In general, there is a difference between SW and GW temperature regimes that is used for inferring rates of SW-GW exchange. GW temperatures are relatively constant through time of measurements. In contrast, stream temperatures fluctuate daily and/or seasonally, depending on the location (Stonestrom and Constantz, 2004). Stream temperature fluctuations result in time-variable thermal gradients between SW and GW that are affected by water flux vertically; in the northern hemisphere, GW is warmer than stream water in winter and cooler than stream water in summer (e.g., Schmidt et al., 2007), as shown in Figure 9.12. As a result, point-in-time temperature profiles in characteristic points in streambeds (T_0, $T_z = T(z)$, and T_L in Figure 9.12) can be used to infer the rate of water flux vertically, assuming temperature profiles are at quasi-steady state (Bredehoeft and Papadopulos, 1965; Turcotte and Schubert, 1982; Conant, 2004; Schmidt et al., 2007). Periodic temperature fluctuations (either diurnal or seasonal) propagate vertically into the subsurface, and the rate of propagation is a function of both the rate of conduction and rate of water flux (Lapham, 1989; Stonestrom and Constantz, 2004), as shown in Figure 9.12. As periodic temperature signals propagate vertically, their amplitude is reduced and their phase is lagged. As a result, temperature time series at multiple depths in streambeds (e.g., depths A, B, and C in Figure 9.12) can be used to observe the degree of amplitude attenuation and phase shift with depth,

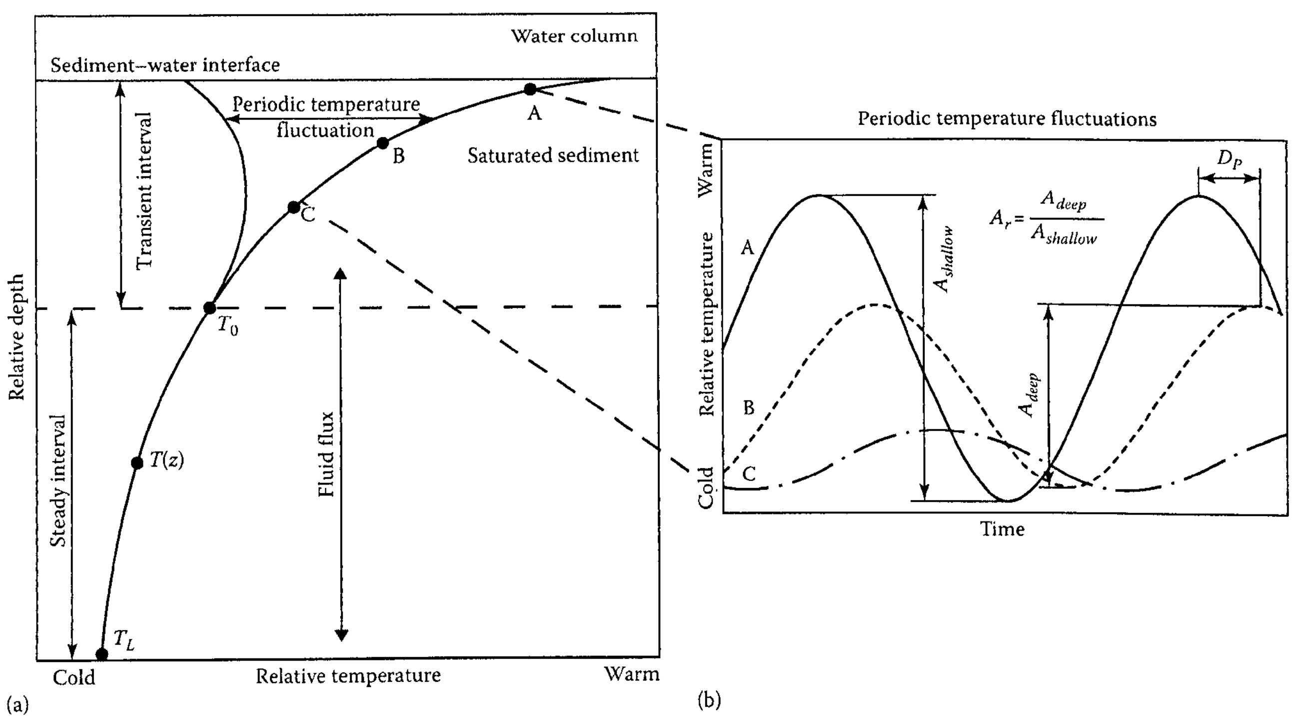

FIGURE 9.12 Schematic temperature profile in streambed sediments. SW undergoes periodic temperature fluctuations and is, on average, warmer than GW: (a) at depth, the temperatures are constant in time, with values that fall between the temperature at the upper and lower boundaries (T_0 and T_L, respectively) and (b) In the shallow region, the temperatures fluctuate periodically, similar to the SW, but with reduced amplitude and increased phase. (Used from Swanson, T.E. and Cardenas, M.B., *Comput. Geosci.*, 37(10), 1664, 2011. With permission.)

which can in turn be used to infer the rate of water flux vertically, assuming a steady-state water flux (Stallman, 1965; Goto et al., 2005; Hatch et al., 2006; Keery et al., 2007; McCallum et al., 2012; Luce et al., 2013).

9.5.3 Heat Transport Parameters

The heat conduction term in Equation 9.38 accounts for two distinct transport processes: (1) heat conduction through the sediment–water matrix and (2) thermal dispersion due to convection (Anderson, 2005; Rau et al., 2012). In practice, the way in which these processes are described in the heat transport equation and analytical solutions is a function of the formulation of effective thermal diffusivity, κ_e. A detailed discussion of this parameter can be found in Rau et al. (2012). In its simplest form, thermal dispersion is ignored (Suzuki, 1960; Stallman, 1965; Goto et al., 2005; Keery et al., 2007; Schmidt et al., 2007; Luce et al., 2013), in which case

$$\kappa_e = \frac{k}{c\rho} \tag{9.40}$$

where k is the thermal conductivity of the sediment–water matrix (J s^{-1} m^{-1} °C^{-1}). If thermal dispersion is not considered negligible, thermal dispersion due to advection is included in the effective thermal diffusivity coefficient as follows:

$$\kappa_e = \frac{k}{c\rho} + \beta\,|q| \tag{9.41}$$

where β is the thermal dispersivity (m) (Anderson, 2005; Hatch et al., 2006; Keery et al., 2007). In this case, the value of κ_e is a function of the water flux rate, q. Recently, an alternative empirical formulation for dispersion has been proposed (Rau et al., 2012), where

$$\kappa_e = \frac{k}{c\rho} + \beta\left(\frac{c_w\rho_w}{c\rho}q\right)^2 \tag{9.42}$$

Table 9.1 shows representative ranges of κ_e from the literature, which are narrow compared to ranges for hydraulic conductivity that can vary over 7–10 orders of magnitude.

TABLE 9.1 Ranges of Values for Heat Transport Parameters

Parameter	Range of Values
Thermal conductivity of sediment–water matrix, k	0.8–2.5 W m^{-1} °C^{-1}
Volumetric heat capacity of sediment–water matrix, $c\rho$	(2.5–3.6) × 10^6 J m^{-3} °C^{-1}
Thermal diffusivity, κ_e	(2.4–9.8) × 10^{-7} m^2 s^{-1}

Sources: Lapham, W.W., Use of temperature profiles beneath streams to determine rates of vertical ground-water flow and vertical hydraulic conductivity, U.S. Geological Survey Water-Supply Paper 2337, 1989; Stonestrom, D.A. and Constantz, J., Heat as a tool for studying the movement of groundwater near streams, U.S. Geological Survey Circular 1260, 2004.

Thermal conductivity, k, of the sediment–water matrix is often estimated as the geometric mean of the water and sediment thermal conductivity, weighted by the sediment porosity, n

$$k = k_w^n k_s^{1-n} \tag{9.43}$$

where k_w and k_s are the thermal conductivity values for water and sediment, respectively (J s^{-1} m^{-1} °C^{-1}) (Hatch et al., 2006; Rau et al., 2014).

The heat capacity of the sediment–water matrix, $c\rho$, is often estimated as the arithmetic mean of the water and sediment heat capacity, weighted by the sediment porosity (Anderson, 2005; Rau et al., 2014):

$$c\rho = (1-n)c_s\rho_s + nc_w\rho_{sw} \tag{9.44}$$

The representative values of k and $c\rho$ are provided in Table 9.2.

9.5.4 Solutions of the One-Dimensional Heat Transport Equation

A series of studies have presented analytical solutions to the 1D heat transport Equation 9.38 that directly determine rates of water flux between streams and GW from temperature observations (Suzuki, 1960; e.g., Bredehoeft and Papadopulos, 1965; Stallman, 1965; Turcotte and Schubert, 1982; Goto et al., 2005; Hatch et al., 2006; Keery et al., 2007; McCallum et al., 2012; Luce et al., 2013). In this section, we summarize the commonly used formulations appearing in the recent literature with an aim of applying heat tracing in field studies, as presented in Section 9.6.

9.5.4.1 Steady-State Temperature Profiles

Heat tracing methods that use point-in-time temperature profiles (e.g., the profile from T_0 to T_L in Figure 9.12) infer the rate of vertical water flux from the degree to which the temperature profile is perturbed from the pure conduction case. Analytical solutions for Equation 9.38 are for steady-state conditions, where the porous medium is homogeneous and isotropic, and the temperature profile is static through time; the temperature at the upper boundary does not change. For this reason, temperature profiles observed in the field must be measured below the zone influenced by short timescale temperature oscillations, such as diurnal fluctuations (Figure 9.12). The solution presented by Turcotte and Schubert (1982) as shown in Table 9.2 is valid for upward flux only and reviewed in detail by Schmidt et al. (2007). The solution presented by Bredehoeft and Papadopulos (1965) shown in Table 9.2 is valid for upward or downward flux (see also Schmidt et al., 2006). The MATLAB® computer program ExStream, which is available at no cost, can be used for time series processing and solving the Turcotte and Schubert (1982) and Bredehoeft and Papadopulos (1965) analytical equations for temperature profiles observed in the field (Swanson and Cardenas, 2011).

9.5.4.2 Temperature Time Series and Periodic Fluctuations

Heat tracing methods can utilize temperature time series and shifts in the periodic temperature fluctuations with depth

TABLE 9.2 Analytical Solutions of 1D Heat Transport for Estimating Vertical Water Flux q (m s^{-1})

References for Method	Data Required	Equation
Methods using point-in-time temperature observations in a vertical profile (e.g., T_0 to T_L in Figure 9.12)		
Turcotte and Schubert (1982), Schmidt et al. (2007), Swanson and Cardenas (2011)	Temperature observations at the sediment–water interface ($z = 0$) and at depths of L, z, and thermal properties of the sediment–water matrix	$q = -\frac{\kappa_e}{z}\ln\left(\frac{T_z - T_L}{T_0 - T_L}\right)$
Bredehoeft and Papadopulos (1965), Schmidt et al. (2006), Schornberg et al. (2010), Swanson and Cardenas (2011)	Temperature observations at the sediment–water interface ($z = 0$) and at depths of L, z, and thermal properties of the sediment–water matrix	$\frac{T_z - T_0}{T_L - T_0} = \frac{\exp((q/k_e)z) - 1}{\exp((q/k_e)L) - 1}$
Methods using temperature time series at multiple depths (e.g., A, B, and C in Figure 9.12)		
Hatch et al. (2006), Swanson and Cardenas (2011), Gordon et al. (2012)	Amplitude ratio (ratio of the amplitude of the deeper periodic signal to the shallow periodic signal $A_r = A_d/A_s$); thermal properties of the sediment–water matrix; period of the temperature oscillation P	$v_t = \frac{2\kappa_e \ln A_r}{\Delta z} + \frac{\left(\alpha + v_t^2\right)^{1/2}}{\sqrt{2}}$ $\alpha = \left[v_t^4 + \left(\frac{8\pi k\kappa_e}{P}\right)^2\right]^{1/2}$
Hatch et al. (2006), Swanson and Cardenas (2011), Gordon et al. (2012)	Phase shift (change in phase between the deeper periodic signal and the upper periodic signal $\Delta\phi = \phi_d - \phi_u$); thermal properties of the sediment–water matrix; period of the temperature oscillation P	$\lvert v_t\rvert = \left[\alpha - 2\left(\frac{4\pi\Delta\phi k_e}{P\Delta z}\right)^2\right]^{1/2}$ $\alpha = \left[v_t^4 + \left(\frac{8\pi k\kappa_e}{P}\right)^2\right]^{1/2}$
Keery et al. (2007), Swanson and Cardenas (2011), Gordon et al. (2012)	Amplitude ratio (ratio of the amplitude of the deeper periodic signal to the shallow periodic signal $A_r = A_d/A_s$); thermal properties of the sediment–water matrix; period of the temperature oscillation P	$\frac{\gamma(Hq)^3}{4} - 1.25\gamma^2(Hq)^2 + 2\gamma^3 Hq + \left(\frac{\pi c\rho}{kP}\right)^2 - \gamma^4 = 0$ $H = \frac{c_w\rho_w}{k}$; $\gamma = \frac{\ln A_r}{\Delta z}$
Keery et al. (2007), Swanson and Cardenas (2011), Gordon et al. (2012)	Phase shift (change in phase between the deeper periodic signal and the upper periodic signal, $\Delta\phi = \phi_d - \phi_u$); thermal properties of the sediment–water matrix; period of the temperature oscillation P	$\lvert q\rvert = \left[\left(\frac{c\rho\Delta z}{\Delta\phi c_w\rho_w}\right)^2 - \left(\frac{4\pi\Delta\phi k}{c_w\rho_w P\Delta z}\right)^2\right]^{1/2}$
Luce et al. (2013)	Amplitude ratio (ratio of the amplitude of the deeper periodic signal to the shallow periodic signal $A_r = A_d/A_s$); thermal properties of the sediment–water matrix; period of the temperature oscillation P	$v_t = \frac{2\pi\Delta z}{P\Delta\phi}\frac{1-\mu^2}{(1+\mu^2)^{1/2}}$; $\mu = \frac{\ln A_r}{\Delta\phi}$
McCallum et al. (2012)	Amplitude ratio (ratio of the amplitude of the deeper periodic signal to the shallow periodic signal $A_r = A_d/A_s$); phase shift (change in phase between the deeper periodic signal and the upper periodic signal $\Delta\phi = \phi_d - \phi_u$); thermal properties of the sediment–water matrix; period of the temperature oscillation P	$v_t = \frac{\Delta z(\theta - 4\pi^2)}{\Delta\phi(16\pi^4 + 8\pi^2\theta + \theta^2)^{1/2}}$, $\theta = \frac{P^2 \ln^2 A_r}{\Delta\phi^2}$

(e.g., the temporal patterns for depths A, B, and C in Figure 9.12). They infer the rate of vertical water flux from the amplitude ratio, A_r

$$A_r = \frac{A_d}{A_s} \tag{9.45}$$

where

A_d is the amplitude at a deeper sensor

A_s is the amplitude at a shallow sensor, phase shift, $\Delta\phi$

$$\Delta\phi = \phi_d - \phi_s \tag{9.46}$$

where

ϕ_d is the phase at a deeper sensor

ϕ_s is the phase at a shallow sensor, or both

Analytical solutions for Equation 9.38 are for a steady-state water flux, but periodic temperature variations with period P at the upper boundary, and assume a homogeneous and isotropic porous media. Temperature time series are observed in the field in the zone of the thermal profile influenced by periodic temperature fluctuations, most commonly diurnal (Figure 9.12). Solutions based on A_r and $\Delta\phi$, individually, are presented by Hatch et al. (2006) and Keery et al. (2007) (Table 9.2). Solutions using A_r and $\Delta\phi$ simultaneously ("combined" methods) are presented by Luce et al. (2013) and McCallum et al. (2012). To extract amplitude and phase information from temperature time series observed in the field, the temperature signal of interest (typically diurnal) must be isolated from other periodic signals, high-frequency noise, and/or long-term trends in temperature. Signal processing techniques include band-pass filtering (Hatch et al., 2006), sinusoidal curve matching (Swanson and Cardenas, 2011), and dynamic harmonic regression (Young et al., 1999; Keery et al., 2007). Two MATLAB computer programs are available at no cost to process temperature time series data and solve the analytical equations: ExStream (Swanson and Cardenas, 2011) and VFLUX (Gordon et al., 2012; hydrology.syr.edu/vflux).

9.5.4.3 Numerical Methods

In addition to the analytical solutions, numerical models can be used to simulate multidimensional heat transport and allow for consideration of streambed heterogeneity when modeling the rates of SW-GW exchange. Although several numerical heat transport models are available, two commonly used programs with graphical user interfaces, available at no cost from the USGS, are VS2DH (Healy and Ronan, 1996; Hsieh et al., 2000) and 1DTempPro (Voytek et al., 2014). VS2DH is a finite difference model that solves Equation 9.38 in one or two dimensions. VS2DH has been used to model the rates of SW-GW exchange in a variety of setting and field studies (e.g., Stonestrom and Constantz, 2004; Su et al., 2004; Naranjo et al., 2012) and has been used to evaluate the performance of the analytical methods under conditions that violate the analytical model assumptions (e.g., Lautz, 2010). 1DTempPro is a graphical user interface for VS2DH that is designed to facilitate calibration of a 1D VS2DH model to observed vertical temperature profiles. Through model calibration to observed data, the user can infer rates of vertical SW-GW exchange and estimate hydraulic conductivity if the hydraulic gradient across the profile is known (Voytek et al., 2014).

9.5.4.4 Empirical Relationships between Temperature and Flux

In addition to analytical and numerical models of heat transport, empirical relationships between streambed temperatures and SW-GW exchange flux rates have been used to map the spatial distribution of vertical water exchange across the streambed interface with relatively high spatial resolution (Conant, 2004; Schmidt et al., 2007; Lautz and Ribaudo, 2012; Gordon et al., 2013). To develop empirical relationships between flux and temperature, temperatures measured at a given point in time in the streambed (point-in-time temperature measurements) are plotted versus SW-GW exchange rates measured at the same time and place, and a rating curve is developed using regression. Rating curves can be linear or nonlinear, depending on the observed relationships between flux and temperature. SW-GW exchange rates must be measured at several (e.g., 10) different locations with contrasting bed temperatures to establish a reliable rating curve, which can then be applied to hundreds of mapped temperatures. Measurements of SW-GW exchange for rating curve development are made using Darcy flux estimates from measurements of hydraulic gradient and conductivity (Conant, 2004) or results of 1D heat transport modeling of vertical temperature profiles (Lautz and Ribaudo, 2012; Gordon et al., 2013), as described earlier. Empirical relationships are valid for one particular point in time and for one particular site, so to create maps of SW-GW exchange for different times or different locations, new empirical relationships must be develop for each instance.

9.5.5 Limitations of One-Dimensional Solutions for Heat Tracing

Commonly used heat tracing of SW-GW exchange (see also Section 9.6) using 1D analytical solutions in Table 9.2 relies on several simplifying assumptions that are often violated in actual field settings. These simplifying assumptions include a homogeneous isotropic saturated sediment matrix, 1D vertical flow only, a sinusoidal temperature signal and no thermal gradient with depth (in the case of time series methods), and a steady-state fluid flux (Bredehoeft and Papadopulos, 1965; Stallman, 1965). A number of recent studies indicated in Table 9.3 have explored the limitations of heat tracing methods under conditions that violate these model assumptions. Methodology of these studies was based on modeling and, to a lesser extent, through controlled laboratory experiments. Very few field studies (e.g., Jensen and Engesgaard, 2011; Briggs et al., 2012) have compared 1D heat tracing with other direct measurements of SW-GW exchange rates. Before applying heat tracing methodology in the field, potential limitations imposed by site-specific field conditions, uncertainty in thermal parameters, and limitations of measurement equipment should be explored.

TABLE 9.3 Examples of Literature Exploring Limitations of 1D Heat Tracing Methodology

Potential Source of Error	References
Non-steady-state temperature profile[a]	Anibas et al. (2009), Schornberg et al. (2010)
Thermal gradient with depth[b]	Lautz (2010)
Flow in 2D or 3D, rather than vertical only	Lautz (2010), Ferguson and Bense (2011), Cuthbert and Mackay (2013)
Nonsinusoidal temperature signals (interpreted both with and without signal processing)	Lautz (2010, 2012)
Non-steady-state water exchange rates through time	Lautz (2012)
Heterogeneity of streambed sediments	Schornberg et al. (2010), Ferguson and Bense (2011), Irvine et al. (2015), Naranjo et al. (2013)
Inaccuracy of temperature observations	Cardenas (2010), Shanafield et al. (2011), Soto-Lopez et al. (2011)
Uncertainty in thermal parameters	Munz et al. (2011), Shanafield et al. (2011)

[a] Violates assumption of Turcotte and Shubert (1982) and Bredehoeft and Papadopulos (1965) methods only.

[b] Violates assumption of Hatch et al. (2006), Keery et al. (2007), Luce et al. (2013), and McCallum et al. (2012) methods only.

9.6 Field Methods for Quantifying GWSWIs

Just as the interest in quantifying exchange between GW and SW continues to rapidly increase, so do the advancements of instruments and methods for quantifying the exchange. This section presents many of the field-based methods available for determining flow across the sediment–water interface in a wide range of physical settings ranging from wetlands to lakes to streams and rivers to estuaries and marine environments. None of these methods are appropriate for all physical settings, but some of the methods can be used in a wide range of applications. Some of the methods are qualitative and are important reconnaissance tools that can be combined with other techniques to efficiently focus efforts in areas of rapid or substantial exchange.

Several reviews of methods for quantifying exchange at the sediment–water interface have been published within the last decade. Although some encompass a wide range of physical settings (Rosenberry and LaBaugh, 2008), most have focused on particular types of environments, including lakes (Rosenberry et al., 2013), streams and rivers (Kalbus et al., 2006), wetlands (Rosenberry and Hayashi, 2013), wetlands in arid settings (Jolly et al., 2008), and marine settings (Burnett et al., 2006; Moore, 2010). Fleckenstein et al. (2010) provide an overview in their introduction to an entire topical journal issue focused on methods and processes at the sediment–water interface; most studies in the special issue were conducted in streams and rivers. Krause et al. (2014) provide an overview for another journal issue devoted primarily to new modeling techniques for quantifying GW-SW exchange.

This section presents a brief summary of methods for quantifying such exchange and then focuses on recent improvements and new methodologies. The reader is directed to the aforementioned review papers for details and equations specific to each method.

Methods for quantifying exchange between GW and SW can be arranged from a watershed scale to a local scale and include (1) net stream/river flow gain or loss (seepage runs), (2) baseflow analysis, (3) water budget or combined water and chemical budget, (4) natural and induced tracers, (5) temperature-based methods, (6) hydraulic-gradient (Darcy) methods including numerical models, and (7) direct measurements (seepage meters). Each is discussed in greater detail below.

9.6.1 Net Gain or Loss in River/Stream Flow

Commonly referred to as a seepage run, measuring the difference in stream discharge at two points on a stream at approximately the same time, and attributing the difference to net exchange between the stream and GW along the stream reach, has been in practice since at least the early 1940s (Meinzer, 1942). An important assumption associated with this method is that runoff, precipitation, and evapotranspiration are all so small that they can be ignored. Therefore, discharge measurements are commonly made when streamflow is relatively stable and ideally also during times when evapotranspiration is expected to be small and no rainfall has occurred for several days prior to stream-discharge measurements. Tributary inputs and off-channel diversions from or to each study reach also are measured and subtracted from the difference between the upstream and downstream discharge measurements. The scale of the determination of the net GW flow to or from the stream is proportional to the distance between the upstream and downstream discharge measurements along each stream reach. The method provides an indication of the net GW exchange with the stream; areas of flow from GW to the stream and flow from the stream to GW, both can exist along a particular stream reach but only the net exchange can be determined (see Equation 9.17). Streams can be partitioned into numerous segments and the net exchange between each pair of stream-discharge locations is determined (e.g., Donato, 1998). The shorter the distance between discharge measurements, the greater the spatial resolution of GW-SW exchange. However, the net exchange between GW and the stream needs to be larger than the uncertainty associated with the discharge measurements (LaBaugh and Rosenberry, 2008). Therefore, this method is best suited for streams where stream discharge is small and gains or losses along stream reaches are relatively large. Because of this constraint, seepage runs are not well suited for rivers with larger discharge because the error associated with measuring river discharge commonly is much larger than the change in discharge along a typical river reach of interest. For streams and rivers that vary substantially in discharge, seepage runs are most often conducted during periods of smaller discharge (Riggs, 1972; Wheeler and Eddy-Miller, 2005).

Additional information can be obtained when other measurements are combined with the standard seepage run (e.g., Dumouchelle, 2001). For example, Simonds and Sinclair (2002) combined GW discharge determined for each stream reach with hydraulic gradient determined with in-stream piezometers at several locations along each stream reach. They were able to determine a scale-appropriate value for hydraulic conductivity for use in a subsequent basin-scale GW flow model. Other studies have made a clever use of stage–discharge relations at gauging stations upstream and downstream of a particular stream reach. Liu and Sheng (2011) related upstream and downstream discharge to determine temporal variability in net GW exchange and distinguished that exchange from evapotranspiration. Others have compared differences in discharge measured at permanently installed gauging stations with synoptic data from subreaches within the same stream reach to show substantial exchanges between GW and stream water even though the net exchange based on differencing data from the permanent gauging stations was too small to distinguish (Becker et al., 2004; Schmadel et al., 2010). Another study (Ruehl et al., 2006) used multiple methods, including a transient storage model (Choi et al., 2000; Harvey and Wagner, 2000) to distinguish between solute losses due to hyporheic exchange and losses due to stream water flowing to GW.

9.6.2 Baseflow Analysis

Another method that provides a measure of GW discharge to a stream integrated over a stream-catchment scale is to distinguish streamflow derived from GW discharge (baseflow) from streamflow derived from runoff in response to rainfall events. The numerous methods used to determine the component of total streamflow derived from discharge of GW to the stream can generally be grouped into (1) those based on separating the streamflow hydrograph into periods influenced by storm events and periods exhibiting low flow or baseflow, commonly termed "hydrograph separation" and (2) those based on the log-linear slope of streamflow recession following storm events, commonly termed "streamflow recession analysis." Several hydrograph-separation algorithms have been developed to separate these two components, such as PULSE, PART, and HYSEP (e.g., Rutledge and Daniel, 1994; Sloto and Crouse, 1996; Rutledge, 1998; Rutledge, 2000). All are arbitrary to some degree. Several of these methods have recently been included in a USGS data analysis user interface called the Groundwater Toolbox (Barlow et al., 2015). Studies have also compared results of multiple methods and demonstrate the variability among methods (Eckhardt, 2008). Automated methods can be used to quickly estimate baseflow across a broad region, extending even to a national scale (Wolock, 2003). One relatively new approach is to substitute hydrographs based on water levels in monitoring wells for the traditional streamflow hydrograph (Rutledge, 2014).

9.6.3 Water and Chemical Budgets

Water budgets have been used for many decades to manage water resources and investigate various hydrologic components (Healy et al., 2007), commonly by measuring the easier-to-quantify components to solve for the more difficult components, notably evaporation or GW. The concept is deceptively simple—water in minus water out equals change in storage, or water in minus water out ± change in storage equals the missing component of interest, in this case GW. A substantial problem with this method is that errors associated with each of the water budget components are also included in the solution for net GW exchange (Winter, 1981a). Another problem is that only net GW (the sum of flow from GW to SW and flow from SW to GW) can be determined with this method. This may not be a problem for some settings where it can be reasonably assumed that exchange between GW and SW is all in the same direction, but those settings are a small subset compared to the much larger number of settings where flow across the sediment–water interface occurs in both directions. A common example is a "seepage lake," where GW flows to one side of a lake and lake water flows to GW along the other side of the lake.

However, if a conservative chemical is present in varying concentrations in all or most of the hydrologic components, measuring the concentration of the conservative constituent for each of the measurable water budget components gives us two equations to solve. With two equations and two unknowns, this method allows a solution for both the volume of GW flow to SW and the volume of SW flow to GW (see Section 9.4). This method has been used for many years, and numerous papers describe the method in great detail (e.g., LaBaugh and Winter, 1984; Krabbenhoft et al., 1990b; Choi and Harvey, 2000), including how to deal with various sources of error and uncertainties (LaBaugh et al., 2009; Winter and Rosenberry, 2009). Uncertainties depend considerably on the conservative constituent of interest and whether that chemical or component actually is conservative. With the advancement in analytical capability and associated reduction in the cost of analysis, deuterium and oxygen-18 isotopes are increasingly becoming the constituents of choice (e.g., Krabbenhoft et al., 1994; Hunt and Krabbenhoft, 1996; Reddy et al., 2006; Cook, 2013; Sacks et al., 2014).

Water and nutrient budgets have been recently combined with other methods to learn more about the geologic setting that controls the distribution of exchange between GW and SW. For example, vertical temperature profiling (described in Section 9.5 and later) was used to determine the percent of nutrients discharged to a lake in areas of focused GW discharge relative to the total nutrient discharge to the lake (Meinikmann et al., 2013). Hydraulic conductivity of a clogging layer at the sediment–water interface of two other lakes was determined by relating hydraulic gradients from a network of wells to GW discharge calculated from a lake water budget (Rudnick et al., 2014).

9.6.4 Natural and Induced Chemical Tracers

Tracers, whether natural or injected, are commonly used in fluvial settings to quantify transport of stream water and its interaction with the subsurface. Fundamentals of GWSW solute exchanges were expounded in Section 9.4. Here, we address important technical aspects that are paramount for obtaining the representative data from chemical tracer tests. Dilution gauging is combined with the knowledge of the injected tracer mass (M_{in}) and the observed in-stream concentration time series, $C_{us}(t)$, to estimate discharge, Q_{us}, as follows:

$$Q_{us} = \frac{M_{in}}{\int_0^t C_{us}(t)dt} \tag{9.47}$$

The application of this method requires that the in-stream observation be conducted as closely as possible to the injection location (to minimize tracer mass loss) but a sufficient distance downstream to achieve complete mixing in the vertical and lateral dimensions (Kilpatrick and Cobb, 1985). Mixing lengths may be calculated based on empirical relationships. Fischer et al. (1979) suggest that estimates can be made by first calculating the lateral dispersion coefficient (E_{lat}, m² s⁻¹)

$$E_{lat} = 0.6HU^* \tag{9.48}$$

where

H is the river depth (m)
U^* is the shear velocity (m s^{-1})

From this value, lengths to achieve complete lateral mixing (L_m, m) can be determined for tracer releases to the stream centerline

$$L_m = 0.1U\frac{B^2}{E_{lat}} \quad (9.49)$$

and for releases at the stream bank

$$L_m = 0.4U\frac{B^2}{E_{lat}} \quad (9.50)$$

where
B is the stream width (m)
U is the mean stream velocity (m s^{-1})

In headwater streams, visual estimates may be more reliable than empirical formulae (Day, 1977). As a practical consideration, release of a visual tracer that does not interfere with the tracer used for dilution gauging can provide visual, rapid confirmation of mixing. Examples include fluorescein dye or milk.

In more recent developments, this injected tracer mass is allowed to be transported downstream through a study reach (commonly 100–200 m), and a second observation of the in-stream tracer concentration is made at a location with known discharge ($C_{ds}(t)$ and Q_{ds}, respectively). Thus, discharge and concentration time series are known at both upstream and downstream ends of the study reach. The tracer mass recovered at the downstream location (M_{rec}) can be calculated as

$$M_{rec} = Q_{ds}\int_0^t C_{ds}(t)dt \quad (9.51)$$

Using these data, Payn et al. (2009) determined the estimate of both net changes in discharge ($\Delta Q = Q_{ds} - Q_{us}$) as well as the gross gains and losses through the study reach.

Stream reaches simultaneously gain water from and lose water to the subsurface through a study reach. For gross gains and losses, end members bounding the possible values include assumptions of gain before loss, or loss before gain. These assumptions, respectively, allow the estimation of minimum and maximum gross losses ($Q_{loss,\,min}$ and $Q_{loss,\,max}$)

$$Q_{loss,min} = \frac{M_{rec} - M_{in}}{\int_0^t C_{us}(t)dt}, \quad Q_{loss,max} = \frac{M_{rec} - M_{in}}{\int_0^t C_{ds}(t)dt} \quad (9.52)$$

These estimates of gross losses, combined with the known ΔQ, can be used to estimate bounds for gross gains as

$$Q_{gain,min} = \Delta Q - Q_{loss,min}, \quad Q_{gain,max} = \Delta Q - Q_{loss,max} \quad (9.53)$$

This analysis has been applied in several recent studies (Payn et al., 2009; Schmadel et al., 2010; Covino et al., 2011; Ward et al., 2013a,b). Exchanges that are based on mass that is lost from the stream and not recovered at the downstream observation are termed "long-term storage" (Ward et al., 2013a,b). The tracer mass that is observed at the downstream location is the complimentary "short-term storage," meaning that the timescales of transport are rapid enough to be observed within the stream (i.e., returns of solute mass to the stream are in large enough magnitude to be observed in $C_{ds}(t)$).

The short-term storage time series, indicating the solute that is primarily advected in the SW body with tailing due to exchange with slower-moving domains such as in-stream dead zones and/or HZs, is commonly interpreted using one of two methods. First, numerical models of transport and fate are commonly applied (see discussion of the transient storage model in this chapter; review by Runkel et al. (2003)). Second, a host of metrics describing the shape of the field observation can be estimated. For example, the skewness of the recovered solute tracer signal (C_{ds}) could be interpreted to estimate the relative interaction of stream water with short-term storage in the study reach. Examples of work using such metrics include Ward et al. (2013a,b), Koestel et al. (2011), Dankwerts (1953), and Schmid (2003).

Finally, tracers recently applied in hyporheic settings for the purpose of quantifying the GW component include carbon-14 contained in dissolved inorganic carbon (Bourke et al., 2014b) to quantify GW discharge and radon-222 (Cook, 2013; Bourke et al., 2014a) to quantify the extent of hyporheic exchange in a stream reach that loses water to GW.

9.6.5 Temperature as a Tracer

Temperature has long been used as a qualitative tool to identify areas of fluxes between GW and SW (Stonestrom and Constantz, 2004; Anderson, 2005), and foundations of this approach have been described in Section 9.5. If GW seepage is sufficiently fast, and the temperatures of GW and SW are sufficiently different, the GW temperature is imparted to the sediment–water interface, resulting in an easily measured difference in the temperature of the sediment bed (e.g., Lee, 1985).

If GW discharge is substantial and occurs where SW is shallow, the temperature signal is transmitted to the water surface and can be detected remotely (Lee and Tracey, 1984; Banks et al., 1996; Gosselin et al., 2000; Tcherepanov et al., 2005; Lewandowski et al., 2013). Discrete measurements of the bed temperature, although much more labor intensive, provide the same ability to isolate areas of focused GW discharge (Conant, 2004; Schmidt et al., 2006).

Discrete measurements of the bed temperature, although labor intensive, provide the ability to map areas of focused GW discharge (Conant, 2004; Schmidt et al., 2006). If GW discharge is substantial and occurs where SW is shallow, the temperature signal is transmitted to the water surface and can be detected remotely (Lee and Tracey, 1984; Banks et al., 1996; Gosselin et al., 2000; Tcherepanov et al., 2005; Lewandowski et al., 2013). High-resolution forward-looking infrared (FLIR) cameras are particularly useful for detecting and displaying areas of the water surface influenced by rapidly discharging GW (Cardenas et al., 2008; Dunckel et al., 2009).

Much of the recent advance of this method has been associated with vertical temperature profiling and dealing with assumptions associated with the method. This method was applied primarily in fluvial settings (Lapham, 1989; Silliman and Booth, 1993; Taniguchi, 1993; Constantz and Thomas, 1996; Constantz et al., 2002). A common assumption is that flow across the sediment–water interface is vertical, allowing for a 1D solution. Some have indicated that flow is not vertical, particularly in hyporheic settings (Naranjo et al., 2012, 2013; Rosenberry et al., 2012), and advances have been made (Lautz, 2010) that allow solutions for nonvertical flow (Gordon et al., 2012). Another assumption is that vertical flow is relatively uniform in space and time, which clearly is not the case in most settings (e.g., Schmidt et al., 2006; Keery et al., 2007; Chen et al., 2009; Lautz, 2010).

Recent technological advances have made temperature measurement at the sediment–water interface vastly more efficient. Multiple thermistors can be buried in a sediment bed and aligned both vertically and horizontally around a central heat source that can be pulsed. The measurement of the thermal response by the surrounding thermistors provides determination of the rate and direction of flow through sediments in the vicinity of the sediment–water interface (Lewandowski et al., 2011). Draping a fiber-optic cable across or along the sediment bed and pulsing a light down the cable allows determining the temperature of the sediment bed continuously in time and space. This method, the distributed temperature system, or DTS (Selker et al., 2006a,b; Tyler et al., 2009), is most often used by draping the fiber-optic cable across the bed to detect spatial heterogeneity in temperature and, therefore, relative GW discharge to SW. However, it can also be used in a vertical orientation. For example, a high-resolution temperature sensors (HRTSs) can be made by wrapping a fiber-optic cable around a rod, such that the spatial resolution of temperature sensing along the cable is improved from the meter-scale to the centimeter-scale along the rod (Vogt et al., 2010; Briggs et al., 2012b). The temperature time series recorded at a multitude of depths can be modeled using 1D analytical solutions presented in Section 9.5 to determine vertical flux rates with high spatial resolution. HRTS can be installed as individual sensors (Vogt et al., 2010) or in series such that several rods can be installed at one field site (Briggs et al., 2012). Alternatively, fiber-optic cables can be spread horizontally and stacked such that one cable is directly above another, running parallel and separated by a small vertical distance. In this manner, temperature time series can be recorded at multiple depths over long horizontal distances (Mamer and Lowry, 2013). DTS has allowed much improved detection of GW discharge in settings ranging from wetlands (Lowry et al., 2007) to streams (Briggs et al., 2012a, 2013; Krause et al., 2012) to lakes (Blume et al., 2013; Sebok et al., 2013) and marine settings (Henderson et al., 2009; Anderson et al., 2014).

9.6.6 Hydraulic-Gradient-Based Methods

Exchange between GW and SW can be determined by measuring the hydraulic gradient between GW and the adjacent SW body, and also the hydraulic conductivity of the porous media through which the GW flows, according to Darcy's law

$$Q = KA\frac{dh}{dl} \tag{9.54}$$

where

K is the hydraulic conductivity
A is the area of exchange between GW and SW
dh/dl is the hydraulic gradient (e.g., LaBaugh and Rosenberry, 2008)

This is one of the most commonly used methods for determining GW-SW exchange and might be used even more if not for the uncertainty in determining the hydraulic conductivity. The geologic complexity of sediments at and near the sediment–water interface, the orders-of-magnitude variability in K, and the scale-dependence of K measurements (Rovey and Cherkauer, 1995) all serve to make determination of this parameter very difficult in many settings. Point measurements of K with single-well slug tests are often not representative on a whole-lake or stream-reach scale. Therefore, numerically simulating flow on a lake-basin or stream-reach scale is often a preferred way to determine a scale-appropriate value for K (Brunner et al., 2010). Several geophysical tools, such as ground-penetrating radar, electrical resistivity, and electromagnetic induction, can be used to better understand the spatial distribution of geologic and associated hydrogeological properties near and beneath sediment beds (e.g., Ong et al., 2010; Toran et al., 2010, 2014; Befus et al., 2012; Briggs et al., 2013). Combining new modeling capability with multiple field-based methods is particularly fruitful for improving understanding of near-shore processes (e.g., Karan et al., 2014).

9.6.7 Direct Measurements with Seepage Meters

A seepage meter is an open-ended cylinder that, when placed on the bed of SW body, collects flow across the portion of the sediment–water interface covered by the meter and routs the flow into a seepage collector (Rosenberry and LaBaugh, 2008). Although this device has been available since the early 1940s, its use increased greatly when a much simplified design was introduced in the late 1970s (Lee, 1977). The device provides a direct measurement of flow as opposed to all other methods that infer the seepage exchange from other measured parameters. One substantial limitation for many studies is the local-scale measurement it provides. Most designs cover only 0.25 m^2 of bed area, introducing issues of the localized scale of the measurement relative to the scale of the investigation. Design improvements include the use of highly flexible, low-resistance bags and operating the bags in the mid-range of bag fullness (Murdoch and

Kelly, 2003), use of larger-diameter bag-connection hardware (Fellows and Brezonik, 1980), placing the bag inside a shelter to eliminate velocity-head effects (Sebestyen and Schneider, 2001), connecting several cylinders to a single bag to increase the surface area and better address bed heterogeneity (Rosenberry, 2005), and several modifications to make the device suitable for use in fluvial settings (Rosenberry, 2008). Duration of measurement depends on the seepage rate and the size of the seepage bag and ranges from minutes to days. One potential drawback is that a time-integrated value is provided with each bag measurement. Several devices have replaced the bag with a flowmeter to provide better temporal resolution (Paulsen et al., 2001; Taniguchi and Iwakawa, 2001; Rosenberry and Morin, 2004; Fritz et al., 2009; Koopmans and Berg, 2011).

Recent studies have addressed concerns related to spatial and temporal heterogeneity. Seepage meters deployed in several fluvial settings indicate seepage is highly variable and is largely controlled by local-scale bed topography (Rosenberry and Pitlick, 2009; Rosenberry et al., 2012). Seepage in near-shore marine settings also has been shown to be highly variable and is commonly a mix of fresh and recirculated water (e.g., Michael et al., 2003; Swarzenski et al., 2007; Bokuniewicz et al., 2008; Stieglitz et al., 2008; Taniguchi et al., 2008; Santos et al., 2009). Seepage meters combined with geophysical methods in a range of settings have indicated that geology greatly controls the distribution of seepage (Simonds et al., 2008; Toran et al., 2010; Russoniello et al., 2013), leading to the conclusion that knowledge of geology is vitally important in understanding seepage heterogeneity. Temporal variability in seepage has recently been shown to be much greater than previously thought; seepage can respond within minutes to wind, evapotranspiration, rainfall, and lake seiche (Rosenberry et al., 2013).

9.6.8 Multiple Methods

Multiple methods are increasingly being used to quantify exchanges between GW and SW both to better determine fluxes and reduce uncertainty and to increase understanding of processes that control seepage exchange (e.g., Burnett et al., 2006; Mulligan and Charette, 2006; Ivkovic, 2009; Kikuchi et al., 2012; Karan et al., 2013; Kidmose et al., 2013; Yang et al., 2014). Continued advances are likely to stem from additional combinations of multiple methods in a wider variety of physical settings.

9.7 Modeling

9.7.1 Simulating at the Interface of Hydrology and Hydrogeology

The interactions between SW and GW are complex and difficult to observe or quantify directly in the field. Numerical modeling techniques are therefore an important tool to understand GWSWIs across different spatial and temporal scales. However, hydrology and hydrogeology have to some degree developed as independent scientific disciplines. This separation is reflected in the conceptual models of the two disciplines: typically, models developed by hydrologists do not explicitly consider the subsurface, whereas most models developed by hydrogeologists conceptualize the surface through simple boundary conditions. Because water fluxes between these two components are naturally continuous, breaking the system down into surface and subsurface components limits a solid understanding of the water as a single resource (Winter et al., 1998). A large number of numerical models simulating GW-SW interactions are now available, including MikeShe (Refsgaard and Storm, 1995), MODFLOW (Harbaugh, 2005), FEFLOW (see e.g., Trefry et al., 2007), and GSFLOW (Markstrom et al., 2008), to mention but a few.

As in any modeling approach, the extent to which a model is suited to simulate a system is intrinsically linked to its conceptualization. Many of the available hydrological and hydrogeological models have limited ability to simulate GWSWIs. For example, if the river is represented through a boundary condition with predefined width, depth, and location, it is impossible to simulate the feedback mechanisms between the surface and the subsurface. In such a model, the reduction of streamflow caused by a nearby pumping cannot be simulated. Also, the increased river discharge or flooding in response to rising GW levels is not reproduced. A related example is the conceptualization of the streambed. If a model couples the surface and the subsurface through a hydraulic conductance approach, the user implicitly employs the assumptions that are embedded in this concept, that is, that the streambed and the aquifer are separate and clearly defined compartments and that the streambed has a constant thickness. A third example is related to the surface flow equations used in the model. Computational fluid dynamics (CFD) approaches have been successfully employed to simulate hyporheic fluxes by solving the Navier–Stokes equation for the water column, and Darcy's law and the continuity equation for the streambed (Cardenas, 2009). Most hydrological and hydrogeological models conceptualize surface flow through the diffusion wave approximation, introducing bias in the pressure distribution along variations of the streambed for turbulent stream conditions and affecting the accuracy of simulations of hyporheic exchange. These examples illustrate the importance of choosing an appropriate model for the problem considered.

9.7.2 Approaches to the GW-SW Coupling

Different approaches to classify hydrological and hydrogeological models exist. Kampf and Burges (2007) presented a thorough review of a distributed hillslope and catchment hydrologic models. They provided a historical perspective on hydrologic modeling and then reviewed existing approaches for catchment modeling. From a hydrogeological point of view, those approaches include models that assume homogeneous subsurface properties, such as TOPMODEL (Beven et al., 1995) or GW flow models that can simulate heterogeneous subsurface properties, but which interact with surface flow through boundary conditions, such as MODFLOW (Harbaugh, 2005).

Morita and Yen (2000) have classified the models according to the coupling between GW and SW. Three levels of coupling exist between them (Morita and Yen, 2000): no coupling, iterative coupling, and full coupling. In a model with no coupling, the equations for the surface and the subsurface are solved without any feedback.

In a model with no coupling, the equations for the surface and the subsurface are solved without any feedback. An infiltration boundary between the surface and subsurface is used as a common boundary condition. This type of coupling is standard for analytical models.

In the second level of coupling, a certain degree of feedback between SW and GW is possible. In this approach, either the surface or subsurface domain is used to update the internal boundary during the simulation. This type of coupling has been referred to as alternative coupling (Morita and Yen, 2000) or iterative coupling (Furman, 2008). MODFLOW and GSFLOW, most widely used models that can account for rivers, streams, and lakes (Merritt and Konikow, 2000; Prudic et al., 2004; Niswonger and Prudic, 2005), fall into the iterative coupling category. GSFLOW (Markstrom et al., 2008) significantly extends the capabilities of MODFLOW for the simulation of coupled GW and SW/watershed processes. This model simulates overland flow via rainfall–runoff relations, soil-zone and one-dimensional (vertical) unsaturated-zone flow, head-dependent GW discharge and SW leakage to streams and lakes, and three-dimensional GW flow. These models are examples of efficient, physically based approaches for the simulation of SW-GW interactions. This is the most commonly achieved level of coupling in applications that follow the Freeze and Harlan (1969) ideas by integrating various processes of hydrological cycle. These ubiquitous and accessible USGS reports provide comprehensive coverage of theory and applications.

In the third and most complex level of coupling, the interface equation and the two systems are solved simultaneously. It is only in this formulation that the physics of the GWSWIs are represented comprehensively. Such models also allow for "self-generating systems," where rivers and lakes can form naturally within the imposed topography in response to the climatic and hydraulic forcing functions. These models are based on a blueprint presented by Freeze and Harlan (1969). Examples of models that are based on the Freeze and Harlan (1969) blueprint include InHM (VanderKwaak, 1999), MODHMS (Panday and Huyakorn, 2004), HydroGeoSphere (Therrien et al., 2010), PARFLOW (Kollet and Maxwell, 2006), FIHM (Kumar et al., 2009), and OpenGeoSys (Kolditz et al., 2012). Maxwell et al. (2014) provide a more detailed description of these models and a set of benchmark problems to assess integrated hydrological models. Those 3D integrated models generally represent 3D subsurface flow by Richards' equation for variably saturated flow and are therefore computationally more demanding, for example, GSFLOW that "takes advantage of the fact that the dominant direction of flow within the unsaturated zone usually is vertical when averaged over large areas" (Markstrom et al., 2008).

Some fully coupled models are capable of jointly simulating fluid flow and solute transport. Typically, they solve 2D advective–dispersive transport for the surface domain and the 3D advective–dispersive equation for the subsurface. Examples of transport solutions are given in Therrien et al. (2010), Panday et al. (2009), and Weill et al. (2011). Heat transport equations, similar to mass transport equations, have been introduced in some models, for example, in the HydroGeoSphere model (Brookfield et al., 2009). A few integrated models have capabilities for sediment transport. Heppner et al. (2006) extended the InHM model to simulate sediment transport in the surface domain.

9.7.3 Setting Up and Interpreting GWSWI Models

Simulating GWSWI brings along some challenges and requirements to the input data set and the discretization of the model. Käser et al. (2014) highlight the importance of streambed and riverbank topography for iterative and fully coupled models, as well as the associated challenges in developing an adequate mesh. As water flows along the topographic gradients of the digital elevation models (DEMs) employed in the model, errors in the elevation data set can result in convergence problems, the erroneous presence (or absence) of lakes and rivers, or the flooding of floodplains due to errors in riverbank elevations. Given that many large-scale DEMs are based on radar data that cannot provide accurate elevation estimates under water-covered areas, DEMs used in numerical models simulating GWSWI typically need to be corrected, as outlined in the tutorials provided by Käser et al. (2014).

A challenge specific to fully coupled models is related to coupling between the surface and the subsurface. A common way to conceptualize the exchange between the surface and the subsurface is through the so-called exchange coefficient (or coupling length) used in, for example, HydroGeoSphere or InHM. Ebel et al. (2009) and Liggett et al. (2012) analyzed the parameter sensitivity for first-order exchange coefficients and provided some guidance on how to select the exchange coefficients. If the coupling between the surface and the subsurface is conceptualized through a continuity of pressure, the streambed properties require an explicit consideration, which naturally raises the question on how the streambed is parameterized and calibrated (see Section 9.7.4).

Finally, iterative and especially coupled models that are based on Richards' equation require a fine vertical discretization. Sciuto and Diekkruger (2010) analyzed the influence of the vertical discretization on a catchments water balance and stressed its importance on the catchments water balance, especially the evapotranspiration rate. Downer and Ogden (2004) highlight the large influence of the vertical discretization on the sensitivity of parameter estimates. The strict requirements to discretization as well as the nonlinear nature of Richards equation and the coupling between the surface and the subsurface lead to very considerable computational times as well as to challenging numerical issues. However, vertical discretization can also be important in models not simulating Richards' equation (e.g., MODFLOW). Brunner et al. (2009a,b) showed that mound height under a disconnected river can be strongly influenced by vertical discretization of the aquifer (corresponding to the number of layers in MODFLOW terminology).

A common limitation to GWSWI models is the inability to directly analyze and interpret flow generation mechanisms and the streamflow hydrograph. Partington et al. (2011) proposed and implemented a hydraulic mixing-cell (HMC) approach in HydroGeoSphere to investigate the GW contribution to streamflow as interpreted at the catchment outlet (i.e., in the streamflow hydrograph). Partington et al. (2013) expanded on the original HMC method to include both overland and in-stream flow generation mechanisms for the broad purpose of deconvolution of a flow hydrograph at any point in space within the model domain. The method could be easily implemented into any other model.

9.7.4 Calibration and Uncertainty Analysis

In any modeling approach, calibration and uncertainty analysis are integral parts of the elaboration of a model. Calibration techniques such as Monte Carlo approaches or Marquardt–Levenberg approaches require a large amount of model runs. Given the typically significant runtimes of GWSWI models, their calibration and subsequent uncertainty analysis are not straightforward, and the computational demand related to the application of standard calibration approaches for physically based models may exceed the capabilities of most researchers and practitioners. This is especially true for fully coupled models and to a certain extent also for iteratively coupled models. Fortunately, a range of new developments in the area of model calibration are opening new possibilities in this regard, including readily available inverse modeling packages such as U-Code (http://igwmc.mines.edu/freeware/ucode/) and PEST (www.pesthomepage.org).

A pragmatic way for calibrating highly parameterized models can be found in the so-called subspace methods, such as the Null space Monte Carlo method (Tonkin and Doherty, 2009). This approach allows to rapidly generate a large amount of parameter combinations that calibrate the available observation data, as opposed to the classical Monte Carlo approaches where most of the generated parameters do not reproduce the observation data sufficiently well to be further considered. Once a sufficiently large range of parameters that calibrate the available observation data has been determined, the uncertainty related to a prediction of interest can be determined. The software package PEST (www.pesthomepage.org) has implemented these advanced calibration and uncertainty concepts. Hill et al. (2015) provide a comprehensive overview on computationally frugal model analysis methods to calculate model uncertainty. Pareto concepts also offer a convenient and relatively model-run-efficient, nonlinear methodology to quantify uncertainty, even where a model employs many parameters. Brunner et al. (2012) combined Pareto methods with linear approaches to calculate predictive uncertainty and parameter identifiability in a complex, fully coupled model. The linear approaches employed allow identifying the data worth of observations under consideration of their measurement accuracy, even before the actual measurement has been carried out. All these approaches can be readily employed in models simulating GWSWIs.

A different approach to calibration and uncertainty analysis is the application of the ensemble Kalman filter for real-time modeling. Real-time observation data are integrated in the modeling process to prevent the model state from diverging from the real systems. Hendricks Franssen et al. (2011) employed this approach successfully in the real-time simulation of GWSWIs using a coupled SW-GW model.

9.7.5 Model-Specific Applications

Sustainable water resource management requires a solid, process-based understanding of GWSWI across vastly different spatial and temporal scales. The choice of the numerical models should take into consideration the spatial scales considered, as well as the dominant processes occurring on the spatial scale under consideration. Owing to their computational efficiency, iteratively coupled models have been widely used to simulate SW interactions on large spatial scales (e.g., for entire river basins or catchments). GSFLOW, for example, has been employed to understand the influence of SW-GW interactions on summertime streamflow in snow-dominated catchments (Huntington and Niswonger, 2012), climate change (Surfleet and Tullos, 2012; Surfleet et al., 2012), or as a tool for integrated decision support systems (Niswonger et al., 2014), to give just some examples on large spatial scales. Iteratively coupled models have also been employed on smaller spatial scales. For example, Fox and Durnford (2003) analyzed the effect of unsaturated flow on stream leakage induced by pumps next to the river by combining the MODFLOW river package with an approximating solution to estimate aquifer drawdown and stream depletion under disconnected (unsaturated) conditions. For an even smaller spatial scale, Käser (2009) used MODFLOW to explore the influence of riffle pool sequences on hyporheic exchanges. These examples demonstrate the polyvalence of applications of iteratively coupled models.

Using fully coupled, physically based models is more challenging for large spatial scales. However, as demonstrated by Kollet et al. (2010), computational power and parallelization of the numerical models have advanced to such a level that it is possible to solve the Richards equation over entire catchments. However, fully coupled models have already been applied previously on a catchment scale, for example, by Li et al. (2008), Abu-El-Shár and Rihani (2007), and Sudicky et al. (2008). Fully coupled models are also increasingly used in the context of climate change simulations, such as Goderniaux et al. (2009, 2011), and Ferguson and Maxwell (2010). Also, fully coupled models have been used to develop hydrological response functions on a catchment scale, for example, Park et al. (2011), Delfs et al. (2012), and Bartsch et al. (2014). Schilling et al. (2014) used HydroGeoSphere to simulate the interactions and feedback mechanisms between SW, GW, and ripairian vegetation along the Tarim River, China. However, the number of applications of fully coupled models on a catchment scale currently remains limited, mainly owing to the significant computational demands in running fully coupled models.

An important application of fully coupled models is in understanding the controls, the physics, and dynamics of SW-GW systems. Frei et al. (2010) used HydroGeosphere to understand how the microtopography of the surface controls the exchange between the surface and the subsurface. PARFLOW has been recently applied to understand how subsurface heterogeneity affects hill slope runoff (Meyerhoff and Maxwell, 2011). Other examples on the application of fully coupled models to explore basic physics are in the area of bank filtration processes (Doble et al., 2012), the disconnection of SW and GW (Brunner et al., 2009a,b), vegetation controls on GWSWI (Banks et al., 2011a), the effect of heterogeneity on surface–subsurface exchange (Frei et al., 2009; Irvine et al., 2012; Kurtz et al., 2013), or the transport and exchange of heat (Brookfield et al., 2009). Fully coupled models have also been applied to assess the credibility of commonly used field approaches. For example, McCallum et al. (2010) simulated solute exchanges between rivers and river banks to quantify the reliability of chemical baseflow separation methods. Partington et al. (2012) used the previously described HMC method to investigate the ability of commonly used hydrograph separation methods to estimate the GW contribution to streamflow by comparison to a synthetic catchment for which the GW contribution could be elicited from the HMC method. Given the difficulties in the field to measure the GW contribution to streamflow, fully coupled modeling approaches are currently the only way to quantitatively compare the performance of hydrograph separation methods.

9.7.6 Challenges and Opportunities

Back in the year 2002, Sophocleous (2002) identified deficiencies in the available GWSWI modeling approaches. A key issue identified was the simplified representation of heterogeneity and anisotropy. He further highlighted that most modeling approaches are 1D or 2D, despite the 3D nature of flow dynamics between SW and GW. An important point to add in this context is that uncertainty analysis is not routinely carried out in the GWSWI modeling community.

With the rapid development of fully coupled models, many of the limitations highlighted in the Sophocleous (2002) paper have, to a certain extent, been addressed on a conceptual basis. For example, 3D flow through the streambed can be simulated in fully coupled models. Also, complex geological structures and topographies can be integrated in the modeling process. The rapid advances in computational power, parallelization of the solvers, and the development of new and powerful approaches for model calibration and uncertainty analysis make the application of such models for catchment scale simulations accessible. Undoubtedly, fully coupled models will also continue to play an important role in developing our process understanding of SW-GW systems. Owing to their computational efficiency, iteratively coupled models will continue to play an essential role in simulating SW-GW interactions for a wide range of water resource management applications.

However, despite this optimistic assessment, important points have to be emphasized. The capabilities of the latest generation of numerical models do not seem to be used to their full extent. With the increased complexity of such models, the need for construction and validation data also increased, and typically the need greatly exceeds the available field data. For example, heterogeneity of the streambed or the subsurface is rarely considered in SW-GW models. The few previously discussed exceptions base their conceptualization of heterogeneity on rather simplistic, multi-Gaussian approaches. More targeted field studies will be required to characterize the subsurface heterogeneity, and the available information has to feed in more advanced geostatstical approaches that go beyond multi-Gaussian simulations. As it is known from the latest studies of HZ, streambed properties are transient and are influenced by sedimentological, thermal, chemical, and biological processes. The modern GWSWI models are currently not capable of simulating such feedback mechanisms fully. Extending the blueprint to this new level of complexity will undoubtedly reveal new insights into the intriguing processes and dynamics and feedback mechanisms between SW and GW systems.

Abbreviations and Glossary

DTS: Distributed temperature sensing
GW: Groundwater
GWSWI: Groundwater–surface water interactions
HZ: Hyporheic zone
SW: Surface water
Bank storage effects: Flow, solute, and heat transport phenomena in the adjacent aquifer, associated with stream-stage changes.
Coupled model of groundwater–surface water interactions: A model that explicitly couples groundwater and surface water flow and sometimes explicitly considers vadose zone, overland flow, and other land surface processes.
Hyporheic zone: The region beneath and alongside a streambed, characterized by mixing of shallow GW and SW and interaction of physical, chemical, and biological processes.
Residence time: The elapsed time from tracer introduction to a moment of achieving a certain characteristic concentration for tracer in groundwater; residence time can be associated with a certain flowpath.
Stream depletion: (Synonymous with "capture") Decrease in discharge of groundwater into the stream plus aquifer recharge (induced infiltration) by the steam, induced by groundwater withdrawals and characterized by rate or volume.

Transient storage zones: Zones of slowly moving surface and subsurface water at channel sides or in shallow subsurface (hyporheic waters), where water, solute, and heat are temporarily stored before re-entering a stream's main channel.

Acknowledgments

The authors acknowledge the thorough and detailed review by P. Barlow, USGS. Any use of trade, firm, or product names is for descriptive purposes only and does not imply endorsement by the U.S. government.

References

Abu-El-Shár, W.Y. and J.F. Rihani (2007) Application of the high performance computing techniques of parflow simulator to model groundwater flow at Azraq basin. *Water Resources Management.* 21(2): 409–425.

Alley, W.M., T.E. Reilly, and O.L. Franke (1999) Sustainability of ground-water resources. U.S. Geological Survey Circular 1186, Denver, CO.

Anderson, M.P. (2005) Heat as a groundwater tracer. *Groundwater.* 43(6): 951–968.

Anderson, M.P. and J.A. Munter (1981) Seasonal reversals of groundwater flow around lakes and the relevance to stagnation points and lake budgets. *Water Resources Research.* 17(4): 1139–1150.

Anderson, R.B., D.L. Naftz, F. Day-Lewis, R.D. Henderson, D.O. Rosenberry, B.J. Stolp, and P. Jewell (2014) Quantity and quality of groundwater discharge in a hypersaline lake environment. *Journal of Hydrology.* 512: 177–194.

Anibas, C., J.H. Fleckenstein, N. Volze, K. Buis, R. Verhoeven, P. Meire, and O. Batelaan (2009) Transient or steady-state? Using vertical temperature profiles to quantify groundwater–surface water exchange. *Hydrological Processes.* 23(15): 2165–2177.

AquaResource Inc. (2011) Integrated Surface and Groundwater Model Review and Technical Guide, Prepared by AquaResource Inc. for The Ontario Ministry of Natural Resources, Peterborough, Ontario, Canada. http://www.scribd.com/doc/134500298/2011-AquaResource-IntegratedModellingGuide#scribd, last accessed on July 14, 2015.

Arrigoni, A.S., G.C. Poole, L.A.K. Mertes, S.J. O'Daniel, W.W. Woessner, and S.A. Thomas (2008) Buffered, lagged, or cooled? Disentangling hyporheic influences on temperature cycles in stream channels. *Water Resources Research.* 44, W09418.

Bakker, M. and E.I. Anderson (2002) Comment on "Numerical investigation of lake bed seepage patterns: Effects of porous medium and lake properties" by Genereux, D., and Bandopadhyay, I., 2001. *Journal of Hydrology.* 241, 286–303; 258: 260–264.

Bakker, M. and E.I. Anderson (2003) Steady flow to a well near a stream with a leaky bed. *Groundwater.* 41(6): 833–840.

Banks, E.W., P. Brunner, and C.T. Simmons (2011a) Vegetation controls on variably saturated processes between surface water and groundwater and their impact on the state of connection. *Water Resources Research.* 47(11): W11517.

Banks, E.W., C.T. Simmons, A.J. Love, and P. Shand (2011b) Assessing spatial and temporal connectivity between surface water and groundwater in a regional catchment: Implications for regional scale water quantity and quality. *Journal of Hydrology.* 404(1–2): 30–49.

Banks, W.S.L., R.J. Paylor, and W.B. Hughes (1996) Using thermal-infrared imagery to delineate ground-water discharge. *Groundwater.* 34: 434–443.

Barlow, P.M., W.L. Cunningham, T. Zhai, and M. Gray (2015) U.S. Geological Survey Groundwater Toolbox, a graphical and mapping interface for analysis of hydrologic data (version 1.0)—User guide for estimation of base flow, runoff, and groundwater recharge from streamflow data. U.S. Geological Survey Techniques and Methods, Reston, VA, Chapter 3-B10, 27p.

Barlow, P.M., L.A. DeSimone, and A.F. Moench (2000) Aquifer response to stream-stage and recharge variations. II. Convolution method and applications. *Journal of Hydrology.* 230: 211–229.

Barlow, P.M. and S.A. Leake (2012) Streamflow depletion by wells—Understanding and managing the effects of groundwater pumping on streamflow. U.S. Geological Survey Circular 1376, Reston, VA.

Barlow, P.M. and A.F. Moench (1999) Analytical solutions and computer programs for hydraulic interaction of stream-aquifer systems. U.S. Geological Survey Open-File Report 98-415A, Marlborough, MA.

Bartsch, S., S. Frei, M. Ruidisch, C.L. Shope, S. Peiffer, B. Kim, and J.H. Fleckenstein (2014) River-aquifer exchange fluxes under monsoonal climate conditions. *Journal of Hydrology.* 509: 601–614.

Battin, T.J. (1999) Hydrologic flow paths control dissolved organic carbon fluxes and metabolism in an alpine stream hyporheic zone. *Water Resources Research.* 35(10): 3159–3169.

Battin, T.J. (2000) Hydrodynamics is a major determinant of streambed biofilm activity: From the sediment to the reach scale. *Limnology and Oceanography.* 45(6): 1308–1319.

Battin, T.J., L.A. Kaplan, S. Findlay, C.S. Hopkinson, E. Marti, A.I. Packman, J.D. Newbold, and F. Sabater (2008) Biophysical controls on organic carbon fluxes in fluvial networks. *Nature Geoscience.* 1(2): 95–100.

Bear, J. (1972) *Dynamics of Fluids in Porous Media.* Dover, New York.

Bear, J. (1979) *Hydraulics of Groundwater.* McGraw-Hill, New York.

Becker, M.W., T. Georgian, H. Ambrose, J. Siniscalchi, and K. Fredrick (2004) Estimating flow and flux of Groundwater discharge using water temperature and velocity. *Journal of Hydrology.* 296: 221–233.

Befus, K.M., M.B. Cardenas, J.B. Ong, and V.A. Zlotnik (2012) Classification and delineation of groundwater–lake interactions in the Nebraska Sand Hills (USA) using electrical resistivity patterns. *Hydrogeology Journal.* 20(8): 1483–1495.

Bencala, K.E. (1983) Simulation of solute transport in a mountain pool-and-riffle stream with a kinetic mass transfer model for sorption. *Water Resources Research.* 19(3): 732–738.

Bencala, K.E and R. Walters (1983) Simulation of solute transport in a mountain pool-and-riffe stream: A transient storage model. *Water Resources Research.* 19(3): 718–724.

Bencala, K.E., G.W. Zellweger, A.P. Jackman, and R.J. Avanzino (1984) Interactions of solutes and streambed sediment: 1. An experimental analysis of cation and anion transport in a mountain stream. *Water Resources Research.* 20(12): 1797–1803.

Bernhardt, E.S. and M.A. Palmer (2007) Restoring streams in an urbanizing world. *Freshwater Biology.* 52(4): 738–751.

Bernhardt, E.S., M.A. Palmer, J.D. Allan, G. Alexander, K. Barnas, S. Brooks, J. Carr et al. (2005) Synthesizing U.S. river restoration efforts. *Science.* 308(5722): 636–637.

Beven, K., P. Lamb, R. Quinn, R. Romanowicz, and J. Freer (1995) TOPMODEL. In V.P. Singh, ed. *Computer Models of Watershed Hydrology.* Water Resources Publications, Highlands Ranch, CO, pp. 627-668.

Blume, T., S. Krause, K. Meinikmann, and J. Lewandowski (2013) Upscaling lacustrine groundwater discharge rates by fiber-optic distributed temperature sensing. *Water Resources Research.* 49: 7929–7944.

Boano, F., J.W. Harvey, A. Marion, A.I. Packman, R. Revelli, L. Ridolfi, and A. Wörman (2014) Hyporheic flow and transport processes: Mechanisms, models, and biogeochemical implications. *Reviews in Geophysics.* 52: 603–679.

Boano, F., R. Revelli, and L. Ridolfi (2007) Bedform-induced hyporheic exchange with unsteady flows. *Advances in Water Resources.* 30: 148–156.

Bokuniewicz, H., M. Taniguchi, T. Ishitoibi, M. Charette, M. Allen, and E.A. Kontar (2008) Direct measurements of submarine groundwater discharge (SGD) over a fractured rock aquifer in Flamengo Bay Brazil. *Estuarine Coastal and Shelf Science.* 76: 466–472.

Born, S.M., S.A. Smith, and D.A. Stephenson (1977) Hydrogeology of glacial-terrain lakes with management and planning applications. *Journal of Hydrology.* 43(1): 7–43.

Bottacin-Busolin, A., A. Marion, T. Musner, M. Tregnaghi, and M. Zaramella (2011) Evidence of distinct contaminant transport patterns in rivers using tracer tests and a multiple domain retention model. *Advances in Water Resources.* 34: 737–746.

Boulton, A.J. (2007) Hyporheic rehabilitation in rivers: Restoring vertical connectivity. *Freshwater Biology.* 52(4): 632–650.

Boulton, A.J., S. Findlay, P. Marmonier, E.H. Stanley, and H.M. Valett (1998) The functional significance of the hyporheic zone in streams and rivers. *Annual Reviews in Ecology and Systematics.* 29(1): 59–81.

Boulton, A.J., T. Tatry, T. Kasahara, M. Mutz, and J.A. Stanford (2010) Ecology and management of the hyporheic zone: Stream–groundwater interactions of running waters and their floodplains. *Journal of North American Benthological Society.* 29(1): 26–40.

Bourg, A.C.M. and C. Bertin (1993) Biogeochemical processes during the infiltration of river water into an alluvial aquifer. *Environmental Science and Technology.* 27(4): 661–666.

Bourke, S.A., P.G. Cook, M. Shanafield, S. Dogramaci, and J.F. Clark (2014a) Characterisation of hyporheic exchange in a losing stream using radon-222. *Journal of Hydrology.* 519(Part A): 94–105.

Bourke, S.A., G.A. Harrington, P.G. Cook, V.E. Post, and S. Dogramaci (2014b) Carbon-14 in streams as a tracer of discharging groundwater. *Journal of Hydrology.* 519: 117–130.

Bouwer, H. (2002) Artificial recharge of groundwater. *Hydrogeology Journal.* 10: 121–142.

Bouwer, H. and T. Maddock, III (1997) Making sense of the interactions between groundwater and streamflow: Lessons for water masters and adjudicators. *Rivers.* 6(1): 19–31.

Bredehoeft, J. (1997) Safe yield and the water budget myth. *Groundwater.* 35(6): 929.

Bredehoeft, J.D. (2002) The water budget myth revisited: Why hydrogeologists model. *Groundwater.* 40(4): 340–345.

Bredehoeft, J.D. (2011) Monitoring regional groundwater extraction—The problem. *Groundwater.* 49(6): 808–814.

Bredehoeft, J.D. and I.S. Papadopulos (1965) Rates of vertical groundwater movement estimated from the Earth's thermal profile. *Water Resources Research.* 1(2): 325–328.

Bredehoeft, J.D., S.S. Papadopulos, and H.H. Cooper, Jr. (1982) Groundwater: The water budget myth. In *Scientific Basis of Water Resource Management*, Studies in Geophysics. National Academy Press, Washington DC, pp. 51–57.

Bridge, J.S. (2003) *Rivers and Floodplains: Forms, Processes, and Sedimentary Record.* Wiley-Blackwell, Oxford, U.K.

Bridge, J.S. and R.V. Demico (2008) *Earth Surface Processes, Landforms and Sediment Deposits.* Cambridge University Press, Cambridge, U.K.

Bridge, J.S. and D.W. Hyndman (2004) Introduction. In Bridge, J.S. and D.W. Hyndman, eds., *Aquifer Characterization.* SEPM Special Publication 80, Tulsa, OK, 176 pp.

Briggs, M.A., M.N. Gooseff, C.D. Arp, and M.A. Baker (2009) A method for estimating surface transient storage parameters for streams with concurrent hyporheic storage. *Water Resources Research.* 45: W00D27.

Briggs, M.A., L.K. Lautz, S.F. Buckley, and J.W. Lane (2014) Practical limitations on the use of vertical temperature profiles to quantify groundwater upwelling. *Journal of Hydrology.* 519(Part B): 1739–1751.

Briggs, M.A., L.K. Lautz, and J.M. McKenzie (2012a) A comparison of fibre-optic distributed temperature sensing to traditional methods of evaluating groundwater inflow to streams. *Hydrological Processes.* 26: 1277–1290.

Briggs, M.A., L.K. Lautz, J.M. McKenzie, R.P. Gordon, and D.K. Hare (2012b) Using high-resolution distributed temperature sensing to quantify spatial and temporal variability in vertical hyporheic flux. *Water Resources Research.* 48(2): 1–16.

Briggs, M.A., E.B. Voytek, F. Day-Lewis, D.O. Rosenberry, and J.W. Lane (2013) Understanding water column and streambed thermal refugia for endangered mussels in the Delaware River. *Environmental Science and Technology*. 47: 11423–11431.

Brookfield, A.E., E.A. Sudicky, Y.J. Park, and B. Conant (2009) Thermal transport modelling in a fully integrated surface/subsurface framework. *Hydrological Processes*. 23(15): 2150–2164.

Broshears, R.E., R.L. Runkel, B.A. Kimball, D.M. McKnight, and K.E. Bencala (1996) Reactive solute transport in an acidic stream: Experimental pH increase and simulation of controls on pH, aluminum, and iron. *Environmental Science and Technology*. 30(10): 3016–3024.

Brunke, M. (1999) Colmation and depth filtration within streambeds: Retention of particles in hyporheic interstices. *International Review of Hydrobiology*. 84: 99–117.

Brunke, M. and T. Gonser (1997) The ecological significance of exchange processes between rivers and groundwater. *Freshwater Biology*. 37: 1–33.

Brunner, P., P.G. Cook, and C.T. Simmons (2009a) Hydrogeologic controls on disconnection between surface water and groundwater. *Water Resources Research*. 45: W01422.

Brunner, P., P.G. Cook, and C.T. Simmons (2011) Disconnected surface water and groundwater—From theory to practice. *Groundwater*. 49(4): 460–467.

Brunner, P., C.T. Simmons, and P.G. Cook (2009b) Spatial and temporal aspects of the transition from connection to disconnection between rivers, lakes and groundwater. *Journal of Hydrology*. 376(1–2): 159–169.

Brunner, P., J. Doherty, and C.T. Simmons (2012) Uncertainty assessment and implications for data acquisition in support of integrated hydrologic models. *Water Resources Research*. 48(7): W07513.

Brunner, P., C.T. Simmons, P.G. Cook, and R. Therrien (2010) Modeling surface water-groundwater interaction with MODFLOW: Some considerations. *Groundwater*. 48: 174–180.

Brutsaert, W. (2005) *Hydrology: An Introduction*. Cambridge University Press, Cambridge, U.K.

Brutsaert, W. and J.L. Nieber (1977) Regionalized drought flow hydrographs from a mature glaciated plateau. *Water Resources Research*. 13(3): 637–643.

Burnett, W.C., P.K. Aggarwal, A. Aureli, H. Bokuniewicz, J.E. Cable, M.A. Charette, E. Kontar et al. (2006) Quantifying submarine groundwater discharge in the coastal zone via multiple methods. *Science of the Total Environment*. 367: 498–543.

Butler, J.J., X. Zhan, and V.A. Zlotnik (2007) Pumping-induced drawdown and stream depletion in a leaky aquifer system. *Groundwater*. 45(2): 178–186.

Butler, J.J., V.A. Zlotnik, and M.S. Tsou (2001) Drawdown and stream depletion produced by pumping in the vicinity of a partially penetrating stream. *Groundwater*. 39(5): 651–659.

Calver, A. (2001) Riverbed permeabilities: Information from pooled data. *Groundwater*. 39(4): 546–553.

Cardenas, M.B. (2009) Stream-aquifer interactions and hyporheic exchange in gaining and losing sinuous streams. *Water Resources Research*. 45: W06429.

Cardenas, M.B. (2010) Thermal skin effect of pipes in streambeds and its implications on groundwater flux estimation using diurnal temperature signals. *Water Resources Research*. 46: W03536.

Cardenas, M.B., J.W. Harvey, A.I. Packman, and D.T. Scott (2008) Ground-based thermography of fluvial systems at low and high discharge reveals complex thermal heterogeneity driven by flow variation and bioroughness. *Hydrological Processes*. 22: 980–986.

Chapelle, F. (1992) *Ground-Water Microbiology and Geochemistry*. John Wiley, New York.

Chen, X. and X.H. Chen (2003) Stream water infiltration, bank storage, and storage zone changes due to stream-stage fluctuations. *Journal of Hydrology*. 280(1–4): 246–264.

Chen, X., Y.Q. Chen, and X.H. Chen (2006) Simulation of baseflow accounting for the effect of bank storage. *Journal of Hydrology*. 327(3–4): 539–549.

Chen, X., J. Sond, C. Cheng, D. Wang, and S. Lackey (2009) A new method for mapping variability in vertical seepage flux in streambeds. *Hydrogeology Journal*. 17: 519–525.

Chen, X.H. (2001) Migration of induced-infiltrated stream water into nearby aquifers due to seasonal groundwater withdrawal. *Groundwater*. 39(5): 721–728.

Cheng, X. and M.P. Anderson (1994) Simulating the influence of lake position on groundwater fluxes. *Water Resources Research*. 30(7): 2041–2049.

Choi, J. and J.W. Harvey (2000) Quantifying time-varying groundwater discharge and recharge in wetlands: A comparison of methods in the Florida Everglades. *Wetlands*. 20(3): 500–511.

Choi, J., J.W. Harvey, and M.H. Conklin (2000) Characterizing multiple timescales of stream and storage zone interaction that affect solute fate and transport in streams. *Water Resources Research*. 36(6): 1511–1518.

Choi, J., S.M. Hulseapple, M.H. Conklin, and J.W. Harvey (1998) Modeling CO_2 degassing and pH in a stream-aquifer system. *Journal of Hydrology*. 209: 297–310.

Christensen, S. (2000) On the estimation of stream flow depletion parameters by drawdown analysis. *Groundwater*. 38(5): 726–734.

Christensen, S., V.A. Zlotnik, and D.M. Tartakovsky (2010) Numerical analysis of implications of designing a pumping test in a leaky aquifer connected to a stream using analytical solutions. *Journal of Hydrology*. 381: 341–351.

COHYST Technical Committee (2004) The 40-year, 28-percent stream depletion lines for the COHYST area west of Elm Creek, Nebraska: Platte River Cooperative Hydrology Study (COHYST), http://cohyst.dnr.ne.gov/adobe/dc012_28-40_lines_092104.pdf, accessed November 20, 2014, 12p.

Conant, B. (2004) Delineating and quantifying groundwater discharge zones using streambed temperatures. *Groundwater.* 42(2): 243–257.

Conant, Jr., B., J.A. Cherry, and R.W. Gillham (2004) A PCE groundwater plume discharging to a river: Influence of the streambed and near-river zone on contaminant distributions. *Journal of Contaminant Hydrology.* 73(1–4): 249–279.

Constantz, J., M.H. Cox, and G.W. Su (2003) Comparison of heat and bromide as groundwater tracers near streams. *Groundwater.* 41(5): 647–656.

Constantz, J., A.E. Stewart, R. Niswonger, and L. Sarma (2002) Analysis of temperature profiles for investigating stream losses beneath ephemeral channels. *Water Resources Research.* 38: 1316.

Constantz, J. and C.L. Thomas (1996) The use of streambed temperature profiles to estimate the depth, duration, and rate of percolation beneath arroyos. *Water Resources Research.* 32: 3597–3602.

Cook, P.G. (2013) Estimating groundwater discharge to rivers from river chemistry surveys. *Hydrologic Processes.* 27: 3694–3707.

Covino, T., B. McGlynn, and J. Mallard (2011) Stream–groundwater exchange and hydrologic turnover at the network scale. *Water Resources Research.* 47: W12521.

Cox, M., D. Rosenberry, G. Su, T. Conlon, K. Lee, and J. Constantz (2002) Comparison of methods to estimate streambed seepage rates. *AWRA Summer Specialty Conference, Ground Water/Surface Water Interactions*, July 1-3, 2002, Middleburg, VA, pp. 519–523.

Cuthbert, M.O. and R. Mackay (2013) Impacts of nonuniform flow on estimates of vertical streambed flux. *Water Resources Research.* 49(1): 19–28.

Dahm, C.N., N.B. Grimm, P. Marmonier, H.M. Valett, and P. Vervier (1998) Nutrient dynamics at the interface between surface waters and groundwaters. *Freshwater Biology.* 40(3): 427–451.

Danckwerts, P. (1953) Continuous flow systems. Distribution of residence times. *Chemical Engineering Science.* 2: 1–13.

Daniel, E.B., J.V. Camp, E.J. LeBoeuf, J.R. Penrod, J.P. Dobbins, and M.D. Abkowitz (2011) Watershed modeling and its applications: A state-of-the-art review. *The Open Hydrology Journal.* 5: 26–50.

Daniluk, T.L., L.K. Lauts, R.P. Gordon, and T.A. Endreny (2013) Surface water–groundwater interaction at restored streams and associated reference reaches. *Hydrological Processes.* 27(25): 3730–3746.

Darama, Y. (2001) An analytical solution for stream depletion by cyclic pumping of wells near streams with semipervious beds. *Groundwater.* 39(1): 79–86.

Day, T.J. (1977) Field procedures and evaluation of a slug dilution gauging method in mountain streams. *New Zealand Journal of Hydrology.* 16(2): 113–133.

Deangelis, D.L., M. Loreau, D. Neegaard, P.J. Mulholland, and E.R. Marzolf (1995) Modeling nutrient-periphyton dynamics in streams—The importance of transient storage zones. *Ecological Modelling.* 80(2–3): 149–160.

Delfs, J.O., F. Blumensaat, W.Q. Wang, P. Krebs, and O. Kolditz (2012) Coupling hydrogeological with surface runoff model in a Poltva case study in Western Ukraine. *Environmental Earth Sciences.* 65(5): 1439–1457.

Dent, C.L., N.B. Grimm, and S.G. Fisher (2001) Multiscale effects of surface–subsurface exchange on stream water nutrient concentrations. *Journal of the North American Benthological Society.* 20(2): 162–181.

Dent, C.L., J.D. Schade, N.B. Grimm, and S.G. Fisher (2000) Subsurface influences on surface biology. In J.B. Jones and P.J. Mulholland, eds., *Streams and Ground Waters*, pp. 381–402, Academic Press, San Diego, CA.

Department of Defense and Environmental Protection Agency (2014) Definition of "Waters of the United States" under the clean water act. *Federal Register.* 79(76): 22188–22247.

Doble, R., P. Brunner, J. McCallum, and P.G. Cook (2012) An analysis of river bank slope and unsaturated flow effects on bank storage. *Groundwater.* 50(1): 77–86.

Domenico, P.A. and F.W. Schwartz (1998) *Physical and Chemical Hydrogeology*, 2nd edn. John Wiley, New York.

Donato, M.M. (1998) Surface-water/ground-water relations in the Lemhi River Basin, East-Central Idaho. U.S. Geological Survey Water-Resources Investigations Report 98-4185, Boise, ID, p. 28.

Doppler, T., H.-J.H. Franssen, H.-P. Kaiser, U. Kuhlman, and F. Stauffer (2007) Field evidence of a dynamic leakage coefficient for modelling river–aquifer interactions. *Journal of Hydrology.* 347: 177–187.

Downer, C.W. and F.L. Ogden (2004) Appropriate vertical discretization of Richards' equation for two-dimensional watershed-scale modelling. *Hydrological Processes.* 18(1): 1–22.

Dumouchelle, D.H. (2001) Evaluation of ground-water/surface-water relations, Chapman Creek, west-central Ohio, by means of multiple methods. U.S. Geological Survey Water-Resources Investigations Report 01-4202, Denver, CO, 13p.

Dunckel, A.E., M.B. Cardenas, A.H. Sawyer, and P.C. Bennett (2009) High-resolution in-situ thermal imaging of microbial mats at El Tatio Geyser, Chile shows coupling between community color and temperature. *Geophysical Research Letters.* 36: L23403.

Ebel, B.A., B.B. Mirus, C.S. Heppner, J.E. VanderKwaak, and K. Loague (2009) First-order exchange coefficient coupling for simulating surface water–groundwater interactions: Parameter sensitivity and consistency with a physics-based approach. *Hydrological Processes.* 23(13): 1949–1959.

Eckhardt, K. (2008) A comparison of baseflow indices, which were calculated with seven different baseflow separation methods. *Journal of Hydrology.* 352: 168–173.

Elliott, A.H. and N.H. Brooks (1997) Transfer of nonsorbing solutes to a streambed with bed forms: Theory. *Water Resources Research.* 33(1): 123 –136.

Ensign, S.H. and M.W. Doyle (2005) In-channel transient storage and associated nutrient retention: Evidence from experimental manipulations. *Limnology and Oceanography.* 50(6): 1740–1751.

Ensign, S.H. and M.W. Doyle (2006) Nutrient spiraling in streams and river networks. *Journal of Geophysical Research*. 111: G04009.

Enzenhoefer, R., W. Nowak, and R. Helmig (2012) Probabilistic exposure risk assessment with advective-dispersive well vulnerability criteria. *Advances in Water Resources*. 36: 121–132.

Fellows, C.R. and P.L. Brezonik (1980) Seepage flow into Florida lakes. *Water Resources Bulletin*. 16: 635–641.

Ferguson, G. and V. Bense (2011) Uncertainty in 1D heat-flow analysis to estimate groundwater discharge to a stream. *Groundwater*. 49(3): 336–347.

Ferguson, I.M. and R.M. Maxwell (2010) Role of groundwater in watershed response and land surface feedbacks under climate change. *Water Resources Research*. 46(10): W00F02.

Fernald, A.G., P.J. Wigington, and D.J. Landers (2001) Transient storage and hyporheic flow along the Willamette River, Oregon: Field measurements and model estimates. *Water Resources Research*. 37(6): 1681–1694.

Ferris, J.G. (1951) Cyclic fluctuations of water levels as a basis for determining aquifer transmissibility. *Proceedings of the International Association of Science Hydrology*, Vol. 2. General Assembly, Brussels, Belgium, pp. 148–155.

Fienen, M.N., J. Luo, and P.K. Kitanidis (2005) Semi-analytical homogeneous anisotropic capture zone delineation. *Journal of Hydrology*. 312(1–4): 39–50.

Findlay, S. (1995) Importance of surface–subsurface exchange in stream ecosystems: The hyporheic zone. *Limnology and Oceanography*. 40(1): 159–164.

Findlay, S. and W.V. Sobczak (2000) Microbial communities in hyporheic sediments. In J.B. Jones and P.J. Mulholland, eds. *Streams and Groundwaters*. Academic Press, San Diego, CA, pp. 287–306.

Fischer, H.B., E.J. List, R.C.Y. Koh, J. Imberger, and N.H. Brooks (1979) *Mixing in Inland and Coastal Waters*. Academic Press, San Diego, CA.

Fisher, S.G., N.B. Grimm, E. Marti, and R. Gomez (1998) Hierarchy, spatial configuration, and nutrient cycling in a desert stream. *Australian Journal of Ecology*. 23(1): 41–52.

Fleckenstein, J., M. Anderson, G. Fogg, and J. Mount (2004) Managing surface water–groundwater to restore fall flows in the Cosumnes River. *Journal of Water Resources Planning and Management*. 130(4): 301–310.

Fleckenstein, J.H., S. Krause, D.M. Hannah, and F. Boano (2010) Groundwater–surface water interactions: New methods and models to improve understanding of processes and dynamics. *Advances in Water Resources*. 33: 1291–1295.

Foglia, L., A. McNally, and T. Harter (2013) Coupling a spatiotemporally distributed soil water budget with stream-depletion functions to inform stakeholder-driven management of groundwater-dependent ecosystems. *Water Resources Research*. 49: 7292–7310.

Fox, G.A. (2004) Evaluation of a stream aquifer analysis test using analytical solutions and field data. *Journal of the American Water Resources Association*. 40(3): 755–763.

Fox, G.A., P. DuChateau, and D.S. Durnford (2002) Analytical model for aquifer response incorporating distributed pumping-induced stream leakage. *Groundwater*. 40(4): 378–384.

Fox, G.A. and D.S. Durnford (2003) Unsaturated hyporheic zone flow in stream/aquifer conjunctive systems. *Advances in Water Resources*. 26(9): 989–1000.

Freeze, R.A. and J.A. Cherry (1979) *Groundwater*. Prentice-Hall, Englewood Cliffs, NJ.

Freeze, R.A. and R.L. Harlan (1969) Blueprint for a physically based, digitally-simulated hydrologic response model. *Journal of Hydrology*. 9: 237–258.

Frei, S., J.H. Fleckenstein, S.J. Kollet, and R.M. Maxwell (2009) Patterns and dynamics of river-aquifer exchange with variably-saturated flow using a fully-coupled model. *Journal of Hydrology*. 375(3–4): 383–393.

Frei, S., G. Lischeid, and J.H. Fleckenstein (2010) Effects of micro-topography on surface–subsurface exchange and runoff generation in a virtual riparian wetland—A modeling study. *Advances in Water Resources*. 33(11): 1388–1401.

Fritz, B.G., D.P. Mendoza, and T.J. Gilmore (2009) Development of an electronic seepage chamber for extended use in a river. *Groundwater*. 47: 136–140.

Furman, A. (2008) Modeling coupled surface–subsurface flow processes: A review. *Vadose Zone Journal*. 7(2): 741–756.

Gandy, C.J., J.W.N. Smith, and P. Jarvis (2007) Attenuation of mining-derived pollutants in the hyporheic zone: A review. *Science of the Total Environment*. 373(2–3): 435–446.

Genereux, D. and I. Bandopadhyay (2001) Numerical investigation of lake bed seepage patterns: Effects of porous medium and lake properties. *Journal of Hydrology*. 241: 286–303.

Gilbert, J., M.J. Dole-Oliver, P. Marmonier, and P. Vervier (1990) Surface water–groundwater ecotones. In R.J. Naiman and H. Decamps, eds., *The Ecology and Management of Aquatic-Terrestrial Ecotones*. The Parthenon Publishing Group, Carnforth, England, pp. 199–225.

Gleeson, T. and A.H. Manning (2008) Regional groundwater flow in mountainous terrain: Three-dimensional simulations of topographic and hydrogeologic controls. *Water Resources Research*. 44: W10403.

Glover, R.E. and G.G. Balmer (1954) River depletion resulting from pumping a well near a river. *Transactions of the American Geophysical Union*. 35(3): 468–470.

Goderniaux, P., S. Brouyère, S. Blenkinsop, A. Burton, H.J. Fowler, P. Orban, and A. Dassargues (2011) Modeling climate change impacts on groundwater resources using transient stochastic climatic scenarios. *Water Resources Research*. 47(12): W12516.

Goderniaux, P., S. Brouyere, H.J. Fowler, S. Blenkinsop, R. Therrien, P. Orban, and A. Dassargues (2009) Large scale surface–subsurface hydrological model to assess climate change impacts on groundwater reserves. *Journal of Hydrology*. 373(1–2): 122–138.

Gomez-Velez, J.D. and J.W. Harvey (2014) A hydrogeomorphic river network model predicts where and why hyporheic exchange is important in large basins. *Geophysical Research Letters.* 41: 6403.

Gooseff, M.N., J. LaNier, R. Haggerty, and K. Kokkeler (2005) Determining in-channel (dead zone) transient storage by comparing solute transport in a bedrock channel-alluvial channel sequence, Oregon. *Water Resources Research.* 41: W06014.

Gooseff, M.N., D.M. McKnight, R.L. Runkel, and J.H. Duff (2004) Denitrification and hydrologic transient storage in a glacial meltwater stream, McMurdo Dry Valleys, Antarctica. *Limnology and Oceanography.* 49(5): 1884–1895.

Gordon, R.P., L.K. Lautz, M.A. Briggs, and J.M. McKenzie (2012) Automated calculation of vertical pore-water flux from field temperature time series using the VFLUX method and computer program. *Journal of Hydrology.* 420–421: 142–158.

Gordon, R.P., L.K. Lautz, and T.L. Daniluk (2013) Spatial patterns of hyporheic exchange and biogeochemical cycling around cross-vane restoration structures: Implications for stream restoration design. *Water Resources Research.* 49(4): 2040–2055.

Gosselin, D.C., D.C. Rundquist, and S.K. McFeeters (2000) Remote monitoring of selected ground-water dominated lakes in the Nebraska Sand Hills. *Journal of American Water Resources Association.* 36: 1039–1051.

Goto, S., M. Yamano, and M. Kinoshita (2005) Thermal response of sediment with vertical fluid flow to periodic temperature variation at the surface. *Journal of Geophysical Research—Solid Earth.* 110: B01106.

Green, T.R., M. Taniguchi, H. Kooi, J.J. Gurdak, D.M. Allen, K.M. Hiscock, and H. Treidel (2011) Beneath the surface of global change: Impacts of climate change on groundwater. *Journal of Hydrology.* 405: 532–560.

Grigoryev, V.M. (1957) The effect of streambed siltation on well-field yield in alluvial aquifers. *Water Supply and Sanitation.* 6: 110–118, in Russian.

Guin, A., R. Ramanathan, R.W. Ritzi, D.F. Dominic, I.A. Lunt, T.D. Scheibe, and V.L. Freedman (2010) Simulating the heterogeneity in braided channel belt deposits: 2. Examples of results and comparison to natural deposits. *Water Resources Research.* 46(4): doi:10.1029/2009WR008112.

Haggerty, R., S.M. Wondzell, and M.A. Johnson (2002) Power-law residence time distribution in the hyporheic zone of a 2nd-order mountain stream. *Geophysical Research Letters.* 29(13): 1640.

Haitjema, H.M. (1995) *Analytic Element Modeling of Groundwater Flow.* Academic Press, San Diego, CA.

Haitjema, H.M. and S. Mitchell-Bruker (2005) Are water tables a subdued replica of the topography? *Groundwater.* 43: 781–786.

Hakenkamp, C.C. and M.A. Palmer (2000) The Ecology of Hyporheic Meiofauna. In J.B. Jones and P.J. Mulholland, eds., *Streams and Ground Waters*, pp. 307–336, Academic Press, San Diego, CA.

Hantush, M.S. (1965) Wells near streams with semipervious beds. *Journal of Geophysical Research.* 70(12): 2829–2838.

Hantush, M.S. (1967a) Depletion of flow in right angle stream bends by steady wells. *Water Resources Research.* 3: 235–240.

Hantush, M.S. (1967b) Growth and decay of groundwater-mounds in response to uniform percolation. *Water Resources Research.* 3(1): 227–234.

Harbaugh, A.W. (2005) MODFLOW-2005, the U.S. Geological Survey modular ground-water model—The ground-water flow process. U.S. Geological Survey Techniques and Methods 6-A16, Reston, VA.

Harvey, J. and M. Gooseff (2015) River corridor science: Hydrologic exchange and ecological consequences from bed forms to basins. *Water Resources Research.* 51: 6893–6922.

Harvey, J.W. and K.E. Bencala (1993) The effect of streambed topography on surface–subsurface water exchange in mountain catchments. *Water Resources Research.* 29(1): 89–98.

Harvey, J.W., J.K. Böhlke, M.A. Voytek, D. Scott, and C.R. Tobias (2013) Hyporheic zone denitrification: Controls on effective reaction depth and contribution to whole-stream mass balance. *Water Resources Research.* 49: 6298–6316.

Harvey, J.W., M.H. Conklin, and R. Koelsch (2003) Predicting changes in hydrologic retention in an evolving semi-arid alluvial. *Advances in Water Resources.* 26: 939–950.

Harvey, J.W. and C.C. Fuller (1998) Effect of enhanced manganese oxidation in the hyporheic zone on basin-scale geochemical mass balance. *Water Resources Research.* 34(4): 623–636.

Harvey, J.W., J.T. Newlin, and J.E. Saiers (2005) Solute transport and storage mechanisms in wetlands of the Everglades, South Florida. *Water Resources Research.* 41: W05009.

Harvey, J.W., B.J. Wagner, and K.E. Bencala (1996) Evaluating the reliability of the stream tracer approach to characterize stream-subsurface water exchange. *Water Resources Research.* 32(8): 2441–2451.

Harvey, J.W. and B.L. Wagner (2000) Quantifying hydrologic interactions between streams and their subsurface hyporheic zones. In J.B. Jones and P.J. Mulholland, eds. *Streams and Groundwaters*, Academic Press, San Diego, CA, pp. 3–44.

Hatch, C.E., A.T. Fisher, J.S. Revenaugh, J. Constantz, and C. Ruehl (2006) Quantifying surface water–groundwater interactions using time series analysis of streambed thermal records: Method development. *Water Resources Research.* 42(10): W10410.

Hayashi, M. and D.O. Rosenberry (2002) Effects of groundwater exchange on the hydrology and ecology of surface water. *Groundwater.* 40(3): 309–316.

Healy, R.W. and A.D. Ronan (1996) Documentation of computer program VS2DH for simulation of energy transport in variably saturated porous media—modification of the USG Geological Survey's computer program VS2DT. U.S. Geological Survey Water-Resources Investigations Report 96-4230, Denver, CO.

Healy, R.W., T.C. Winter, J.W. LaBaugh, and O.L. Franke (2007) Water budgets: Foundations for effective water-resources and environmental management. U.S. Geological Survey Circular 1308, Reston, CO.

Henderson, R.D., F. Day-Lewis, and C.F. Harvey (2009) Investigation of aquifer-estuary interaction using wavelet analysis of fiber-optic temperature data. *Geophysical Research Letters*. 36: L06403.

Hendricks Franssen, H., H. Kaiser, U. Kuhlmann, G. Bauser, F. Stauffer, R. Müller, and W. Kinzelbach (2011) Operational real-time modeling with ensemble Kalman filter of variably saturated subsurface flow including stream-aquifer interaction and parameter updating. *Water Resources Research*. 47(2): W02532.

Heppner, C.S., Q.H. Ran, J.E. VanderKwaak, and K. Loague (2006) Adding sediment transport to the integrated hydrology model (InHM): Development and testing. *Advances in Water Resources*. 29(6): 930–943.

Hester, E.T. and M.N. Gooseff (2010) Moving beyond the banks: Hyporheic restoration is fundamental to restoring ecological services and functions of streams, *Environmental Science and Technology*. 44(5): 1521–1525.

Hester, E.T. and M.N. Gooseff (2011) Hyporheic restoration in streams and rivers. In A. Simon, S.J. Bennett, and J.M. Castro, eds. *Stream Restoration in Dynamic Fluvial Systems: Scientific Approaches, Analyses, and Tools*. Geophysical Monograph Series 194. American Geophysical Union, Washington, DC, pp. 167–187.

Hill, M.C., D. Kavetski, M. Clark, M. Ye, M. Arabi, D. Lu, L. Foglia, and S. Mehl (2015) Practical use of computationally frugal model analysis methods. *Groundwater*.

Hiscock, K.M. and T. Grischek, eds. (2002) Attenuation of groundwater pollution by bank filtration, Special issue. *Journal of Hydrology*. 266: 139–184.

Hsieh, P.A., W. Wingle, and R.W. Healy (2000) VS2DI—A graphical software package for simulating fluid flow and solute or energy transport in variably saturated porous media. U.S. Geological Survey Water-Resources Investigations Report 99-4130, Lakewood, CO.

Hubbart, J., T. Link, C. Campbell, and D. Cobos (2005) Evaluation of a low-cost temperature measurement system for environmental applications. *Hydrological Processes*. 19(7): 1517–1523.

Hunt, B. (1999) Unsteady stream depletion from groundwater pumping. *Groundwater*. 37(1): 98–102.

Hunt, B. (2014) Review of stream depletion solutions, behavior, and calculations. *Journal of Hydrologic Engineering—ASCE*. 19(1): 167–178.

Hunt, B., J. Weir, and B. Clausen (2001) A stream depletion field experiment. *Groundwater*. 39(2): 283–289.

Hunt, R.J., D.T. Feinstein, C.D. Pint, and M.P. Anderson (2005) The importance of diverse data types to calibrate a watershed model of the Trout Lake Basin, northern Wisconsin, USA. *Journal of Hydrology*. 321(1–4): 286–296.

Hunt, R.J. and D.P. Krabbenhoft (1996) Groundwater inflow measurements in wetland systems. *Water Resources Research*. 32: 495–507.

Huntington, J.L. and R.G. Niswonger (2012) Role of surface-water and groundwater interactions on projected summertime streamflow in snow dominated regions: An integrated modeling approach: *Water Resources Research*. 48: W11524.

Irvine, D.J., P. Brunner, H.-J.H. Franssen, and C.T. Simmons (2012) Heterogeneous or homogeneous? Implications of simplifying heterogeneous streambeds in models of losing streams. *Journal of Hydrology*. 424–425: 16–23.

Irvine, D.J., R.H. Cranswick, C.T. Simmons, M.A. Shanafield, and L.K. Lautz (2015) The effect of streambed heterogeneity on groundwater–surface water exchange fluxes inferred from temperature time series. *Water Resources Research*. 51(1): 198–212.

Ivkovic, K.M. (2009) A top–down approach to characterise aquifer–river interaction processes. *Journal of Hydrology*. 365: 145–155.

Jackman, A.P., R.A. Walters, and V.C. Kennedy (1984) Transport and concentration controls for chloride, strontium, potassium and lead in Uvas Creek, a small cobble-bed stream in Santa Clara County, California, U.S.A. Part 2: Mathematical modeling. *Journal of Hydrology*. 75: 111–141.

Jackson, T.R., R. Haggerty, and S.V. Apte (2013) A fluid-mechanics based classification scheme for surface transient storage in riverine environments: Quantitatively separating surface from hyporheic transient storage. *Hydrology and Earth System Science*. 17: 2747–2779.

Jeffrey, K.A., F.W.H. Beamish, S.C. Ferguson, R.J. Kolton, and P.D. MacMahon (1986) Effects of the lampricide, 3-trifluoromethyl-4-nitrophenol (TFM) on the macroinvertebrates within the hyporheic region of a small stream. *Hydrobiologia*. 134(1): 43–51.

Jenkins, C.T. (1968) Techniques for computing rate and volume of stream depletion by wells. *Groundwater*. 6(2): 37– 46.

Jenkins, C.T. (1970) Computation of rate and volume of stream depletion by wells. Techniques of Water Resources Investigations of the USGS, Book 4, Chapter D1, USGS, Reston, VA.

Jensen, J.K. and P. Engesgaard (2011) Nonuniform groundwater discharge across a streambed: Heat as a tracer. *Vadose Zone Journal*. 10(1): 98–109.

Johnson, A.N., B.R. Boer, W.W. Woessner, J.A. Stanford, G.C. Poole, S.A. Thomas, and S.J. O'Daniel (2005) Evaluation of an inexpensive small-diameter temperature logger for documenting groundwater–river interactions. *Groundwater Monitoring and Remediation*. 25(4): 68–74.

Jolly, I.D., K.L. McEwan, and K.L. Holland (2008) A review of groundwater–surface water interactions in arid/semi-arid wetlands and the consequences of salinity for wetland ecology. *Ecohydrology*. 1: 43–58.

Jones, J.B. and P.J. Mulholland (2000) Surface—Subsurface exchange and nutrient spiraling. In J.B. Jones and P.J. Mulholland, eds. *Streams and Groundwaters*. Academic Press, San Diego, CA, pp. 149–166.

Jonsson, K., H. Johanson, and A. Wörman (2003) Hyporheic exchange of reactive and conservative solutes in streams—Tracer methodology and model interpretation. *Journal of Hydrology*. 278: 153–171.

Kalbus, E., F. Reinstorf, and M. Schirmer (2006) Measuring methods for groundwater-surface water interactions: A review. *Hydrology and Earth System Sciences*. 10: 873–887.

Kampf, S.K. and S.J. Burges (2007) A framework for classifying and comparing distributed hillslope and catchment hydrologic models. *Water Resources Research*. 43(5): W05423.

Karan, S., P. Engesgaard, M.C. Looms, T. Laier, and J. Kazmierczak (2013) Groundwater flow and mixing in a wetland–stream system: Field study and numerical modeling. *Journal of Hydrology*. 488: 73–83.

Karan, S., J. Kidmose, P. Engesgaard, B. Nilsson, M. Frandsen, D.A.O. Ommen, M.R. Flindt, F.Ø. Andersen, and O. Pedersen (2014) Role of a groundwater–lake interface in controlling seepage of water and nitrate. *Journal of Hydrology*. 517: 791–802.

Kaser, D.H., A.M. Binley, A.L. Heathwaite, and S. Krause (2009) Spatio-temporal variations of hyporheic flow in a riffle-step-pool sequence. *Hydrological Processes*. 23(15): 2138–2149.

Käser, D., T. Graf, F. Cochand, R. McLaren, R. Therrien, and P. Brunner (2014) Channel representation in physically based models coupling groundwater and surface water: Pitfalls and how to avoid them. *Groundwater*. 52(6): 827–836.

Käser, D.H., A. Binley, A.L. Heathwaite, and S. Krause (2009) Spatio-temporal variations of hyporheic flow in a riffle-step-pool sequence. *Hydrological Processes*. 23(15): 2138–2149.

Keery, J., A. Binley, N. Crook, and J.W.N. Smith (2007) Temporal and spatial variability of groundwater–surface water fluxes: Development and application of an analytical method using temperature time series. *Journal of Hydrology*. 336: 1–16.

Kennedy, C.D., D.P. Genereux, D.R. Corbett, and H. Mitasova (2009) Spatial and temporal dynamics of coupled groundwater and nitrogen fluxes through a streambed in an agricultural watershed. *Water Resources Research*. 45: W09401.

Kidmose, J., B. Nilsson, P. Engesgaard, M. Frandsen, S. Karan, F. Landkildehus, F.Søndergaard, and E. Jeppesen (2013) Focused groundwater discharge of phosphorus to a eutrophic seepage lake (Lake Væng, Denmark): Implications for lake ecological state and restoration. *Hydrogeology Journal*. 21(8): 1787–1802.

Kiel, B.A. and M.B. Cardenas (2014) Lateral hyporheic exchange throughout the Mississippi River network. *Nature Geosciences*. 7: 413–417.

Kikuchi, C.P., T.P.A. Ferré, and J.M. Welker (2012) Spatially telescoping measurements for improved characterization of groundwater–surface water interactions. *Journal of Hydrology*. 446–447: 1–12.

Kilpatrick, F.A. and E.D. Cobb (1985) Measurement of discharge using tracers. Report of the U.S. Geological Survey, Techniques of Water-Resources Investigations, Book 3, Chapter A16, U.S. Geological Survey, Washington DC.

Kim, B.K.A., A.P. Jackman, and F.J. Triska (1990) Modeling transient storage and nitrate uptake kinetics in a flume containing a natural periphyton community. *Water Resources Research*. 26(3): 505–515.

Kim, B.K.A., A.P. Jackman, and F.J. Triska (1992) Modeling biotic uptake by periphyton and transient hyporheic storage of nitrate in a natural stream. *Water Resources Research*. 28(10): 2743–2752.

Kim, H., H.F. Hemond, L.R. Krumholz, and B.A. Cohen (1995) In-situ biodegradation of toluene in a contaminated stream. Part 1. Field studies. *Environmental Science and Technology*. 29(1): 108–116.

Kimball, B.A., R.E. Broshears, K.E. Bencala, and D.M. McKnight (1994) Coupling of hydrologic transport and chemical-reactions in a stream affected by acid-mine drainage. *Environmental Science and Technology*. 28(12): 2065–2073.

Knight, J.H., M. Gilfedder, and G. Walker (2005) Impacts of irrigation and dryland development on GW discharge to rivers-a unit response approach to cumulative impacts analysis. *Journal of Hydrology*. 303: 79–91.

Koestel, J.K., J. Moeys, and N.J. Jarvis (2011) Evaluation of nonparametric shape measures for solute breakthrough curves. *Vadose Zone Journal*. 10(4): 1261–1275.

Kolditz, O., S. Bauer, L. Bilke, N. Böttcher, J.O. Delfs, T. Fischer, U.J. Görke et al. (2012) OpenGeoSys: An open-source initiative for numerical simulation of thermo-hydro-mechanical/chemical (THM/C) processes in porous media. *Environmental Earth Sciences*. 67(2): 589–599.

Kollet, S.J. and R.M. Maxwell (2006) Integrated surface–groundwater flow modeling: A free-surface overland flow boundary condition in a parallel groundwater flow model. *Advances in Water Resources*. 29(7): 945–958.

Kollet, S.J., R.M. Maxwell, C.S. Woodward, S. Smith, J. Vanderborght, H. Vereecken, and C. Simmer (2010) Proof of concept of regional scale hydrologic simulations at hydrologic resolution utilizing massively parallel computer resources. *Water Resources Research*. 46(4): W04201.

Kollet, S.J. and V.A. Zlotnik (2003) Stream depletion predictions using pumping test data from a heterogeneous stream-aquifer system (a case study from the Great Plains, U.S.A.). *Journal of Hydrology*. 281(1): 96–114.

Kollet, S.J., V.A. Zlotnik, and G. Ledder (2002) "A Stream Depletion Field Experiment," by Bruce Hunt, Julian Weir, and Bente Clausen. *Groundwater*. 40(4): 448–449.

Konikow, L.F. and E. Kendy (2005) Groundwater depletion: A global problem. *Hydrogeology Journal*. 13: 317–320.

Koopmans, D. and P. Berg (2011) An alternative to traditional seepage meters: Dye displacement. *Water Resources Research*. 47: W01506.

Krabbenhoft, D.P., M.P. Anderson, and C.J. Bowser (1990a) Estimating groundwater exchange with lakes: 2. Calibration of a three-dimensional, solute transport model to a stable isotope plume. *Water Resources Research*. 26(10): 2455–2462.

Krabbenhoft, D.P., C.J. Bowser, M.P. Anderson, and J.W. Valley (1990b) Estimating groundwater exchange with lakes, 1: Use of the stable isotope method. *Water Resources Research*. 26(10): 2445–2453.

Krabbenhoft, D.P., C.J. Bowser, C. Kendall, and J.R. Gat (1994) Use of oxygen-18 and deuterium to assess the hydrology of groundwater-lake systems. In L.A. Baker, ed. *Environmental Chemistry of Lakes and Reservoirs*. American Chemical Society, Washington, DC, pp. 67–90.

Krause, S., T. Blume, and N.J. Cassidy (2012) Investigating patterns and controls of groundwater up-welling in a lowland river by combining fibre-optic distributed temperature sensing with observations of vertical hydraulic gradients. *Hydrology and Earth System Sciences*. 16: 1775–1792.

Krause, S., F. Boano, M.O. Cuthbert, J.H. Fleckenstein, and J. Lewandowski (2014) Understanding process dynamics at aquifer–surface water interfaces: An introduction to the special section on new modeling approaches and novel experimental technologies. *Water Resources Research*. 50: 1847–1855.

Krause, S., D.M. Hannah, J.H. Fleckenstein, C.M. Heppell, D. Kaeser, R. Pickup, G. Pinay, A.L. Robertson, and P.J. Wood (2011) Inter-disciplinary perspectives on processes in the hyporheic zone. *Ecohydrology*. 4(4): 481–499.

Krause, S., L. Heathwaite, A. Binley, and P. Keenan (2009) Nitrate concentrations changes at the groundwater–surface water interface of a small Cumbrian river. *Hydrological Processes*. 23: 2195–2211.

Kumar, M., C.J. Duffy, and K.M. Salvage (2009) A second-order accurate, finite volume-based, integrated hydrologic modeling (FIHM) framework for simulation of surface and subsurface flow. *Vadose Zone Journal*. 8(4): 873–890.

Kurtz, W., H.-J. Hendricks Franssen, P. Brunner, and H. Vereecken (2013) Is high-resolution inverse characterization of heterogeneous river bed hydraulic conductivities needed and possible? *Hydrology and Earth System Sciences*. 17(10): 3795–3813.

Kuwayama, Y. and N. Brozović (2013) The regulation of a spatially heterogeneous externality: Tradable groundwater permits to protect streams. *Journal of Environmental Economics and Management*. 66(2013): 364–382.

LaBaugh, J.W., D.C. Buso, and G.E. Likens (2009) Evaluation of methods and uncertainties in the chemical budgets. In T.C. Winter and G.E. Likens, eds. *Mirror Lake: Interactions among Air, Land, and Water*. University of California Press, Berkeley, CA, pp. 225–299.

LaBaugh, J.W. and D.O. Rosenberry (2008) Introduction and characteristics of flow. In D.O. Rosenberry and J.W. LaBaugh, eds. *Field Techniques for Estimating Water Fluxes between Surface Water and Groundwater*. U.S. Geological Survey Techniques and Methods 4-D2, Reston, VA, pp. 1–38.

LaBaugh, J.W. and T.C. Winter (1984) The impact of uncertainties in hydrologic measurement on phosphorus budgets and empirical models for two Colorado reservoirs. *Limnology and Oceanography*. 29: 322–339.

Lapham, W.W. (1989) Use of temperature profiles beneath streams to determine rates of vertical ground-water flow and vertical hydraulic conductivity. U.S. Geological Survey Water-Supply Paper 2337, Denver, CO.

Larkin, R.G. and J.M. Sharp (1992) On the relationship between river-basin geomorphology, aquifer hydraulics, and ground-water flow direction in alluvial aquifers. *Bulletin of the Geological Society of America*. 104(12): 1608–1620.

Lautz, L.K. (2010) Impacts of non-ideal field conditions on vertical water velocity estimates from streambed temperature time series. *Water Resources Research*. 46: W01509.

Lautz, L.K. (2012) Observing temporal patterns of vertical flux through streambed sediments using time-series analysis of temperature records. *Journal of Hydrology*. 464: 199–215.

Lautz, L.K. and R.M. Fanelli (2008) Seasonal biogeochemical hotspots in the streambed around restoration structures. *Biogeochemistry*. 91(1): 85–104.

Lautz, L.K. and R.E. Ribaudo (2012) Scaling up point-in-space heat tracing of seepage flux using bed temperatures as a quantitative proxy. *Hydrogeology Journal*. 20(7): 1223–1238.

Lautz, L.K., D.I. Siegel, and R.L. Bauer (2006) Impact of debris dams on hyporheic interaction along a semi-arid stream. *Hydrological Processes*. 20(1): 183–196.

Leake, S.A., H.W. Reeves, and J.E. Dickinson (2010) A new capture fraction method to map how pumpage affects surface water flow. *Groundwater*. 48(5): 690–700.

Lee, D.R. (1977) A device for measuring seepage flux in lakes and estuaries. *Limnology and Oceanography*. 22: 140–147.

Lee, D.R. (1985) Method for locating sediment anomalies in lakebeds that can be caused by groundwater flow. *Journal of Hydrology*. 79: 187–193.

Lee, D.R. and J.P. Tracey (1984) Identification of groundwater discharge locations using thermal infrared imagery. *Ninth Canadian Symposium on Remote Sensing*. Canadian Aeronautics and Space Institute, Saint Johns, Newfoundland, Canada, pp. 301–308.

Lewandowski, J., L. Angermann, G. Nützmann, and J.H. Fleckenstein (2011) A heat pulse technique for the determination of small-scale flow directions and flow velocities in the streambed of sand-bed streams. *Hydrological Processes*. 25: 3244–3255.

Lewandowski, J., K. Meinikmann, T. Ruhtz, F. Pöschke, and G. Kirillin (2013) Localization of lacustrine groundwater discharge (LGD) by airborne measurement of thermal infrared radiation. *Remote Sensing of Environment*. 138: 119–125.

Li, Q., A.J.A. Unger, E.A. Sudicky, D. Kassenaar, E.J. Wexler, and S. Shikaze (2008) Simulating the multi-seasonal response of a large-scale watershed with a 3D physically-based hydrologic model. *Journal of Hydrology.* 357(3–4): 317–336.

Liggett, J.E., A.D. Werner, and C.T. Simmons (2012) Influence of the first-order exchange coefficient on simulation of coupled surface–subsurface flow. *Journal of Hydrology.* 414: 503–515.

Liu, Y. and Z. Sheng (2011) Trend-outflow method for understanding interactions of surface water with groundwater and atmospheric water for eight reaches of the upper Rio Grande. *Journal of Hydrology.* 409: 710–723.

Lohman, S.W. (1972) Definitions of selected groundwater terms—Revision and conceptual refinements. U.S. Geological Survey Water-Supply Paper 1988, Washington, DC.

Lough, H.K. and B. Hunt (2006) Pumping test evaluation of stream depletion parameters. *Groundwater.* 44(4): 540–546.

Lowry, C.S., J.F. Walker, R.J. Hunt, and M.P. Anderson (2007) Identifying spatial variability of groundwater discharge in a wetland stream using a distributed temperature sensor. *Water Resources Research.* 43: W10408.

Luce, C.H., D. Tonina, F. Gariglio, and R. Applebee (2013) Solutions for the diurnally forced advection-diffusion equation to estimate bulk fluid velocity and diffusivity in streambeds from temperature time series. *Water Resources Research.* 49(1): 488–506.

Luther, K.H. and H.M. Haitjema (2000) Approximate analytic solutions to 3D unconfined groundwater flow within regional 2D Models. *Journal of Hydrology.* 226: 101–117.

Mamer, E.A. and C.S. Lowry (2013) Locating and quantifying spatially distributed groundwater/surface water interactions using temperature signals with paired fiber-optic cables. *Water Resources Research.* 49(11): 7670–7680.

Markstrom, S.L., R.G. Niswonger, R.S. Regan, D.E. Prudic, and P.M. Barlow (2008) GSFLOW—Coupled ground-water and surface-water flow model based on the integration of the precipitation-runoff modeling system (PRMS) and the modular ground-water flow model (MODFLOW-2005). U.S. Geological Survey Techniques and Methods, Reston, VA, Book 6, D1, p. 240.

Marsily de, G., F. Delay, J. Gonçalvès, P. Renard, V. Tales, and S. Violette (2005) Dealing with spatial heterogeneity. *Hydrogeology Journal.* 13: 161–183.

Maxwell, R.M. and S.J. Kollet (2008) Interdependence of groundwater dynamics and land-energy feedbacks under climate change. *Nature Geoscience.* 1: 665–669.

Maxwell, R.M., M. Putti, S. Meyerhoff, J.O. Delfs, I.M. Ferguson, V. Ivanov, J. Kim et al. (2014) Surface–subsurface model intercomparison: A first set of benchmark results to diagnose integrated hydrology and feedbacks. *Water Resources Research.* 50(2): 1531–1549.

McBride, M.S. and H.O. Pfannkuch (1975) The distribution of seepage within lakebeds. *U.S. Geological Survey Journal of Research.* 3: 505–512.

McCallum, A.M., M.S. Andersen, G.C. Rau, and R.I. Acworth (2012) A 1-D analytical method for estimating surface water–groundwater interactions and effective thermal diffusivity using temperature time series. *Water Resources Research.* 48, W11532, doi:10.1029/2012WR012007, 8 p.

McCallum, J.L., P.G. Cook, P. Brunner, and D. Berhane (2010) Solute dynamics during bank storage flows and implications for chemical base flow separation. *Water Resources Research.* 46: W07541.

McDonald, M.G. and A.W. Harbaugh (1983) A modular three-dimensional finite-difference ground-water flow model. U.S. Geological Survey Open-File Report 83-875, Reston, VA.

McDowell, W. (1985) Kinetics and mechanisms of dissolved organic carbon retention in a headwater stream. *Biogeochemistry.* 1: 329–352.

Meinikmann, K., J. Lewandowski, and G. Nützmann (2013) Lacustrine groundwater discharge: Combined determination of volumes and spatial patterns. *Journal of Hydrology.* 502: 202–211.

Meinzer, O.E., ed. (1942) *Hydrology.* McGraw-Hill, New York.

Merill, L. and D.J. Tonjes (2014) A Review of the hyporheic zone, stream restoration, and means to enhance denitrification. *Critical Reviews in Environmental Science and Technology.* 44(21): 2337–2379.

Merritt, M.L. and L.F. Konikow (2000) Documentation of a computer program to simulate lake-aquifer interaction using the MODFLOW ground-water flow model and the MOC3D solute-transport model. U.S. Geological Survey Water-Resources Investigations Report 00-4167, Tallahassee, FL, 146p.

Meyerhoff, S.B. and R.M. Maxwell (2011) Quantifying the effects of subsurface heterogeneity on hillslope runoff using a stochastic approach. *Hydrogeology Journal.* 19(8): 1515–1530.

Michael, H.A., J.S. Lubetsky, and C.F. Harvey (2003) Characterizing submarine groundwater discharge: A seepage meter study in Waquoit Bay, Massachusetts. *Geophysical Research Letters.* 30: 1297.

Miller, C.D., D. Durnford, M.R. Halstead, J. Altenhofen, and V. Flory (2007) Stream depletion in alluvial valleys using the SDF semianalytical model. *Groundwater.* 45(4): 506–514.

Moench, A.F. and P.M. Barlow (2000) Aquifer response to stream-stage and recharge variations. I. Analytical step-response functions. *Journal of Hydrology.* 230: 192–210.

Moore, W.S. (2010) The effect of submarine groundwater discharge on the ocean. *Annual Review of Marine Science.* 2: 59–88.

Morita, M. and B.C. Yen (2000) Numerical methods for conjunctive two-dimensional surface and three-dimensional subsurface flows. *International Journal for Numerical Methods in Fluids.* 32(8): 921–957.

Mulholland, P.J. (1992) Regulation of nutrient concentrations in a temperate forest stream: Roles of upland, riparian, and instream processes. *Limnology and Oceanography.* 37(7): 1512–1526.

Mulholland, P.J., E.R. Marzolf, J.R. Webster, D.R. Hart, and S. P Hendricks (1997) Evidence that hyporheic zones increase heterotrophic metabolism and phosphorus uptake in forest streams. *Limnology and Oceanography.* 42(3): 443–451.

Mulligan, A.E. and M.A. Charette (2006) Intercomparison of submarine groundwater discharge estimates from a sandy unconfined aquifer. *Journal of Hydrology.* 327: 411–425.

Munz, M., S.E. Oswald, and C. Schmidt (2011) Sand box experiments to evaluate the influence of subsurface temperature probe design on temperature based water flux calculation. *Hydrology and Earth System Sciences.* 15: 3495–3510.

Murdoch, L.C. and S.E. Kelly (2003) Factors affecting the performance of conventional seepage meters. *Water Resources Research.* 39(6): 1163–1169.

Naranjo, R.C., R.G. Niswonger, M. Stone, C. Davis, and A. Mckay (2012) The use of multiobjective calibration and regional sensitivity analysis in simulating hyporheic exchange. *Water Resources Research.* 48: W01538.

Naranjo, R.C., G. Pohll, R.G. Niswonger, M. Stone, and A. Mckay (2013) Using heat as a tracer to estimate spatially distributed mean residence times in the hyporheic zone of a riffle-pool sequence, *Water Resources Research.* 49: 3697–3711.

Neilson, B.T., D.K. Stevens, S.C. Chapra, and C. Bandaragoda (2010) Two-zone transient storage modeling using temperature and solute data with multiobjective calibration: 2. Temperature and solute. *Water Resources Research.* 46(12): W12521.

Nelson, R.W. (1978) Evaluating the environmental consequences of groundwater contamination: 2. Obtaining location/arrival time and location/outflow quantity distributions for steady flow systems. *Water Resources Research.* 14(3): 416–428.

Newbold, J.D., J.W. Elwood, R.W. O'Neill, and A.L. Sheldon (1983) Phosphorus dynamics in a woodland stream ecosystem—A study of nutrient spiraling. *Ecology.* 64(5): 1249–1265.

Newsom, J.M. and J.L. Wilson (1988) Flow of groundwater to a well near a stream—Effect of ambient ground-water flow direction. *Groundwater.* 26: 703–711.

Nield, S.P., L.R. Townley, and A.D. Barr (1994) A framework for quantitative analysis of surface water–groundwater interaction: Flow geometry in a vertical section. *Water Resources Research.* 30(8): 2461–2475.

Niswonger, R.G., K.K. Allander, and A.E. Jeton (2014) Collaborative modelling and integrated decision support system analysis of a developed terminal lake basin. *Journal of Hydrology.* 517: 521–537.

Niswonger, R.G. and D.E. Prudic (2005) Documentation of the Streamflow-Routing (SFR2) Package to include unsaturated flow beneath streams—A modification to SFR1. U.S. Geological Survey Techniques and Methods 6-A13, Reston, VA, 62p.

Nyholm, T., S. Christensen, and K.R. Rasmussen (2002) Flow depletion in a small stream caused by groundwater abstraction from wells. *Groundwater.* 40(4): 425–437.

Nyholm, T., K.R. Rasmussen, and S. Christensen (2003) Estimation of stream flow depletion and uncertainty from discharge measurements in a small alluvial stream. *Journal of Hydrology.* 274: 129–144.

O'Connor, B.L., M. Hondzo, and J.W. Harvey (2010) Predictive modeling of transient storage and nutrient uptake. *Journal of Hydraulic Engineering—ASCE.* 136(12): 1018–1032.

Ong, J., J. Lane, V. Zlotnik, T. Halihan, and E. White (2010) Combined use of frequency-domain electromagnetic and electrical resistivity surveys to delineate near-lake groundwater flow in the semi-arid Nebraska Sand Hills, USA. *Hydrogeology Journal.* 18(6): 1539–1545.

Orghidan, T. (1959) Ein neuer Lebensraum des unterirdischen Wassers, der hyporheische Biotop. *Archiv fur Hydrobiologie.* 55: 392–414.

Panday, S., N. Brown, T. Foreman, V. Bedekar, J. Kaur, and P.S. Huyakorn (2009) Simulating dynamic water supply systems in a fully integrated surface–subsurface flow and transport model. *Vadose Zone Journal.* 8(4): 858–872.

Panday, S. and P.S. Huyakorn (2004) A fully coupled physically-based spatially-distributed model for evaluating surface/subsurface flow. *Advances in Water Resources.* 27(4): 361–382.

Park, Y.J., E.A. Sudicky, A.E. Brookfield, and J.P. Jones (2011) Hydrologic response of catchments to precipitation: Quantification of mechanical carriers and origins of water. *Water Resources Research.* 47: W12515.

Partington, D., P. Brunner, S. Frei, C. Simmons, A. Werner, R. Therrien, H. Maier, G. Dandy, and J. Fleckenstein (2013) Interpreting streamflow generation mechanisms from integrated surface-subsurface flow models of a riparian wetland and catchment. *Water Resources Research.* 49(9): 5501–5519.

Partington, D., P. Brunner, C.T. Simmons, R. Therrien, A.D. Werner, G.C. Dandy, and H.R. Maier (2011) A hydraulic mixing-cell method to quantify the groundwater component of streamflow within spatially distributed fully integrated surface water–groundwater flow models. *Environmental Modelling and Software.* 26(7): 886–898.

Partington, D., P. Brunner, C.T. Simmons, A.D. Werner, R. Therrien, H.R. Maier, and G.C. Dandy (2012) Evaluation of outputs from automated baseflow separation methods against simulated baseflow from a physically based, surface water–groundwater flow model. *Journal of Hydrology.* 458–459: 28–39.

Paulsen, R.J., C.F. Smith, D. O'Rourke, and T. Wong (2001) Development and evaluation of an ultrasonic groundwater seepage meter. *Groundwater.* 39: 904–911.

Payn, R.A., M.N. Gooseff, B.L. McGlynn, K.E. Bencala, and S.M. Wondzell (2009) Channel water balance and exchange with subsurface flow along a mountain headwater stream in Montana, United States. *Water Resources Research.* 45: W11427.

Pfannkuch, H.O. and T.C. Winter (1984) Effect of anisotropy and ground-water system geometry on seepage through lakebeds, 1. Analog and dimensional analysis. *Journal of Hydrology*. 75: 213–237.

Pinay, G., T.C. O'Keefe, R.T. Edwards, and R.J. Naiman (2009) Nitrate removal in the hyporheic zone of a salmon river in Alaska. *River Research and Applications*. 25(4): 367–375.

Prudic, D.E., L.F. Konikow, and E.R. Banta (2004) A new Streamflow-Routing (SFR1) Package to simulate stream-aquifer interaction with MODFLOW-2000. U.S. Geological Survey Open-File Report 2004-1042, Carson City, NV, 95p.

Prudic, D.E., R.G. Niswonger, and R.W. Plume (2006) Trends in streamflow on the Humboldt River between Elko and Imlay, Nevada, 1950–99. U.S. Geological Survey Scientific Investigations Report 2005-5199, Carson City, NV.

Pugsley, C. and H.B.N. Hynes (1986) Three-Dimensional distribution of winter stonefly nymphs, Allocapnia pygmaea, within the substrate of a Southern Ontario River. *Canadian Journal of Fisheries and Aquatic Sciences*. 43: 1812–1817.

Rau, G.C., M.S. Andersen, and R.I. Acworth (2012) Experimental investigation of the thermal dispersivity term and its significance in the heat transport equation for flow in sediments. *Water Resources Research*. 48: W03511.

Rau, G.C., M.S. Andersen, A.M. McCallum, H. Roshan, and R.I. Acworth (2014) Heat as a tracer to quantify water flow in near-surface sediments. *Earth Science Reviews*. 129: 40–58.

Reddy, M.M., P. Schuster, C. Kendall, and M.B. Reddy (2006) Characterization of surface and groundwater $d^{18}O$ seasonal variation and its use for estimating groundwater residence times. *Hydrological Processes*. 20: 1753–1772.

Reeves, H.W. (2008) STRMDEPL08—An extended version of STRMDEPL with additional analytical solutions to calculate streamflow depletion by nearby pumping wells. U.S. Geological Survey Open-File Report 2008-1166, Reston, VA.

Reeves, H.W., D.A. Hamilton, P.W. Seelbach, and A.J. Asher (2009) Ground-water-withdrawal component of the Michigan water-withdrawal screening tool. U.S. Geological Survey Scientific Investigations Report 2009-5003, Reston, VA, 36p.

Refsgaard, J.C. and B. Storm (1995) MIKE-SHE. In V.P. Singh, ed. *Computer Models of Watershed Hydrology*. Water Resources Publications, Highlands Ranch, CO, pp. 809–846.

Riggs, H.C. (1972) Low-flow investigations. U.S. Geological Survey Techniques of Water-Resources Investigations, Washington, DC, Book 4, Chapter B1, 18p.

Rosen, M. (1994) The importance of groundwater in playas: A review of playa classifications and the sedimentology and hydrology of playas. *Geological Society of America Special Papers* 289: 1–18,

Rosenberry, D.O. (2005) Integrating seepage heterogeneity with the use of ganged seepage meters. *Limnology and Oceanography: Methods*. 3: 131–142.

Rosenberry, D.O. (2008) A seepage meter designed for use in flowing water. *Journal of Hydrology*. 359: 118–130.

Rosenberry, D.O. and M. Hayashi (2013) Assessing and measuring wetland hydrology. In J.T. Anderson and C.A. Davis, eds. *Wetland Techniques*, Vol. 1: Foundations. Springer, Dordrecht, the Netherlands, pp. 87–225.

Rosenberry, D.O., P.Z. Klos, and A. Neal (2012) In situ quantification of spatial and temporal variability of hyporheic exchange in static and mobile gravel-bed rivers. *Hydrological Processes*. 26: 604–612.

Rosenberry, D.O. and J.W. LaBaugh (2008) Field techniques for estimating water fluxes between surface water and groundwater. U.S. Geological Survey Techniques and Methods, Denver, CO, Chapter 4-D2, p. 128.

Rosenberry, D.O. and R.H. Morin (2004) Use of an electromagnetic seepage meter to investigate temporal variability in lake seepage. *Groundwater*. 42: 68–77.

Rosenberry, D.O. and J. Pitlick (2009) Local-scale spatial and temporal variability of seepage in a shallow gravel-bed river. *Hydrological Processes*. 23: 3306–3318.

Rosenberry, D.O., R.W. Sheibley, S.E. Cox, F.W. Simonds, and D.L. Naftz (2013) Temporal variability of exchange between groundwater and surface water based on high-frequency direct measurements of seepage at the sediment–water interface. *Water Resources Research*. 49: 2975–2986.

Rossman, N.R.,and V.A. Zlotnik (2013) Review: Regional groundwater flow modeling in heavily irrigated basins of selected states in the western United States. *Hydrogeology Journal*. 21, 1173–1192.

Rötting, T., J. Carrera, J. Bolzicco, and J.M. Salvany (2006) Stream-stage response tests and their joint interpretation with pumping tests. *Groundwater*. 44(3): 371–385.

Rovey, II, C.W. and D.S. Cherkauer (1995) Scale dependency of hydraulic conductivity measurements. *Groundwater*. 33: 769–780.

Rubin, Y. and S. Hubbard, eds. (2005) *Hydrogeophysics*. Springer, the Netherlands.

Rudnick, S., J. Lewandowski, and G. Nützmann (2014) Investigating groundwater-lake interactions by hydraulic heads and a water balance. *Groundwater*. 53(2): 227–237.

Ruehl, C., A.T. Fisher, C. Hatch, M.L. Huertos, G. Stemler, and C. Shennan (2006) Differential gauging and tracer tests resolve seepage fluxes in a strongly-losing stream. *Journal of Hydrology*. 330: 235–248.

Runkel, R.L. (1998) One-dimensional transport with inflow and storage (OTIS): A solute transport model for streams and rivers. U.S. Geological Survey Water-Resources Investigations Report 98-4018, Denver, CO.

Runkel, R.L. (2010) One-dimensional transport with equilibrium chemistry (OTEQ)—A reactive transport model for streams and rivers. U.S. Geological Survey Techniques and Methods, Reston, VA, Book 6, Chapter B6.

Runkel, R.L., K.E. Bencala, R.E. Broshears, and S.C. Chapra (1996a) Reactive solute transport in streams: 1. Development of an equilibrium-based model. *Water Resources Research*. 32(2): 409–418.

Runkel, R.L., B.A. Kimball, D.M. McKnight, and K.E. Bencala (1999) Reactive solute transport in streams: A surface complexation approach for trace metal sorption. *Water Resources Research*. 35(12): 3829–3840.

Runkel, R.L., D.M. McKnight, K.E. Bencala, and S.C. Chapra (1996b) Reactive solute transport in streams: 2. Simulation of a pH Modification Experiment. *Water Resources Research*. 32(2): 419–430.

Runkel, R.L., D.M. McKnight, and H. Rajaram (2003) Modeling hyporheic zone processes. *Advances in Water Resources*. 26: 901–905.

Russoniello, C.J., C. Fernandez, J.F. Bratton, J.F. Banaszak, D.E. Krantz, A.S. Andres, L.F. Konikow, and H.A. Michael (2013) Geologic effects on groundwater salinity and discharge into an estuary. *Journal of Hydrology*. 498: 1–12.

Rutledge, A.T. (1998) Computer programs for describing the recession of ground-water discharge and for estimating mean ground-water recharge and discharge from streamflow records. Update. U.S. Geological Survey Water-Resources Investigations Report 98-4148, Reston, VA.

Rutledge, A.T. (2000) Considerations for use of the RORA program to estimate ground-water recharge from streamflow records. U.S. Geological Survey Open-File Report 00-156, Reston, VA, p. 44.

Rutledge, A.T. (2014) Use of groundwater levels with the PULSE analytical model. *Groundwater*. 52(5): 789–797.

Rutledge, A.T. and C.C. Daniel, III (1994) Testing an automated method to estimate ground-water recharge from streamflow records. *Groundwater*. 32: 180–189.

Sacks, L.A., T.M. Lee, and A. Swancar (2014) The suitability of a simplified isotope-balance approach to quantify transient groundwater–lake interactions over a decade with climatic extremes. *Journal of Hydrology*. 519(Part D): 3042–3053.

Sambrook Smith, G.H., J.L. Best, O. Orfeo, M.E. Vardy and J.A. Zinger (2013) Decimeter-scale in situ mapping of modern cross-bedded dune deposits using parametric echo sounding: A new method for linking river processes and their deposits. *Geophysical Research Letters*. 40: 3883–3887.

Santos, I.R., W.C. Burnett, J. Chanton, N. Dimova, and R.N. Peterson (2009) Land or ocean? Assessing the driving forces of submarine groundwater discharge at a coastal site in the Gulf of Mexico. *Journal of Geophysical Research—Oceans*. 114: C04012.

Schilling, K.E., K.S. Chan, H. Liu, and Y.K. Zhang (2010) Quantifying the effect of land cover land use change on increasing discharge in the Upper Mississippi River. *Journal of Hydrology*. 387: 343–345.

Schilling, O.S., J. Doherty, W. Kinzelbach, H. Wang, P.N. Yang, and P. Brunner (2014) Using tree ring data as a proxy for transpiration to reduce predictive uncertainty of a model simulating groundwater–surface water–vegetation interactions. *Journal of Hydrology*. 519(Part B): 2258–2271.

Schmadel, N.M., B.T. Neilson, and D.K. Stevens (2010) Approaches to estimate uncertainty in longitudinal channel water balances. *Journal of Hydrology*. 394(3–4): 357–369.

Schmid, B.H. (2003) Temporal moments routing in streams and rivers with transient storage. *Advances in Water Resources*. 26(9): 1021–1027.

Schmidt, C., M. Bayer-Raich, and M. Schirmer (2006) Characterization of spatial heterogeneity of groundwater–stream water interactions using multiple depth streambed temperature measurements at the reach scale. *Hydrology and Earth System Sciences*. 10(6): 849–859.

Schmidt, C., B. Conant, Jr., M. Bayer-Raich, and M. Schirmer (2007) Evaluation and field scale application of an analytical method to quantify groundwater discharge using mapped streambed temperatures. *Journal of Hydrology*. 347: 292–307.

Schornberg, C., C. Schmidt, E. Kalbus, and J.H. Fleckenstein (2010) Simulating the effects of geologic heterogeneity and transient boundary conditions on streambed temperatures—Implications for temperature-based water flux calculations. *Advances in Water Resources*. 33(11): 1309–1319.

Sciuto, G. and B. Diekkruger (2010) Influence of soil heterogeneity and spatial discretization on catchment water balance modeling. *Vadose Zone Journal*. 9(4): 955–969.

Sebestyen, S.D. and R.L. Schneider (2001) Dynamic temporal patterns of nearshore seepage flux in a headwater Adirondack lake. *Journal of Hydrology*. 247: 137–150.

Sebok, E., C. Duque, J. Kazmierczak, P. Engesgaard, B. Nilsson, S. Karan, and M. Frandsen (2013) High-resolution distributed temperature sensing to detect seasonal groundwater discharge into Lake Væng, Denmark. *Water Resources Research*. 49: 5355–5368.

Selker, J., N. van de Giesen, M. Westhoff, W. Luxemburg, and M.B. Parlange (2006a) Fiber optics opens window on stream dynamics. *Geophysical Research Letters*. 33, L24401, doi:10.1029/2006GL027979, 4 p.

Selker, J.S., L. Thevenaz, H. Huwald, A. Mallet, W. Luxemburg, N.V. de Giesen, M. Stejskal, J. Zeman, M. Westhoff, and M.B. Parlange (2006b) Distributed fiber-optic temperature sensing for hydrologic systems. *Water Resources Research*. 42, W12202, doi:10.1029/2006WR005326, 8 p.

Shanafield, M. and P.G. Cook (2014) Transmission losses, infiltration and groundwater recharge through ephemeral and intermittent streambeds: A review of applied methods. *Journal of Hydrology*. 511: 518–529.

Shanafield, M., C. Hatch, and G. Pohll (2011) Uncertainty in thermal time series analysis estimates of streambed water flux. *Water Resources Research*. 47: W03504.

Silliman, S.E. and D.F. Booth (1993) Analysis of time-series measurements of sediment temperature for identification of gaining vs. losing portions of Juday Creek, Indiana. *Journal of Hydrology*. 146: 131–148.

Simonds, F.W. and K.A. Sinclair (2002) Surface water–groundwater interactions along the Lower Dungeness River and vertical hydraulic conductivity of streambed sediments, Clallam County, Washington, September 1999–July 2001. U.S. Geological Survey Water-Resources Investigations Report 02-4161, Tacoma, WA, 60p.

Simonds, F.W., P.W. Swarzenski, D.O. Rosenberry, C.D. Reich, and A.J. Paulson (2008) Estimates of nutrient loading by ground-water discharge into the Lynch Cove Area of Hood Canal, Washington. U.S. Geological Survey Scientific Investigations Report 2008-5078, Reston, VA, 54p.

Singh, S.K. (2003) Flow depletion of semipervious streams due to pumping. *Journal of Irrigation and Drainage Engineering, ASCE*. 129(6): 449–453.

Sloto, R.A. and M.Y. Crouse (1996) HYSEP: A computer program for streamflow hydrograph separation and analysis. U.S. Geological Survey Water-Resources Investigations Report 96-4040, Lemoyne, PA.

Smerdon, B.D., C.A. Mendoza, and K.J. Devito (2007) Simulations of fully coupled lake-groundwater exchange in a subhumid climate with an integrated hydrologic model. *Water Resources Research*. 43: W01416, doi:10.1029/2006WR005137.

Smith, A.J. and L.R. Townley (2002) The influence of regional setting on the interaction between shallow lakes and aquifers. *Water Resources Research*. 38(9): 1170.

Sophocleous, M. (1991) Stream-floodwave propagation through the Great Bend alluvial aquifer, Kansas: Field measurements and numerical simulations. *Journal of Hydrology*. 124: 207–228.

Sophocleous, M. (2000) From safe yield to sustainable development of water resources—The Kansas experience. *Journal of Hydrology*. 235: 27–43.

Sophocleous, M. (2002) Interactions between groundwater and surface water: The state of the science. *Hydrogeology Journal*. 10: 52–67.

Sophocleous, M., M.A. Townsend, L.D. Vogler, T.J. McClain, E.T. Marks, and G.R. Coble (1988) Experimental studies in stream-aquifer interaction along the Arkansas River in central Kansas—Field testing and analysis. *Journal of Hydrology*. 98: 249–273.

Soto-Lopez, C.D., M. Meixner, and T.P.A. Ferre (2011) Effects of measurement resolution on the analysis of temperature time series for stream–aquifer flux estimation. *Water Resources Research*. 47(12): 12602.

Stallman, R.W. (1962) Channel methods—Line sink or line source (constant head, nonsteady state, no recharge). In J.G. Ferris, D.B. Knowles, R.H. Brown, and R.W. Stallman, eds. *Theory of Aquifer Tests*. U.S. Geological Survey Water-Supply Paper 1536-E, Washington, DC, p. 126.

Stallman, R.W. (1965) Steady one-dimensional fluid flow in a semi-infinite porous medium with sinusoidal surface temperature. *Journal of Geophysical Research*. 70(12): 2821–2827.

Stanford, J.A. and J.V. Ward (1988) The hyporheic habitat of river ecosystems. *Nature*. 335(6185): 64–66.

Stanford, J.A. and J.V. Ward (1993) An ecosystem perspective of alluvial rivers: Connectivity and the hyporheic corridor. *Journal of the North American Benthological Society*. 12(1): 48–60.

Stanford, J.A. and J.V. Ward (1999) An ecosystem perspective of alluvial rivers: connectivity and the hyporheic corridor. *Journal of North American Benthological Society*. 12: 48–60.

Stanley, E.H. and J.B. Jones (2000) Surface-subsurface interactions: past, present, and future, In J.B. Jones and P.J. Mulholland, eds., *Streams Ground Waters*, pp. 381–402, Academic Press, San Diego, CA.

Stauffer, F., A. Guadagnini, A. Butler, H.J.H. Franssen, N.V.D. Wiel, M. Bakr, M. Riva et al. (2005) Delineation of source protection zones using statistical methods. *Water Resources Management*. 19(2): 163–85.

Stieglitz, T., J. Rapaglia, and H. Bokuniewicz (2008) Estimation of submarine groundwater discharge from bulk ground electrical conductivity measurements. *Journal of Geophysical Research*. 113: C08007.

Stonedahl, S.H., J.W. Harvey, and A.I. Packman (2013) Interactions between hyporheic flow produced by streammeanders, bars, and dunes. *Water Resources Research*. 9: 5450–5461.

Stonestrom, D.A. and J. Constantz (2004) Heat as a tool for studying the movement of groundwater near streams. U.S. Geological Survey Circular 1260, Reston, VA.

Stonestrom, D.A., B.R. Scanlon, and L. Zhang (2009) Introduction to special section on impacts of land use change on water resources. *Water Resources Research*. 45: W00A00.

Storey, R.G., K.W.F. Howard, and D.D. Williams (2003) Factors controlling riffle-scale hyporheic exchange flows and their seasonal changes in a gaining stream: A three-dimensional groundwater flow model. *Water Resources Research*. 39(2): 1034.

Stream Solute Workshop (1990) Concepts and methods for assessing solute dynamics in stream ecosystems. *Journal of North American Benthological Society*. 9: 95–119.

Su, G.W., J. Jasperse, D. Seymour, and J. Constantz (2004) Estimation of hydraulic conductivity in an alluvial system using temperatures. *Groundwater*. 42(6): 890–901.

Sudicky, E.A., J.P. Jones, Y.J. Park, A.E. Brookfield, and D. Colautti (2008) Simulating complex flow and transport dynamics in an integrated surface-subsurface modeling framework. *Geosciences Journal*. 12(2): 107–122.

Surfleet, C.G. and D. Tullos (2012) Uncertainty in hydrologic modeling for estimating hydrologic response due to climate change (Santiam River, Oregon). *Hydrological Processes*.

Surfleet, C.G., D. Tullos, C. Desiree, H. Chang, Heejun, and I.-W. Jun (2012) Selection of hydrologic modeling approaches for climate change assessment: A comparison of model scale and structures. *Journal of Hydrology*. 464–465: 233–248.

Suzuki, S. (1960) Percolation measurements based on heat flow through soil with special reference to paddy fields. *Journal of Geophysical Research*. 65(9): 2883–2885.

Swanson, T.E. and M.B. Cardenas (2011) Ex-Stream: A MATLAB program for calculating fluid flux through sediment–water interfaces based on steady and transient temperature profiles. *Computers & Geosciences*. 37(10): 1664–1669.

Swarzenski, P.W., F.W. Simonds, A.J. Paulson, S. Kruse, and C. Reich (2007) Geochemical and geophysical examination of submarine groundwater discharge and associated nutrient loading estimates into Lynch Cove, Hood Canal, WA. *Environmental Science and Technology.* 41: 7022–7029.

Szilagyi, J. (2003) Sensitivity analysis of aquifer parameter estimations based on the Laplace equation with linearized boundary conditions. *Water Resources Research.* 39(6): 1156.

Taniguchi, M. (1993) Evaluation of vertical groundwater fluxes and thermal properties of aquifers based on transient temperature-depth profiles. *Water Resources Research.* 29: 2021–2026.

Taniguchi, M. and H. Iwakawa (2001) Measurements of submarine groundwater discharge rates by a continuous heat-type automated seepage meter in Osaka Bay, Japan. *Japanese Journal of Groundwater Hydrology.* 43: 271–277.

Taniguchi, M., T. Stieglitz, and T. Ishitobi (2008) Temporal variability of water quality of submarine groundwater discharge in Ubatuba, Brazil. *Estuarine Coastal and Shelf Science.* 76: 484–492.

Tcherepanov, E.N., V.A. Zlotnik, and G.M. Henebry (2005) Using Landsat thermal imagery and GIS for identification of groundwater discharge into shallow groundwater-dominated lakes. *International Journal of Remote Sensing.* 26: 3649–3661.

Thackston, E.L. and K.B. Schnelle (1970) Predicting effects of dead zones on stream mixing, *Journal of Sanitary Engineering Division—ASCE.* 96: 319–331.

Theis, C.V. (1940) The source of water derived from wells—Essential factors controlling the response of an aquifer to development. *Civil Engineering.* 10(5): 277–280.

Theis, C.V. (1941) The effect of a well on the flow of a nearby stream. *Transactions of the American Geophysical Union.* 22(3): 734–738.

Therrien, R., R.G. McLaren, E.A. Sudicky, and S.M. Panday (2010) HydroGeoSphere: A three-dimensional numerical model describing fully-integrated subsurface and surface flow and solute transport. Groundwater Simulations Group, University of Waterloo, Waterloo, Ontario, Canada.

Tonkin, M. and J. Doherty (2009) Calibration-constrained Monte Carlo analysis of highly parameterized models using subspace techniques. *Water Resources Research.* 45(12): W00B10.

Toran, L., M. Johnson, J. Nyquist, and D.O. Rosenberry (2010) Delineating a road-salt plume in lakebed sediments using electrical resistivity, piezometers, and seepage meters at Mirror Lake, New Hampshire, U.S.A. *Geophysics.* 53: 841–850.

Toran, L., J. Nyquist, D. Rosenberry, M. Gagliano, N. Mitchell, and J. Mikochik (2014) Geophysical and hydrologic studies of lake seepage variability. *Groundwater.*

Tóth, J. (1963) A theoretical analysis of groundwater flow in small drainage basins. *Journal of Geophysical Research.* 68(16): 4795–4812.

Townley, L.R. (2015) Personal web site: Visualizations, http://www.townley.com.au/, last accessed May 12, 2016.

Townley, L.R. and M.G. Trefry (2000) Surface water–groundwater interaction near shallow circular lakes: Flow geometry in three dimensions. *Water Resources Research.* 36(4): 935–948.

Traylor, J.P. and V.A. Zlotnik (2016) Analytical modeling of irrigation and land use effects on streamflow in semi-arid conditions. *Journal of Hydrology.* 533: 591–602.

Trefry, M.G. and C. Muffels (2007) FEFLOW: A finite-element ground water flow and transport modeling tool. *Groundwater.* 45: 525–528.

Triska, F.J., V.C. Kennedy, R.J. Avanzino, G.W. Zellweger, and K.E. Bencala (1989) Retention and transport of nutrients in a third-order stream in northwestern California: Hyporheic processes. *Ecology.* 70(6): 1893–1905.

Turcotte, D.L. and G. Schubert (1982) *Geodynamics: Applications of Continuum Physics to Geological Problems.* John Wiley, New York.

Turner, J.V and L.R. Townley (2006) Determination of groundwater flow-through regimes of shallow lakes and wetlands from numerical analysis of stable isotope and chloride tracer distribution patterns. *Journal of Hydrology.* 320: 451–483.

Tyler, S.W., J.S. Selker, M.B. Hausner, C.E. Hatch, T. Torgersen, C.E. Thodal, and S.G. Schladow (2009) Environmental temperature sensing using Raman spectra DTS fiber-optic methods. *Water Resources Research.* 45: W00D23.

Valentine, E. and I. Wood (1979) Experiments in longitudinal dispersion with dead zones. *Journal of Hydraulics Division—ASCE.* 105: 999–1016.

Valett, H.M., S.G. Fischer, N.B. Grimm, and P. Camil (1994) Vertical hydrologic exchange and ecological stability of a desert stream ecosystem. *Ecology.* 75(2): 548–560.

Valett, H.M., S.G. Fisher, and E.H. Stanley (1990) Physical and chemical characteristics of the hyporheic zone of a Sonoran Desert stream. *Journal of North American Benthological Society.* 9(3): 201–215.

Valett, H.M., C.N. Dahm, M.E. Campana, J.A. Morrice, M.A. Baker, and C.S. Fellows (1997) Hydrologic influences on groundwater-surface water ecotones: Heterogeneity in nutrient composition and retention. *Journal of the North American Benthological Society.* 239–247.

Valett, H.M., C.G.C. Hakenkamp, and A.J. Boulton (1993) Perspectives on the hyporheic zone: Integrating hydrology and biology. Concluding remarks. *Journal of North American Benthological Society.* 12(1): 94–99.

Valett, H.M., J.A. Morrice, C.N. Dahm, and M.E. Campana (1996) Parent lithology, surface-groundwater exchange, and nitrate retention in headwater streams. *Limnology and Oceanography.* 333–345.

VanderKwaak, J.E. (1999) Numerical simulation of flow and chemical transport in integrated surface–subsurface hydrologic system. PhD dissertation, University of Waterloo, Waterloo, Ontario, Canada.

Vervier, P., J. Gibert, P. Marmonier, and M.J. Dole-Oliver (1992) A perspective on the permeability of the surface freshwater–groundwater ecotone. *Journal of North American Benthological Society*. 11(1): 93–102.

Vidon, P.G. et al. (2010) Hot spots and hot moments in riparian zones: Potential for improved water quality management, *Journal of the American Water Resources Association*. 46(2): 278–298.

Vogt, T., P. Schneider, L. Hahn-Woernle, and O.A. Cirpka (2010) Estimation of seepage rates in a losing stream by means of fiber-optic high-resolution vertical temperature profiling. *Journal of Hydrology*. 380(1–2): 154–164.

Von Gunten, H. and C. Lienert (1993) Decreased metal concentrations in ground-water caused by controls of phosphate emissions. *Nature*. 364: 220–222.

Voytek, E.B., A. Drenkelfuss, F.D. Day-Lewis, R. Healy, J.W. Lane, and D. Werkema (2014) 1DTempPro: Analyzing temperature profiles for groundwater/surface-water exchange. *Groundwater*. 52(2): 298–302.

Wada, Y., L.P.H. van Beek, and M.F.P. Bierkens (2012) Nonsustainable groundwater sustaining irrigation: A global assessment. *Water Resources Research*. 48, W00L06, doi:10.1029/2011WR010562, 18 p.

Wagner, B.J. and S.M. Gorelick (1986) A statistical methodology for estimating transport parameters: Theory and application to one-dimensional advective-dispersive systems. *Water Resources Research*. 22(8): 1303–1315.

Wagner, B.J. and J.W. Harvey (1997) Experimental design for estimating parameters of rate-limited mass transfer: Analysis of stream tracer studies. *Water Resources Research*. 33(7): 1731–1741.

Wahl, K.L. and R.L. Tortorelli (1997) Changes in flow in the Beaver–North Canadian River Basin upstream from Canton Lake, Western Oklahoma. U.S. Geological Survey Water-Resources Investigations Report 96-4304, Oklahoma City, OK.

Wallace, R.B., Y. Darama, and M.D. Annable (1990) Stream depletion by cyclic pumping of wells. *Water Resources Research*. 26(6): 1263–1270.

Ward, A.S., M.N. Gooseff, and P.A. Johnson (2011) How can subsurface modifications to hydraulic conductivity be designed as stream restoration structures? Analysis of Vaux's conceptual models to enhance hyporheic exchange. *Water Resources Research*. 47(8): W08512.

Ward, A.S., M.N. Gooseff, T.J. Voltz, M. Fitzgerald, K. Singha, and J.P. Zarnetske (2013a), How does rapidly changing discharge during storm events affect transient storage and channel water balance in a headwater mountain stream? *Water Resources Research*. 49: 5473–5486.

Ward, A.S., R.A. Payn, M.N. Gooseff, B.L. McGlynn, K.E. Bencala, C.A. Kelleher, S.M. Wondzell, and T. Wagener (2013b) Variations in surface water-groundwater interactions along a headwater mountain stream: Comparisons between transientstorage and water balance analyses. *Water Resources Research*. 49: 3359–3374.

Ward, J.V. (1989) The four-dimensional nature of lotic ecosystems the four-dimensional nature of lotic ecosystems. *Journal of North American Benthological Society*. 8(1): 2–8.

Ward, N.D. and P. Callander (2010) Distribution of stream depletion. *Journal of Hydraulic Engineering—ASCE*. 136(3): 170–174.

Weill, S., A. Mazzia, M. Putti, and C. Paniconi (2011) Coupling water flow and solute transport into a physically-based surface–subsurface hydrological model. *Advances in Water Resources*. 34(1): 128–136.

Wheeler, J.D. and C.A. Eddy-Miller (2005) Seepage investigation on selected reaches of Fish Creek, Teton County, Wyoming, 2004. U.S. Geological Survey Scientific Investigations Report 2005-5133, Reston, VA, 15p.

White, D.S. (1993) Perspectives on defining and delineating hyporheic zones. *Journal of the North American Benthological Society*. 12(1): 61–69.

Wilson, J.L. (1993) Induced infiltration in aquifers with ambient flow. *Water Resources Research*. 29(10): 3503–3512.

Winter, T.C. (1978) Numerical simulation of steady state three-dimensional groundwater flow near lakes. *Water Resources Research*. 14(2): 245–254.

Winter, T.C. (1981a) Uncertainties in estimating the water balance of lakes. *Water Resources Bulletin*. 17: 82–115.

Winter, T.C. (1981b) Effects of water-table configuration on seepage through lake beds. *Limnology and Oceanography*. 26(5): 925–934.

Winter, T.C. (1986) Effect of ground-water recharge on configuration of the water table beneath sand dunes and on seepage in lakes in the sandhills of Nebraska, U.S.A. *Journal of Hydrology*. 86: 221–237.

Winter, T.C. (1999) Relation of streams, lakes, and wetlands to groundwater flow systems. *Hydrogeology Journal*. 7: 28–45.

Winter, T.C., J.W. Harvey, O.L. Franke, and W.M. Alley (1998) Ground water and surface water; a single resource. U.S. Geological Survey Circular 1139, Denver, CO.

Winter, T.C. and D.O. Rosenberry (2009) Evaluation of methods and uncertainties in the water budget. In T.C. Winter and G.E. Likens, eds. *Mirror Lake: Interactions among Air, Land, and Water*. University of California Press, Berkeley, CA, pp. 205–224.

Woessner, W.W. (2000) Stream and fluvial plain ground water interactions: Rescaling hydrogeologic thought. *Groundwater*. 38(3): 423.

Wolock, D.M. (2003) Estimated mean annual natural groundwater recharge in the conterminous United States. U.S. Geological Survey Open-File Report 03-311, Reston, VA, 16p.

Wondzell, S.M. and M.N. Gooseff (2013) Geomorphic controls on hyporheic exchange across scales: Watersheds to particles. In J. Shroder (Editor in Chief), E. Wohl, eds. *Treatise on Geomorphology*, Vol. 9: Fluvial Geomorphology. Academic Press, San Diego, CA, pp. 203–218.

Wondzell, S.M. and F.J. Swanson (1996) Seasonal and storm dynamics of the hyporheic zone of a 4th-order mountain stream. 2: Nitrogen cycling. *Journal of North American Benthological Society.* 15(1): 3–19.

Wondzell, S.M. and F.J. Swanson (1999) Floods, channel change, and the hyporheic zone. *Water Resources Research.* 35(2): 555–567.

Wörman, A. (2000) Comparison of models for transient storage of solutes in small streams. *Water Resources Research.* 36(2): 455–468.

Wörman, A., A. Packman, and K. Jonsson (2002) Effect of flow-induced exchange in hyporheic zones on longitudinal transport of solutes in stream and rivers. *Water Resources Research.* 38: 1001.

Wroblicky, G.J., M.E. Campana, H.M. Valett, and C.N. Dahm (1998) Seasonal variation in surface–subsurface water exchange and lateral hyporheic area of two stream-aquifer systems. *Water Resources Research.* 34(3): 317–328.

Yang, Z., Y. Zhou, J. Wenninger, and S. Uhlenbrook (2014) A multi-method approach to quantify groundwater/surface water-interactions in the semi-arid Hailiutu River basin, northwest China. *Hydrogeology Journal.* 22: 527–541.

Yeh, H.D., Y.C. Chang, and V.A. Zlotnik (2008a) Stream depletion rate and volume from groundwater pumping in wedge-shape aquifers. *Journal of Hydrology.* 349: 501–511.

Yeh, T.-C., C.-H. Lee, K.-C. Hsu, W.A. Illman, W. Barrash, X. Cai, J. Daniels, E.A. Sudicky, L. Wan, G. Li, and C.L. Winter (2008b) A view towards the future of subsurface characterization: CAT scanning groundwater basins. *Water Resources Research.* 44: W03301.

Yeh, T.J., J. Xiang, R.M. Suribhatla, K. Hsu, C. Lee, and J. Wen (2009) River stage tomography: A new approach for characterizing groundwater basins, *Water Resources Research.* 45: W05409.

Young, P.C., D.J. Pedregal, and W. Tych (1999) Dynamic harmonic regression. *Journal of Forecasting.* 18(6): 369–394.

Zlotnik, V. (2015) Analytical methods for assessment of land-use change effects on stream runoff. *Journal of Hydrologic Engineering—ASCE.* 20(7): 06014009.

Zlotnik, V.A. (2004) A concept of maximum stream depletion rate for leaky aquifers in alluvial valleys. *Water Resources Research.* 40: W06507.

Zlotnik, V.A. and H. Huang (1999) Effect of partial penetration and streambed sediments on aquifer response to stream stage fluctuations. *Groundwater.* 37(4): 599–605.

Zlotnik, V.A., H. Huang, and J.J. Butler (1999) Evaluation of stream depletion considering finite stream width, shallow penetration, and properties of streambed sediments. *Proceedings of Water 99 Joint Congress*, Brisbane, Queensland, Australia, July 6–8, 1999, pp. 221–226.

Zlotnik, V.A., F. Olaguera, and J.B. Ong (2009) An approach to assessment of flow regimes of groundwater-dominated lakes in arid environments. *Journal of Hydrology.* 371: 22–30.

Zlotnik, V.A. and D.M. Tartakovsky (2008) Stream depletion by groundwater pumping in leaky aquifers. *Journal of Hydrologic Engineering—ASCE.* 13(2): 43–50.

Further Reading

Field methods for quantifying GWSWIs were addressed by Rosenberry and LaBaugh (2008) and Flekenstein et al. (2010).

General overview of GWSWI issues is given in a classic publication by Winter et al. (1998).

Heat transport across the GW and SW interface was reviewed by Stonestrom and Constantz (2004), Anderson (2005), and Rau et al. (2014).

Hydraulics of GWSWI for streams is well covered in the review of Barlow and Leake (2012).

Hyporheic zone concepts with physical, chemical, and biological aspects can be found in Aquatic Ecology series volume (e.g., Harvey and Wagner, 2000).

Modeling of GWSWI processes has been described by Furman (2008). Most commonly used model (GSFLOW) is described in a report by Markstrom et al. (2008), and intercomparison of several widely known coupled models is available from AquaResource Inc. (2011)